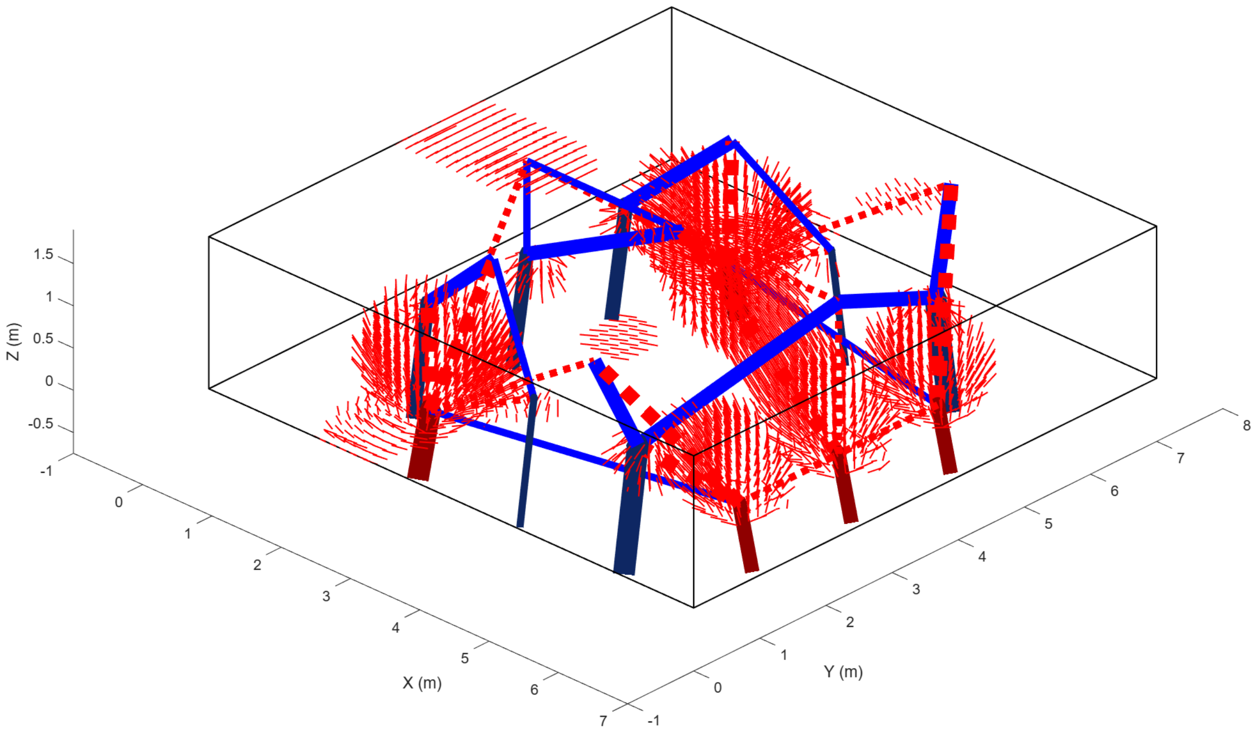

A 3D Finite Element Approach for Stress Field Analysis of Mooring Dolphin Pile Caps for Strut-and-Tie Modeling

A Parametric Study with acting Mooring Load

Master's thesis in Structural Engineering and Building Technology

EMELIE EKLUND
WILMA ERIKSSON

DEPARTMENT OF ARCHITECTURE AND CIVIL ENGINEERING
CHALMERS UNIVERSITY OF TECHNOLOGY
Gothenburg, Sweden 2026
www.chalmers.se

Master's thesis 2026

A 3D Finite Element Approach for Stress Field Analysis of Mooring Dolphin Pile Caps for Strut-and-Tie Modeling

A Parametric Study with acting Mooring Load

Emelie Eklund
Wilma Eriksson

CHALMERS
UNIVERSITY OF TECHNOLOGY

Department of Architecture and civil engineering
Division of Structural Engineering and Building Technology
Chalmers University of Technology
Gothenburg, Sweden 2026

A 3D Finite Element Approach for Stress Field Analysis of Mooring Dolphin Pile Caps for Strut-and-Tie Modeling
A Parametric Study with acting Mooring Load

EMELIE EKLUND
WILMA ERIKSSON

Examiner and Supervisor: Carlos Gil Berrocal, Department of Architecture and Civil Engineering
Supervisor: Hugo von Kraemer, Ramboll
Supervisor: Hadi Mazaheripour, Ramboll

Master's Thesis 2026
Department of Architecture and civil engineering
Division of Structural Engineering and Building Technology
Chalmers University of Technology
SE-412 96 Gothenburg
Telephone +46 31 772 1000

Cover: One of the final STMs for a mooring dolphin pile cap under self-weight and mooring loading. The red stress field is represented by compressive principal stress tensors.

Typeset in LaTeX
Printed by Chalmers Reproservice
Gothenburg, Sweden 2026

A 3D Finite Element Approach for Stress Field Analysis of Mooring Dolphin Pile Caps for Strut-and-Tie Modeling
A Parametric Study with acting Mooring Load
EMELIE EKLUND
WILMA ERIKSSON
Department of Architecture and Civil Engineering
Chalmers University of Technology

Abstract

A mooring dolphin is a marine structure designed to secure a vessel by mooring lines. These structures are typically equipped with pile caps to accommodate piles, anchors and bollards. Conventionally, a two-dimensional strut-and-tie model (STM) is used in the design of mooring dolphin pile caps.

This thesis proposes an alternative design methodology involving the development of a three-dimensional finite element (FE) model for a specific mooring dolphin. This approach aims to mitigate the uncertainties arising from the assumptions inherent in traditional two-dimensional STM applications. Furthermore, the three-dimensional model was processed using a self developed computational script, to sort and visualize principal stress tensors, enabling the systematic mapping of the internal strut-and-tie network within the structural volume. The script also includes the possibility of drawing the struts and ties directly within the structural volume and its stress field.

The assessed mooring dolphin was analyzed for self-weight combined with four mooring load directions, and varying pile cap thickness and anchor length. When subjected to the mooring load, the expected structural response was simultaneously piles in compression and anchors in tension with struts stretching in between the pile plate and anchor plate. This was confirmed and the analysis revealed that the magnitude of the struts and ties changed with the mooring load's inclination, while their configuration remained intact.

The three-dimensional FE model provides a comprehensive visualization of the global internal stresses within the pile cap and thereby can be used as guidance for the derivation of strut-and-tie models. Although this approach may reduce uncertainties regarding the internal stresses, it remains dependent on the design engineer to connect and map the nodes. To address this, in this thesis, a set of guidelines were established to support the engineer through these decisions.

Keywords: Mooring Dolphin, Mooring Load, Pile Cap, Deep Slab, Strut-and-Tie Model (STM), Finite Element Analysis (FEA), Three-dimensional, Internal Stress Field.

Ett 3D-finita elementmetods tillvägagångssätt för spänningsfältsanalys av förtöjningsdelfinpålkapslar för modellering av fackverksmodell
En parameterstudie med verkande förtöjningslast
EMELIE EKLUND
WILMA ERIKSSON
Institutionen för arkitektur och samhällsbyggnadsteknik
Chalmers tekniska högskola

Sammanfattning

En förtöjningsdykdalb är en marin struktur utformad för att säkra ett fartyg med hjälp av förtöjningslinor. Dessa strukturer är vanligtvis utrustade med en pålplint som förbinder pålar, ankare och pollare. Konventionellt används en tvådimensionell fackverksmodell vid namn strut-and-tie-modell (STM) för konstruering av dessa dykdalb pålplintar.

Denna avhandling föreslår en alternativ designmetodik som involverar utvecklingen av en tredimensionell finita elementmodell för en specifik förtöjnings dykdalb. Metoden syftar till att reducera osäkerheterna som uppstår från de antaganden som görs vid traditionella tvådimensionella STM-tillämpningar. Dessutom bearbetades resultatet från den tredimensionella modellen med hjälp av en egenutvecklad beräkningskod för att sortera och visualisera huvudspänningstensorer, vilket möjliggjorde en systematisk kartläggning av det inre strut-and-tie-nätverket inom den strukturella volymen. Koden inkluderar även möjligheten att rita tryck- (struts) och dragsträvorna (ties) direkt in i den strukturella volymen och dess spänningsfält.

Förtöjningsdykdalben analyserades för egentyngd kombinerad med fyra förtöjningslastriktningar, och för en varierande pålplinttjocklek samt ankarlängd. Vid verkande förtöjningslast var det förväntade strukturella beteendet att pålar verkade i tryck och ankare i drag med trycksträvor mellan pålplattan och ankarplattan. Detta bekräftades och analysen visade även att storleken på tryck- och dragsträvorna förändrades med förtöjningslastens lutning, medan deras konfiguration förblev intakt.

Den tredimensionella FE-modellen ger en omfattande visualisering av de globala inre spänningarna i pålplinten och kan därmed användas som vägledning för modellering av STM. Även om denna metod minskar osäkerheterna gällande det inre spänningsfältet, är metoden fortfarande beroende av konstruktören att förbinda och kartlägga noderna. För att hantera detta upprättades i denna avhandling en uppsättning riktlinjer för att stödja ingenjören genom dessa beslut.

Nyckelord: Förtöjningsdykdalb, Förtöjningslast, Pålplint, Fackverksmodell, Finit elementanalys (FEA), Tredimensionell, Inre spänningsfält.

Acknowledgements

This thesis was conducted at the Department of Architecture and Civil Engineering at Chalmers University of Technology as a final step towards our masters degree in Structural engineering and Building technology. The thesis topic, 3D FE modeling and STM analysis of mooring dolphin, was presented by Ramboll Ports and Marine, and Ramboll serves the roll as an important collaboration partner.

Our gratitude goes towards Ramboll and everybody at the division of Ports and marine who has engaged in our work, by providing valuable insights, information and encouragement. A special thanks goes to Hugo von Kraemer and Hadi Mazaheripour whom both has showed great engagement, and supported us through out the whole process from defining the thesis to discussing the final result.

We also express our deepest thanks to Carlos Gil Berrocal for always being available for us and his continuous feedback, endorsement, and technical support on substantive issues. Further thanks goes to Karin Lundgren and the SOFiSTiK team for aiding us in our work.

Emelie Eklund & Wilma Eriksson, Gothenburg, June 2026

Use of Artificial Intelligence

The use of artificial intelligence was limited to large language models (LLM), more specifically ChatGTP, Gemini and Overleaf AI. AI was applied to streamline the work and ensure high quality by refining the report content, debugging scripts in MATLAB and SOFiSTiK, and navigating sources. The authors take full responsibility for the academic decisions and conclusions within this thesis.

Emelie Eklund & Wilma Eriksson, Gothenburg, June 2026

List of Acronyms

Below is the list of acronyms that have been used throughout this thesis listed in alphabetical order:

BSI	British Standards Instituition
FE	Finite Element
FEA	Finite Element Analysis
FEM	Finite Element Method
LC	Load Case
LEA	Linear Elastic Analysis
LPM	Load Path Method
NLA	Nonlinear Analysis
SIS	Swedish Institute for Standards
SLS	Service Limit State
STM	Strut and Tie Model
ULS	Ultimate Limit State

Nomenclature

Below is the nomenclature of sets, parameters, and variables that have been used throughout this thesis.

Sets

$a - d$	Set of load cases
$A - F$	Set of parametric models

Parameters

$F_{mooring}$	Mooring load
h_s	Slab height from pile head
h_a	Distance between bottom of slab and anchor head
L_a	Support center distance
L_s	Anchor rod length
L_z	Slab height from pile head

Variables

σ_x	Nodal stress in global X-direction
σ_y	Nodal stress in global Y-direction
σ_z	Nodal stress in global Z-direction
τ_{xy}	Nodal shear stress XY plane
τ_{xz}	Nodal shear stress XZ plane
τ_{yz}	Nodal shear stress YZ plane
σ_1	Maximum nodal principal stress
σ_2	Intermediate nodal principal stress
σ_3	Minimum nodal principal stress

Contents

Abstract v

Sammanfattning vi

Acknowledgements vii

Use of Artificial Intelligence viii

List of Acronyms ix

Nomenclature xi

List of Figures xix

List of Tables xxiii

1 Introduction 1
1.1 Background 2
1.2 Aim 3
1.3 Objectives 3
1.4 Scope and Limitations 4
1.5 Methodology 5
1.6 Societal, Ethical and Ecological aspects 6

2 Theory 7
2.1 Mooring Dolphins 7
2.1.1 Mooring Equipment 9
2.1.2 Pile Cap 9
2.1.3 Piles and Anchors 10
2.1.4 Pile Anchor - Pile Cap Connection 12
2.2 Design Practice of Mooring Dolphins 13
2.3 Recommended Loads for Mooring Dolphin Design 14
2.3.1 Mooring Load 14
2.3.1.1 Operational factors 15
2.3.2 Environmental Loads 15
2.3.3 General Loads 16
2.3.4 Load Combination 16
2.4 Strut-and-Tie 17

2.4.1 Stress Distribution in Deep Slabs 19
2.4.1.1 B-regions and D-regions 19
2.4.1.2 Deep Slabs and Pile Caps 19
2.4.1.3 Influence of Embedded Supports 20
2.4.2 Load Path Method 21
2.4.3 Three Dimensional Strut-and-Tie 23
2.4.4 Struts, Ties and Nodes 24
2.4.4.1 Shape of Concrete Struts and Ties 24
2.4.4.2 Strength of Concrete Struts and Ties 25
2.4.4.3 Strength of Concrete Struts - Experimental Study . . 25
2.5 The Finite Element Method 26
2.5.1 Finite Elements 26
2.5.2 Pile Head Connection - FE Modeling Recommendations . . . 28
2.5.3 Shell Model - How it Worked 28
2.6 Nonlinearity 29
2.6.1 Modified Newton-Raphson Method 29
2.7 SOFiSTiK FEA 30
2.7.1 Overview Element Types 30
2.7.2 SOFiSTiK Stress Visualization 31

3 FE Model 33
3.1 FE models' main Structural Elements 34
3.2 Evolution of the FE Model 35
3.2.1 Pile Cap 35
3.2.2 Piles and Anchors 36
3.2.3 Bollard Attachment 41
3.3 Final FE Model 43
3.3.1 Properties 45
3.3.2 Parameters 47
3.4 Pile Cap Mesh 49
3.4.1 Convergence Analysis 49
3.4.2 Analysis Run Time 52
3.4.3 Stress Field Visualization 53
3.4.4 Final Mesh Size 55
3.5 Verification 56
3.6 Load Cases 57
3.7 Principle Stress FE Analysis 58

4 Strut-and-Tie Modeling 59
4.1 Stress Field in 3D 59
4.1.1 Stress Visualization Tools 60
4.2 Interpretation of the Stress Field 62
4.2.1 Expert Input 62
4.2.2 Strut-and-Tie Representation 63

5 STM Result 65
5.1 Load case a & d 66

5.2 Load case b & c 69

6 Discussion **73**
6.1 Stress Patterns 73
6.1.1 Load case a & d 75
6.1.2 Load case b & c 79
6.2 Method Evaluation 81
6.3 Additional Findings 82

7 Conclusion **85**
7.1 Further Research 86

References **89**

A Appendix **I**
A.1 Nonlinear Material Curves I
A.2 TRUS Pile Reasoning III
A.3 Nodal von Mises Stress IV
A.4 Slab Displacement VII
A.5 Reaction Force VIII
A.6 Load case c XVIII
A.7 Load case d XXIII
A.8 Verification of pile response XXVIII

List of Figures

1.1 Old mooring dolphin featuring timber piles. *Comment:* Adapted from: Vy från Skeppsholmen mot Strandvägen i Stockholm [photo], of H. Ellgaard, 2005, Wikimedia Commons. Licensed under CC-BY-SA-3.0. 2
1.2 Modern mooring dolphin featuring concrete pile cap *Comment:* Adapted from: Dykdalber Flekkefjord 005 Vest Betong [photo], of Vest Betong, 2021, Vestbetong.no/prosjekt/dykdalber-flekkefjord/. Reprinted with permission. 2
1.3 Schematic for the general method. 5

2.1 Marine port layout with belonging structures and components. 8
2.2 Rigid piled mooring dolphin with structural components. 8
2.3 Mooring equipment bollard securing a vessel. 9
2.4 Pile cross section with possible parts. 10
2.5 a) Pile - bedrock connection without grout. b) Anchor - bedrock connection with grout. 11
2.6 Simplified Pile - Pile Cap Connection with main components. 12
2.7 Struts forming between load application point and supporting piles following the red stress field. 17
2.8 Schematic for the Strut and Tie Method. 18
2.9 Stress field for concrete block with discontinuity (D) and continuity (B) regions. 19
2.10 Stress distribution for different slab heights (Park and Paulay, 1975, p.702). 20
2.11 Possible pile cap cross section with supports within the structure. . . . 20
2.12 Schematic for the Load Path Method. 21
2.13 Different load paths for the same loaded structure. Red - load path. Blue - stress field. Dotted black - load divider. 22
2.14 Strut-and-Tie Model with load paths. Red - load path. Blue - stress field. Dotted black - load divider. Circle - node. Solid black - tie. Dashed black - strut. 22
2.15 3D STM using two different approaches, a combination of 2D STM and a general 3D STM. 23
2.16 Strut shapes: a) Prismatic, b) Bottle, c) Fan. 25
2.17 Internal forces and moments in shell elements 26
2.18 Eight-node hexahedral element 27

2.19 FE model of mooring dolphin using lower order elements. 28

3.1 Final mooring dolphin FE model. 33
3.2 Bottom slab with holes for pile insertion. 35
3.3 Intended 8 pile, and final 12 pile configuration. 36
3.4 Resulting normal force in the elements from a horizontal load. 37
3.5 Simple geometry with nonlinear spring elements. Left: FE model. Middle: Spring under self-weight - pile spring in compression. Right: Spring under negative self-weight - anchor spring in tension. 38
3.6 Tension and compression over the pile heads in the rigid links for load case self-weight 40
3.7 Illustration of strain distribution in the connection plate. 41
3.8 Evolution of the bollard attachment for the mooring dolphin FE model. 41
3.9 Bollard FE design connecting TRUS bolt to BRIC node 42
3.10 Transparent pile cap of final FE mooring dolphin model. 43
3.11 Pile cap attachments showing pile head, anchor plate and bollard plate as yellow rigid links. 43
3.12 Pile and anchor hinged supports. 44
3.13 Bollard range - orientation and inclination 45
3.14 Plan for mooring dolphin model. 46
3.15 Section for mooring dolphin model. 46
3.16 Parametric models A-F to be studied in the thesis. 47
3.17 Average von Mises stress for all BRIC nodes for the self-weight analysis with different mesh sizes 50
3.18 Nodal von Mises stress for a mesh size of 49×49×14 51
3.19 Location of nodal strip in top BRIC nodal layer, see dashed blue line 51
3.20 Average BRIC nodal von Mises stress for a nodal strip for the self-weight analysis with different mesh sizes 52
3.21 Run time for self-weight analysis with different mesh sizes 53
3.22 Principal nodal stress σ_3 [Pa] for coarse mesh 54
3.23 Principal nodal stress σ_3 [Pa] for intermediate mesh 54
3.24 Principal nodal stress σ_3 [Pa] for dense mesh 55
3.25 Reaction forces, global Z, in piles for slab thickness 1.8m. 56
3.26 Mooring load application. 57

4.1 Different stress thresholds for the same parametric and load case - tensor plot. a) Threshold 8e5 Pa, b) Threshold 6e5 Pa. 60
4.2 Plot types: a) Tensor plot, b) Magnitude tensor plot, c) Magnitude plot. 61

5.1 STM for model A, load case a. 66
5.2 STM for model B & E, load case a. 67
5.3 STM for model C, load case a. 67
5.4 STM for model D, load case a. 68
5.5 STM for model F, load case a. 68
5.6 STM for model A, load case b. 69
5.7 STM for model B & E, load case b. 70

5.8 STM for model C, load case b. 70
5.9 STM for model D, load case b. 71
5.10 STM for model F, load case b. 71

6.1 Local tensor stress field around active anchor tension plate at height 0.7m. Blue - σ_1, Red - σ_3. 74
6.2 a) Pile head - Anchor head strut. b) Roof truss strut and tie. Blue - σ_1, Red - σ_3. 74
6.3 Back end strut comparison for models D and F. Blue - σ_1, Red - σ_3. . 75
6.4 Back end stress σ_3 tensor plot for model A, load case "imperfection". Note that no new strut is added to the STM, for the now visible strut on the right side. 76
6.5 Front (x = 3.3-7.0 m) three stress σ_3 struts for model A. Threshold 0.2 MPa. 77
6.6 Front (x = 3.3-7.0 m) three stress σ_3 struts for model A. Threshold 0.1 MPa. 77
6.7 Front (x = 3.3-7.0 m) three stress σ_3 struts for model C. Threshold 0.2 MPa. 78
6.8 Back three (x = 0.0-3.7 m) stress σ_1 ties for model A. Threshold 0.2 MPa. 78
6.9 Wavy stress (σ_1) flow bends of load cases b and c - Model B, clarified by a light blue line indicating the stress path. 79
6.10 Compression bottom stress σ_3 for load case b, model D, with additional bottom struts. 80
6.11 Global support reaction [kN] in the local pile axis for the FE model with truss-beam piles, either hinged or fixed to the pile cap. Red indicates compressive force, and blue indicates tensile force. 83

A.1 Nonlinear material curve for compression pile used in nonlinear material evolution of the FE model in SOFiSTiK. Y-axis [MPa] X-axis [‰]. I
A.2 Nonlinear material curve for tension anchor used in nonlinear material evolution of the FE model in SOFiSTiK.Y-axis [MPa] X-axis [‰]. . . II
A.3 BEAM pile moment force [kNm] and shear force [kN] for self-weight. . III
A.4 Pile head principal stress field. III
A.5 Nodal von Mises stress for a mesh size of 19×19×5. IV
A.6 Nodal von Mises stress for a mesh size of 29×29×8. IV
A.7 Nodal von Mises stress for a mesh size of 39×39×11. V
A.8 Nodal von Mises stress for a mesh size of 49×49×14. V
A.9 Nodal von Mises stress for a mesh size of 69×69×20. VI
A.10 Nodal von Mises stress for a mesh size of 99×99×25. VI
A.11 Model A, pile cap displacement [mm] for mooring load case a. VII
A.12 Reaction force model A, load case a. Red compressive forces represents pile reactions, blue tensile forces represents anchor reactions. . . VIII
A.13 Reaction force model B & E, load case a. Red compressive forces represents pile reactions, blue tensile forces represents anchor reactions.VIII

A.14 Reaction force model C, load case a. Red compressive forces represents pile reactions, blue tensile forces represents anchor reactions. . . IX
A.15 Reaction force model D, load case a. Red compressive forces represents pile reactions, blue tensile forces represents anchor reactions. . . IX
A.16 Reaction force model F, load case a. Red compressive forces represents pile reactions, blue tensile forces represents anchor reactions. . . X
A.17 Reaction force model A, load case b. Red compressive forces represents pile reactions, blue tensile forces represents anchor reactions. . . X
A.18 Reaction force model B & E, load case b. Red compressive forces represents pile reactions, blue tensile forces represents anchor reactions. XI
A.19 Reaction force model C, load case b. Red compressive forces represents pile reactions, blue tensile forces represents anchor reactions. . . XI
A.20 Reaction force model D, load case b. Red compressive forces represents pile reactions, blue tensile forces represents anchor reactions. . . XII
A.21 Reaction force model F, load case b. Red compressive forces represents pile reactions, blue tensile forces represents anchor reactions. . . XII
A.22 Reaction force model A, load case c. Red compressive forces represents pile reactions, blue tensile forces represents anchor reactions. . . XIII
A.23 Reaction force model B & E, load case c. Red compressive forces represents pile reactions, blue tensile forces represents anchor reactions.XIII
A.24 Reaction force model C, load case c. Red compressive forces represents pile reactions, blue tensile forces represents anchor reactions. . . XIV
A.25 Reaction force model D, load case c. Red compressive forces represents pile reactions, blue tensile forces represents anchor reactions. . . XIV
A.26 Reaction force model F, load case c. Red compressive forces represents pile reactions, blue tensile forces represents anchor reactions. . . XV
A.27 Reaction force model A, load case d. Red compressive forces represents pile reactions, blue tensile forces represents anchor reactions. . . XV
A.28 Reaction force model B & E, load case d. Red compressive forces represents pile reactions, blue tensile forces represents anchor reactions.XVI
A.29 Reaction force model C, load case d. Red compressive forces represents pile reactions, blue tensile forces represents anchor reactions. . . XVI
A.30 Reaction force model D, load case d. Red compressive forces represents pile reactions, blue tensile forces represents anchor reactions. . . XVII
A.31 Reaction force model F, load case d. Red compressive forces represents pile reactions, blue tensile forces represents anchor reactions. . . XVII
A.32 STM for model A, lc c. XVIII
A.33 STM for model B & E, lc c. XIX
A.34 STM for model C, lc c. XX
A.35 STM for model D, lc c. XXI
A.36 STM for model F, lc c. XXII
A.37 STM for model A, lc d. XXIII
A.38 STM for model B & E, lc d. XXIV
A.39 STM for model C, lc d. XXV
A.40 STM for model D, lc d. XXVI
A.41 STM for model F, lc d. XXVII

List of Tables

3.1 Material and geometry properties 45
3.2 Boundary conditions for mooring dolphin FE-model 47
3.3 Parametric values for Models A-F. 48
3.4 Structured mesh sizes and corresponding total number of nodes . . . 49
3.5 Reaction force verification for slab thickness 1.8 m 56
3.6 Mooring load cases applied in SOFiSTiK 57

6.1 Global support reaction in the local pile axis for the FE model with truss - beam piles as either hinged or fixed to the pile cap. 82

1 Introduction

Maritime transport vessels more than 80% (UN Trade and Development, 2025) of the volumetric international trade worldwide. Ports play a significant role in the global supply chain acting as the link between the marine and terrestrial transport networks. These harbors are complex infrastructural systems consisting of many action specific structures designed for securing vessels, loading goods, and integrated transport hubs to distribute the goods further on land.

A mooring dolphin is one such maritime structure, see Figures 1.1 and 1.2. It intends to secure a vessel at its berth by line, typically equipped with bollards or hooks mounted on the structure (The British Standards Institution, 2019 p.3). This thesis focuses on an open piled rigid dolphin which can be designed with raking piles and anchors embedded in a concrete slab, also known as a pile cap (The British Standards Institution, 2019 p.16).

Conventionally, deep concrete slabs for mooring dolphins are designed using the strut-and-tie method, a labor-intensive approach that requires simplification of load paths, stress distribution, and structure geometry, making the model highly dependent on the designer's interpretation of the internal stress field (Leu et al., 2006). These simplifications can potentially lead to unrealistic slab behavior and overly conservative designs, consequently being more expensive and having a higher carbon footprint due to the increase in material.

This thesis develops three-dimensional STMs for mooring dolphin pile caps using finite element analysis (FEA) to reduce two-dimensional idealization uncertainties. The mooring dolphins have altering slab heights and anchor rod penetration length, with mooring load acting in different directions. The resulting internal stress fields and STM configurations are visualized and used to establish guidelines to support the design of mooring dolphin pile caps.

Figure 1.1: Old mooring dolphin featuring timber piles. *Comment:* Adapted from: Vy från Skeppsholmen mot Strandvägen i Stockholm [photo], of H. Ellgaard, 2005, Wikimedia Commons. Licensed under CC-BY-SA-3.0.

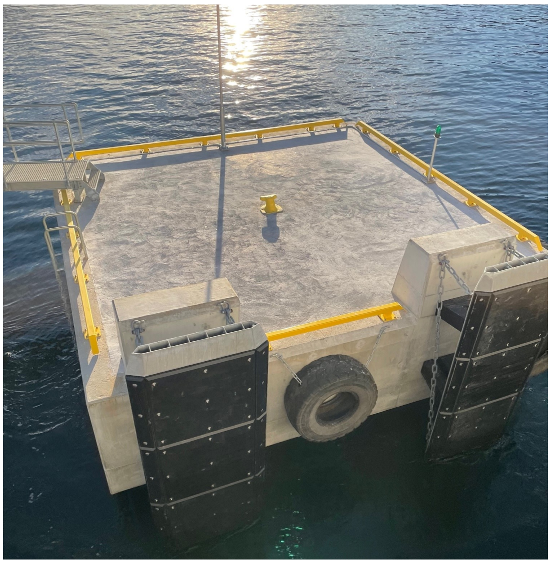

Figure 1.2: Modern mooring dolphin featuring concrete pile cap *Comment:* Adapted from: Dykdalber Flekkefjord 005 Vest Betong [photo], of Vest Betong, 2021, Vestbetong.no/prosjekt/dykdalber-flekkefjord/. Reprinted with permission.

1.1 Background

A mooring dolphin is a marine structure designed to facilitate a vessel. They are typically equipped with deep concrete slabs known as pile caps to accommodate piles and anchors, and mooring equipment such as bollards. Raking piles are considered effective only in compression, while tensile forces causing uplift are resisted by rock anchors (The British Standards Institution, 2019 p.105). A common approach to further reduce net uplift is to employ a deep pile cap with a thickness between 1.5 and 2.5 meters. The cap needs to be thick enough to accommodate the fastener connections for the piles, anchors, and bollards. In addition to that, the cap adds a lot of weight to the structure which reduces the demanded capacity of the anchors, while increasing the demand on the piles. Furthermore, the thick concrete cap improves shear resistance by distributing stresses in the piles and ensures structural rigidity. For a more in depth description of mooring dolphins, read Section 2.1.

Pile caps can be designed with the use of strut-and-tie models (STM) in accordance with Swedish Institute for Standards (2005). The method is mainly applied on discontinuity regions and utilizes the stress field to map struts, ties and nodes for structural analysis and reinforcement design. It is common practice to simplify the problem by working in two-dimensional sections, but it is possible to model three-dimensional strut-and-tie networks as well. For STM theory, read Section 2.4.

The finite element model that is conventionally used in addition to the two-dimensional STM, primarily focuses on the pile response. In such models, the pile cap is typically modeled using planar (shell) elements (see Section 2.5.1), resulting in a structural response governed mainly by in-plane behavior.

An alternative approach, with a stronger emphasis on the global structural behavior of the mooring dolphin, is to model the pile cap using solid elements. A three-dimensional approach provides insight into internal stress trajectories and force transfer mechanisms. Such information can be valuable for developing a three-dimensional STM representation, which in turn contribute to more refined understanding and potentially improved design practice for future applications.

1.2 Aim

This thesis aims to reduce uncertainties associated with idealizations inherent in two-dimensional strut-and-tie modeling. By conducting a finite element analysis, with focus on the pile cap, the global stress field is analyzed and post-processed to produce three-dimensional strut-and-tie configurations. The aim is to establish guidelines to support engineers in the interpretative process of designing STMs for mooring dolphin pile caps.

1.3 Objectives

The objectives of the thesis include the following:

- Develop and validate a FE model utilizing solid volume elements for the mooring dolphin pile cap.
- Extract and plot the principal stress field from the FE results of the solid volume elements.
- Investigate internal stress fields within the pile cap.
- Conduct a parametric study to evaluate geometric influences.
- Propose guidelines for three-dimensional strut-and-tie design configurations.

The first objective entails the construction of an FE model that accurately represents the global structural behavior of a mooring dolphin, with focus on the pile cap, and once validated, the FE analysis begins.

The parametric study involves alternating the geometry of the mooring dolphin to assess the influence of the parameters on the structural response of complex deep concrete slabs. By evaluating these analytical results and comparing the resulting strut-and-tie configurations, the thesis aims to propose STM design guidelines for specific deep concrete slabs under various operational circumstances.

The specific actions taken to achieve these objectives are described in Section 1.5 with regard to the defined limitations of the study. Furthermore, these actions are detailed in Chapters 2.5 and 4, describing the process.

1.4 Scope and Limitations

Limitations are acknowledged to constrain the scope of this work. This study is dedicated to the structural behavior of the pile cap and consequently, the design of structural members other than the concrete slab are excluded in the analysis. Furthermore, the study is focused on the global behavior of the pile cap response, meaning that details and connections are not designed and taken into account when meshing the FE model. Additionally, the local stress fields will not be evaluated within the thesis.

The research methodology is numerical and intuition based, with the FE analysis restricted to the use of the SOFiSTiK software and additional computational MATLAB scripts. No experimental testing or alternative analytical methods are included.

The STM is heavily dependent on the specific load case and structural geometry, and this thesis is limited to a single unique pile configuration, and set geometry excluding the alternating parameters, see Sections 3.3.1 and 3.3.2. Additionally, the piles are end-bearing hollow circular steel (HCS) founded on rock, with hinged connections in both ends. The concrete is modeled as linear elastic, state I concrete. Load wise, the thesis considers mooring action combined with self-weight.

1.5 Methodology

A schematic overview of the general method is shown in Figure 1.3. For an in depth description of the finite element modeling see Section 3.2, and see Chapter 4 for the stress field analysis and the strut-and-tie modeling.

To achieve the objective of providing guidelines for the strut-and-tie design in pile caps, the first step of the thesis commenced with a comprehensive literature study. The purpose of the literature study was to gather knowledge regarding the structural characteristics of mooring dolphins and to investigate established FE models and analytical methods. Furthermore, the literature review included theoretical foundations and practical applications of the STM, and practices for implementing the FE model. Based on these findings, a more specific objective and method were formulated.

The second phase of the project involved the development of the pile cap FE model using solid volume elements in SOFiSTiK. Nodal principal stresses from the three-dimensional elements in the FE model were utilized to visualize the internal load paths and stress fields in three dimensions. These visualizations were executed in MATLAB by self-developed computational scripts. The visualizations tools within the script allowed one to analyze and to directly draw the struts and ties along the principal stress tensors to form a complete strut-and-tie model. This procedure was repeated for the other parameters and load cases defined by the parametric study.

Finally, a comparative evaluation of the STMs and stress fields was performed to formulate design guidelines to support engineering decision making when designing STMs for mooring dolphin pile caps.

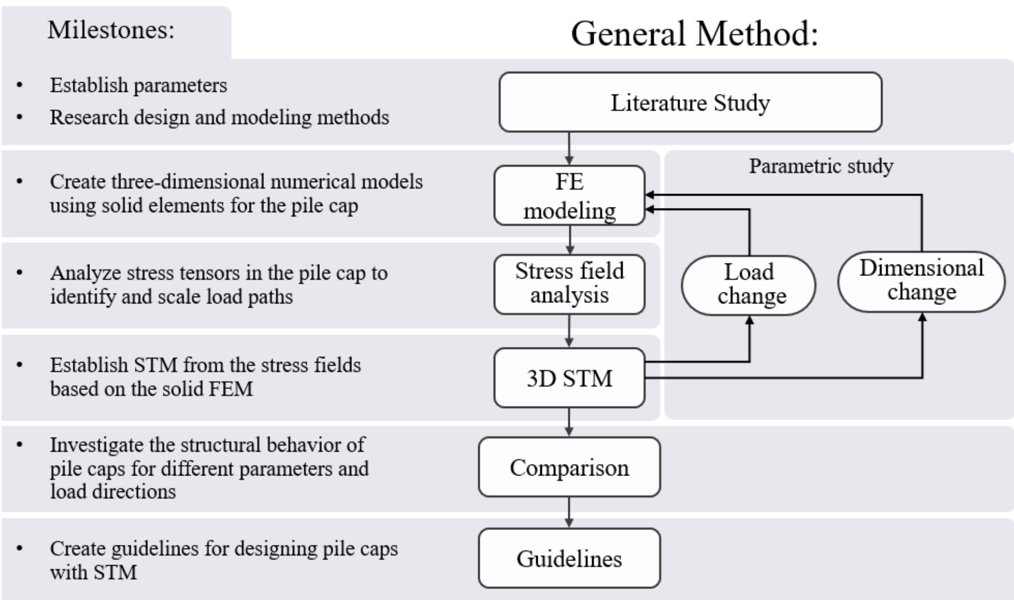

Figure 1.3: Schematic for the general method.

1.6 Societal, Ethical and Ecological aspects

The maritime environment addresses sustainable development by involving the societal, ethical, and ecological dimensions. The development of infrastructure can be beneficial for the maritime industry and it is important to consider additional aspects to ensure that the designs benefit society at multiple scales. This section aims to explore these dimensions within the scope of the thesis to work towards a holistic approach.

Societal
The thesis does not address individual citizens directly, although, the development of improved design approaches could enhance maritime commerce by contributing to more reliable infrastructure. The primary goal is to provide tools that support engineering practices in creating sustainable and resilient structures, while establishing standardized guidelines for pile cap design.

Ethical
Engineers play a crucial role in shaping infrastructure and they bear responsibility for the long-term consequences of their decisions. Ethical engineering practice requires balancing social, environmental, and economic dimensions throughout the design process. As each project presents specific opportunities and constraints, ethical considerations must be addressed within the individual project. This thesis aims to generate results that provide new insights that contribute to the exchange of knowledge and the sustainable development of civil engineering.

Ecological
Global warming poses the challenge of designing for a changing environment, including an altering sea-level and increased storminess (The British Standards Institution, 2017, p.33). Maritime design can address these challenges by reviewing factors that contribute to more resilient and durable structures. In this thesis, this is explored by considering different load cases to visualize a harsher and more variable environment.

Another important factor to consider is the environmental impact from the maritime structure itself (The British Standards Institution, 2019, p.20), such as its effects on water quality and CO_2 emissions associated with material use. The numerical results obtained with the three-dimensional modeling can be used to assess the potential for optimized cross-sectional design, including reducing concrete volume and reinforcement amount, while maintaining adequate structural performance and durability.

2 Theory

This chapter includes theory on mooring dolphins, strut-and-tie, and finite elements to gain a better understanding of the thesis topic. It contains specifics of the piled mooring dolphin addressed in the thesis and information about additional components. Recommendations and practices for mooring dolphin design and load application. The strut-and-tie method is included with a focus on three-dimensional STM applicable for pile cap design. Lastly, the sections covering the finite element method covers the FE elements, applications, and the specified FE software SOFiSTiK applied in the thesis.

2.1 Mooring Dolphins

A dolphin is defined by The British Standards Institution (BSI) as an "isolated structure or strong point used to maneuver a vessel or to hold it in position at its berth"(The British Standards Institution, 2019, p.3). These structures are essential for mooring and breasting of vessels, enabling cargo loading, maintenance, and long term storage. Among the various types of dolphin structures, the mooring dolphin is primarily designed to secure the vessel using hooks or bollards connected via mooring lines.

Generally, the mooring dolphin is often located further out in the water behind the line of breasting dolphins and is connected to the quay by a jetty and/or a walkway. While breasting dolphins are engineered to absorb energy from vessel impacts and maintain the vessel's position against the quay, mooring dolphins serve to resist outward forces and prevent the vessel from drifting. Figure 2.1 illustrates a typical layout of dolphins and their associated structures.

The specific structure investigated in this thesis is a rigid, mooring dolphin with raking piles. Its primary components are shown in Figure 2.2. The number and dimensions of piles and bollards etc vary depending on the vessels that are facilitated and the environmental conditions. Furthermore, the included components also depends on load and environment such that in arctic climates, piles are often equipped with ice protectors in the splash zone to mitigate ice-induced loads and abrasion. Anchors are also not a necessary component but depends on the anchoring capacity demanded by the different governing design drivers.

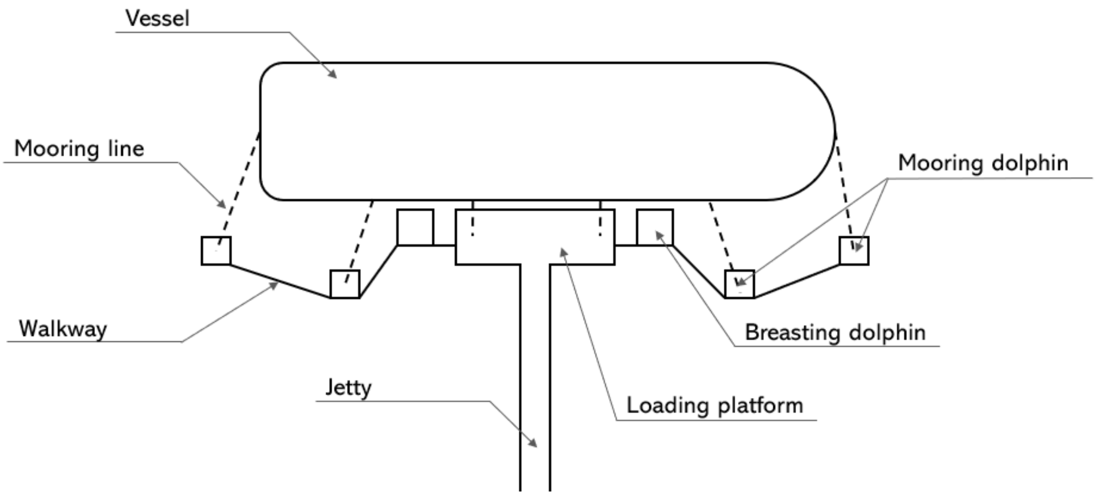

Figure 2.1: Marine port layout with belonging structures and components.

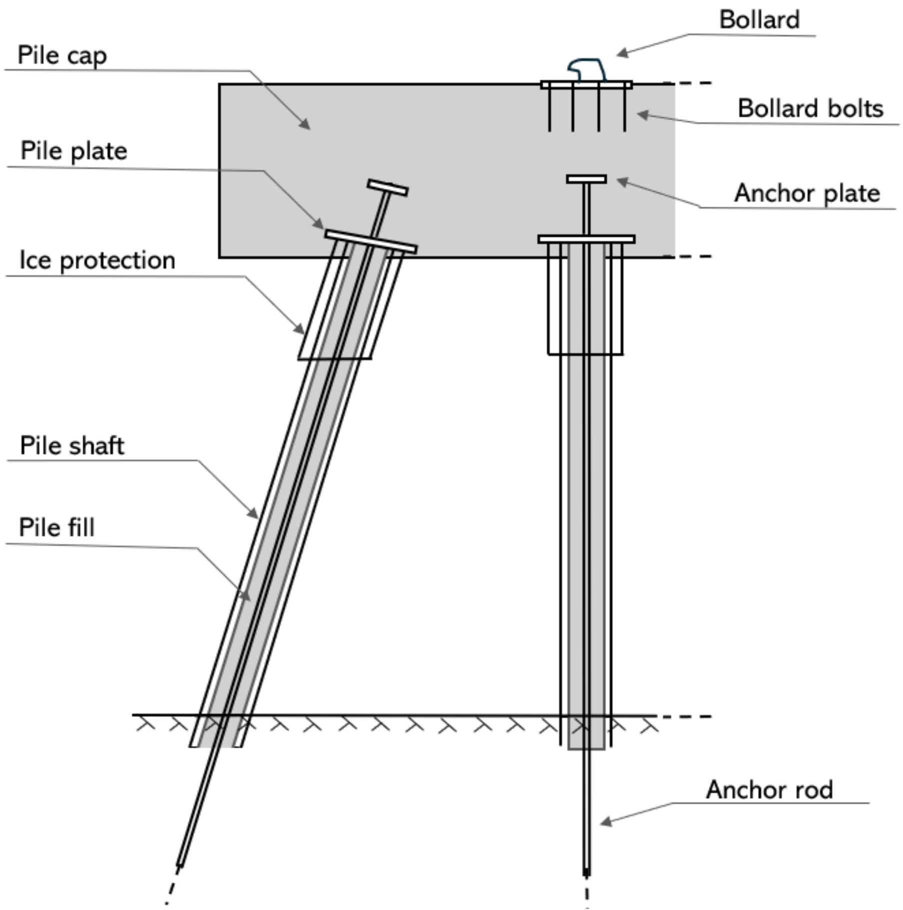

Figure 2.2: Rigid piled mooring dolphin with structural components.

2.1.1 Mooring Equipment

A bollard is a type of mooring equipment that secures a vessel by mooring line, see Figure 2.3. Larger vessels are attached to these in multiple places to ensure that the vessel is facilitated. Traditionally, this is done by knots or eye loops around a bollard which can differ in shape, for example, a T-head, bitt, or kidney bollard (as in Figure 2.3). The shape prevents the rope from sliding of the compartment. In Figure 1.2 a yellow bollard can be seen located in the middle of a dolphin pile cap.

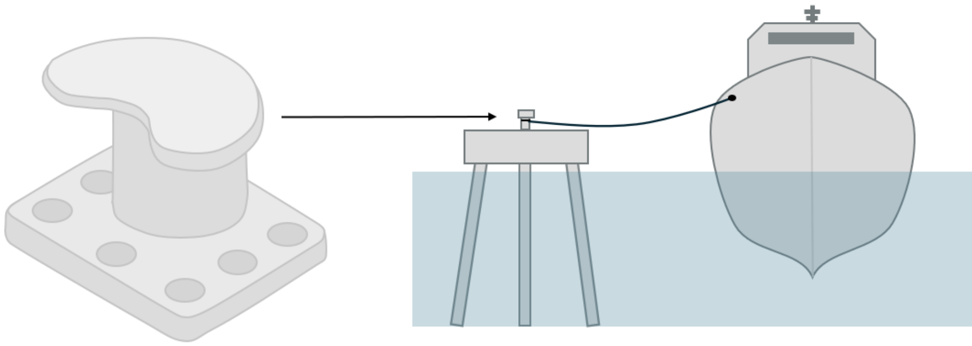

Figure 2.3: Mooring equipment bollard securing a vessel.

Quick release hooks (QRH) are a kind of mooring equipment with automatic release of the vessel. They are equipped with one or more hooks to attach to the eye loops. By releasing the vessel one can simultaneously off-hook the lines from all hooks and bollards.

2.1.2 Pile Cap

The pile cap is designed as a concrete deep slab that accommodates attachments for bollards, piles, and anchors. Beyond transferring the load from the bollard to the ground through the slab and piles, the pile cap also reduces tensile stresses in the anchors by dispersing concentrated forces. Also, the self-weight assists with resisting uplift and rotation. This is of high importance as the piles otherwise would need much higher capacity and demand a more expensive method of anchoring to resist the uplift forces. To what extent the slab assists in transferring the loads depends on its stiffness and therefore its thickness, leading to the implementation of deep slabs commonly between 1.5 and 2.5 m (The British Standards Institution, 2019, p.105). However, the use of a deep slab entails high material consumption, which increases production costs and greenhouse gas emissions.

Furthermore, a thicker slab enhances the punching-shear resistance of the cap. Alternative methods to increase the capacity is to increase the amount of reinforcement to strengthen the slab and to use larger connection points for the piles to disperse the stresses.

2.1.3 Piles and Anchors

The primary focus of the piles and anchors is to transfer the loads down to the foundation. The mooring dolphin is subjected to downward compressive forces as well as uplift and horizontal forces. The horizontal forces applied to the mooring dolphin are resisted through the axial strength of the raking piles, according to the BSI (The British Standards Institution, 2019, p.99). The compressive forces are handled by the piles while the tensile forces are resisted by the anchors. It is possible for a mooring dolphin to function without anchors if the mooring load is relatively small compared to the thickness and weight of the slab. Additionally, the piles can carry tension to some extent, depending on pile design - bedrock support connection. However, this is generally an unwanted behavior due to the limited ground anchoring capacity for larger piles, as well as the more difficult production procedure.

Since some mooring dolphins must resist significant uplift forces, the connections must be capable of transferring tensile forces through the entire structure, from the pile cap, through the pile structure, and into the bedrock. This is achieved by an anchor rod extended through the hollow circular steel (HCS) pile, as illustrated in Figure 2.4. The anchor is secured within the pile cap via an anchor plate (see Figure 2.6) and driven deep into the bedrock.

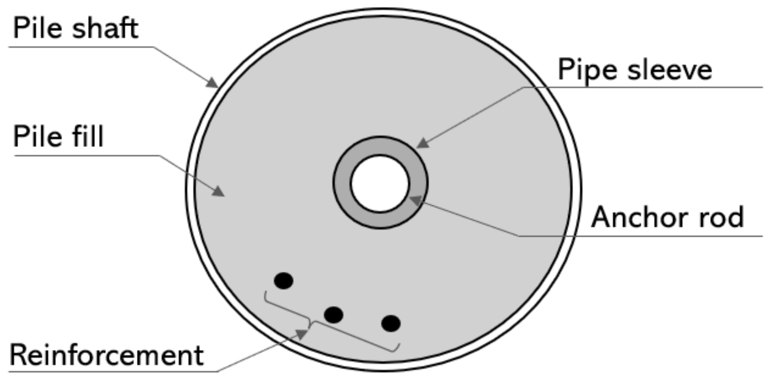

Figure 2.4: Pile cross section with possible parts.

As seen in Figure 2.4 the pile may be filled with a sort of fill, for example sand or concrete, and can furthermore be reinforced. The Swedish Commission on Piles (Bredenberg et al., 2010) highlights that the fill protects from corrosion and also increases the stiffness and the dead-weight of the hollow piles. Between the fill and the anchor rod it is common to install a pipe sleeve. The sleeve is installed to minimize the risk of corrosion of the anchor rod and to ensure no load transfer between the anchorage and the pile takes place, since they serve different purposes, namely the anchorage handling the tensile forces and the pile the compression forces. The anchor "rod" itself, if present, can be solid, hollow or entirely be made out of rope.

The bedrock connection for pile and anchor can be seen in Figure 2.2. The pile toe is typically driven or drilled 0.5 to 1.5 m into the bedrock to ensure that the pile toe has full contact with the bedrock and that it reaches a load bearing layer that is more load bearing than the surface layer, which is known to contain cracks, which could reduce the capacity. The anchor rod is drilled deeper through the rock and grouted. The depth depends on the dimensioning tensile forces. (Bredenberg et al., 2010)

Due to the different methods of driving, drilling, and grouting, the pile and anchor can have different support conditions. The pocket for the pile is commonly wider than the pile as the drill bit is wider than the piles, see Figure 2.5 (a). Because of this, the connection will allow for some horizontal movement and allow the pile to lift from the bedrock if loaded by a vertical upward force, like a mooring load. In theory, it is possible to make the connection fixed, but in a marine environment this would require additional and more complex installation methods, such as removing particles left from drilling (Karlsson et al., 2024).

The anchor bedrock connection is produced much stiffer than the pile, with additional concrete grout to ensure anchoring capacity. Grout is injected as seen in Figure 2.5 (b) in the space between the anchor and the wall of the hole (SSAB, 2025). The embedment length into the bedrock and the amount of grout depend on the anchoring capacity.

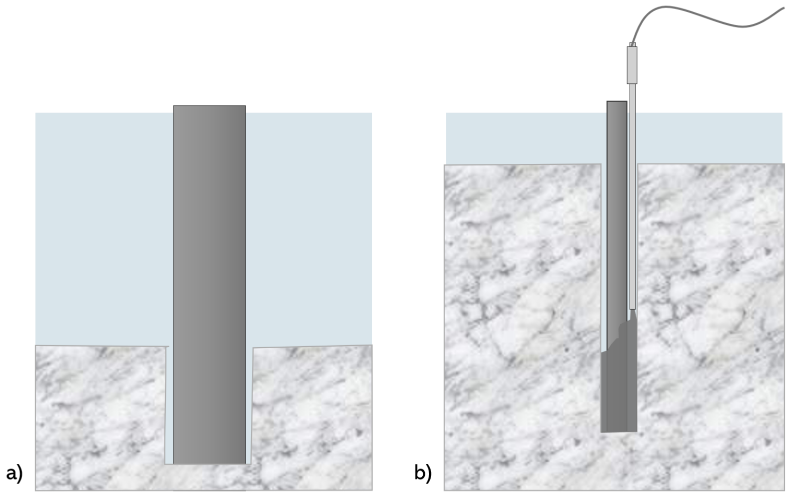

Figure 2.5: a) Pile - bedrock connection without grout. b) Anchor - bedrock connection with grout.

The ice-protections seen in Figure 2.2, are used to protect the piles from the impact of ice floes and are installed around the pile cap in the splash zone. It also reduces the risk of corrosion by minimizing the cycles of wetting and drying. (Bredenberg et al., 2010

2.1.4 Pile Anchor - Pile Cap Connection

Mooring dolphins, unlike standard foundation pile caps, are dominated by the mooring load. This mooring load demands that the pile anchor - pile cap connection does not only transfer load down to the soil/bedrock, but also resists horizontal forces, uplift forces, and can carry in tension.

The anchor tension plate distributes the tensile forces to the anchor while the pile compression plate distributes the compressive forces to the pile. The plates are placed perpendicular to the pile/anchor inclination and can differ in shape. They are generally wider than the the radius of the anchor rod respectively pile shaft, to enable welding of the connection. See Figure 2.6 for the main components of the connection.

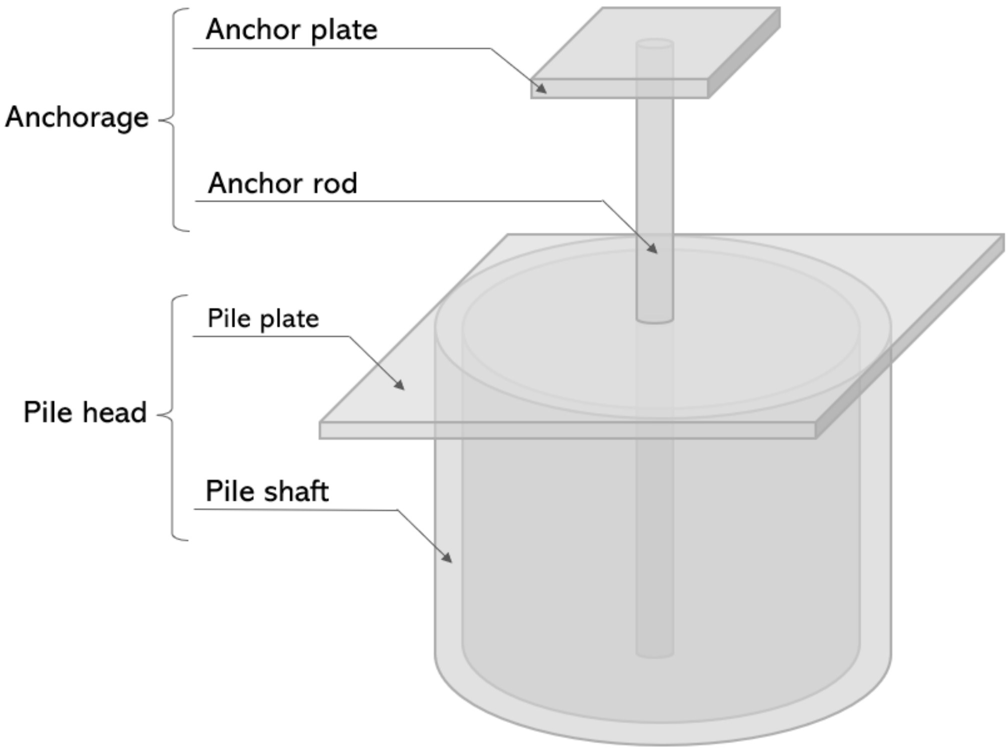

Figure 2.6: Simplified Pile - Pile Cap Connection with main components.

Occasionally must the pile compression plate additionally transfer the load to the pile filling. To ensure effective transfer of the load through the fill, it is important that the fill is packed to the top of the pile and has full contact with the pile plate. The same is true for the other end of the pile, that the pile toe must have uniform contact with the bedrock, including the fill. (Bredenberg et al., 2010)

2.2 Design Practice of Mooring Dolphins

Marine structures are designed according to Eurocode standards as other structures are, but compared to buildings and bridges, marine structures lack a dedicated national standard. Consequently, design practices often rely on international guidelines. PIANC is The World Association for Waterborne Transport Infrastructure and they unite experts worldwide to publish technical reports related to sustainable waterborne transport infrastructure.

Sweden is one of 43 countries who is a qualified member of PIANC, meaning that the country is connected to the organization via government, state or private companies (PIANC, 2026). The qualified members must endorse and encourage the use of the guidelines presented by PIANC with the ambition to create a unified maritime transport infrastructure. As for Sweden, PIANC is represented by PIANC Sverige, an association of private companies currently presided by a representative from the state owned research institutes RISE (Research Institutes of Sweden) (PIANC Sverige, 2026).

PIANC refers frequently to other studies and other countries' standards, such as the British Standards. The British Standards Institution (BSI) provide information and guidelines on how mooring dolphins could and should be designed, and what needs to be considered.

A common design practice consists of a two dimensional strut-and-tie model to dimension the concrete pile cap and associated reinforcement, and is approved by Swedish Institute for Standards (2005). The supporting piles can be dimensioned with finite element software, as was the case for the model referred to in Section 2.5.3.

2.3 Recommended Loads for Mooring Dolphin Design

Numerous loads act on a mooring dolphin, and both environmental influences and the structural characteristics must be considered in the design process. Forces arise from operational activities such as mooring, as well as from natural phenomena within the marine environment (The British Standards Institution, 2017, p.51). These actions may either be beneficial or adverse, depending on the load combination.

The BSI (The British Standards Institution, 2017, p.28-29) recommend that the following actions should be accounted for:

- Vehicular traffic loads
- Pedestrian-only traffic loads
- Equipment loads
- Cargo loads
- Environmental loads
- Operational loads
- Construction and installation loads

2.3.1 Mooring Load

Mooring actions occur when a vessel is secured, subjecting the bollard to significant loads through the mooring line (The British Standards Institution, 2019, p.18). The mooring load capacity of a mooring dolphin should be robust enough to withstand the dynamic nature of the load. Since the secured vessel reacts to its environment, affected by waves, winds, and the bypassing of other vessels, the load can shift in magnitude, orientation, and inclination (The British Standards Institution, 2019, p.11).

Mooring actions should be calculated in accordance with The British Standards Institution, 2017 and The British Standards Institution, 2014, including actions from breast, head and stern lines, and from spring lines. The mooring loads are assessed as dynamic loads caused by the vessel according to the BSI (The British Standards Institution, 2017). The load can act from a range of angles depending on the vessel's position and the mooring dolphin must be designed accordingly, and the mooring equipment selected based on the dimensioned capacity.

The magnitude of the mooring load is a decisive factor in bollard selection, as the component must be capable of resisting peak operational forces and efficiently distributing them to the pile cap. Furthermore, the design and specification of the bollard are governed by the specific orientation and vertical inclination of the mooring lines. The inclination and orientation depends on the type of vessel the dolphin secures, but also depends on the water level.

2.3.1.1 Operational factors

The capacity of a bollard is limited by a minimum breaking load (MBL), which is defined based on the maximum capacity obtained in a line mooring the vessel (The British Standards Institution, 2017, p.68). Each bollard should obtain a safe working load (SWL) that is greater or equal to the MBL.

The load transmitted through the bollard is limited by the MBL, which is lower than the corresponding accidental load case. This is possible due to a safety measurement taken in design. In the event of an accidental overload, neither the dolphin nor the vessel should break. The mooring system components are designed to fail progressively so that the weak link of the mooring equipment is the mooring line. The capacity of the mooring line is less than the SWL and that of the remaining mooring equipment, such that when exceeded the vessel breaks free and the mooring dolphin remains intact. (The British Standards Institution, 2017, p.69)

2.3.2 Environmental Loads

The main environmental loads in Sweden acting on a mooring dolphin include ice and wave actions. Ice loads impose horizontal loads, either from floating ice floes or static loads resulting from ice formation. According to Trafikverket (Trafikverket, 2023, p.82), it should be assumed that the ice load acts unilaterally on the structure. The design must account for varying load application points, acting at levels between the mean high water (MHW) and the mean low water (MLW) level. Subsequently, depending on the water level, it may be applied directly onto the piles, or to the pile cap.

In addition to horizontal loading, wave action can generate a vertical uplift force to the underside of the pile cap. The magnitude and nature of these loads depends on the coastal environment, fluctuations in water level, and the behavior of local currents and waves. In accordance with the BSI (The British Standards Institution, 2017), mooring dolphin design must account for a various number of load cases, for example steady current action, slamming action of waves on piles and slab, and wave induced vibrations. To reduce the number of dimensioning load cases the BSI (The British Standards Institution, 2019, p.11) stipulates that decks can be suspended such that the pile cap is located high enough to avoid the waves.

2.3.3 General Loads

The mooring dolphin is subjected to its own self-weight. However, buoyancy will act on the components submerged in the water (such as piles), reducing the effective contribution of their self-weight.

A live load equally distributed on the pile cap is commonly assessed for. This live load is not included for the purpose of the mooring dolphin, but it may be taken into account if the pile cap would for instance be used for storing or loading cargo.

2.3.4 Load Combination

SIS (Swedish Institute for Standards, 2026, p.27) states that structures should be designed to adequate reliability throughout their intended life, including sufficient durability, serviceability, and resilience. To meet these requirements, the application of appropriate load combinations together with partial safety factors is essential. These combinations primarily consider permanent and variable actions, as outlined by the The British Standards Institution, 2017, in order to generate the most adverse structural response for design.

One critical example is vertical uplift induced by mooring forces, which represents a case of governing design condition. This total uplift may be amplified by wave slamming actions on the soffit of the mooring dolphin pile cap, though it could also be resisted by possible live loads acting in opposite vertical direction. Furthermore, the dolphin is influenced by buoyancy, which reduces the effective self-weight of the piles and anchors. Ultimately, these loads are combined to determine the governing load cases for structural design.

2.4 Strut-and-Tie

The strut-and-tie method is a design and analysis practice for reinforced concrete members (Engström, 2015). It is typically applied for members with discontinuity regions (D-regions) with nonlinear strain distributions. The method can be applied for both two- and three-dimensional analysis and is suitable for both linear and nonlinear analysis.

The core principle of the strut-and-tie method is to identify the internal stress distribution and load paths for a cracked reinforced concrete section as a truss system, to find an appropriate strut-and-tie model (STM) consisting of compression struts, tension ties and connecting nodes. While the method is used to determine the ultimate limit state (ULS) capacity by assuming plastic redistribution for deep elements, it is recommended that the chosen truss geometry follows the elastic stress field. This ensures that the reinforcement is placed where the tensile stresses actually occur within the section, which improves performance in the serviceability limit state (SLS) by for instance limiting crack widths which could be dimensioning, especially for structures in a marine environment. (Engström, 2015, p.15)

The forces within a concrete structure can be solved by equilibrium conditions at the nodes. The struts represent the compressive stress fields within the concrete, while the tension ties usually represent some kind of reinforcement needed to resist the internal tensile stresses. In Figure 2.14, a simple model is illustrated with struts and internal compressive principal stresses, displaying the load path. (Engström, 2015, p.20-21)

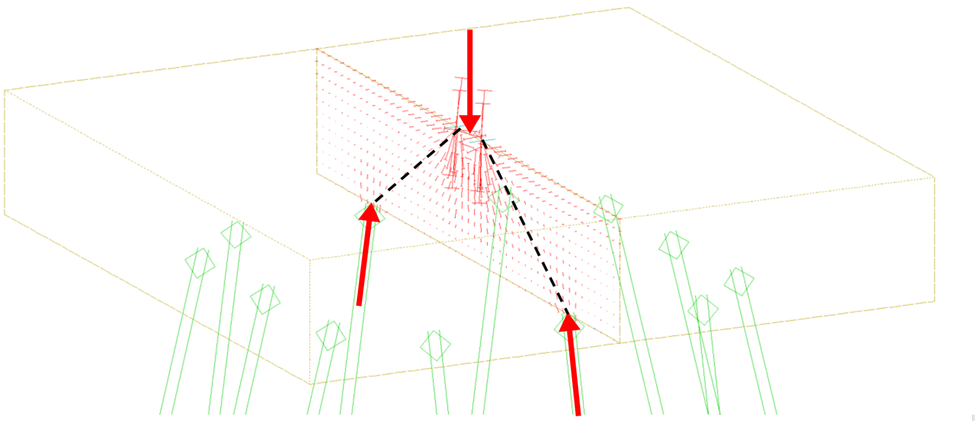

Figure 2.7: Struts forming between load application point and supporting piles following the red stress field.

The capacity of the STM is determined by the concrete failure criteria. Concrete is stronger in compression than in tension, and therefore the model is designed such that the struts represent the compression experienced by the concrete, while ties are most often associated with the need for reinforcement rather than directly representing the tensile field. The design choice depends on the magnitude of the stress and the preference of the engineer (Leu et al., 2006). Because the STM is used to determine the reinforcement demand in terms of struts and ties, the model is best suited for for ULS analysis of cracked cases, when the tensile strength of concrete is exceeded and the ties become active.

In Figure 2.8 the general workflow of the strut-and-tie method is summarized. The process begins with a structural analysis in which loads, boundary conditions, and reactions are determined. The reactions can be calculated by hand, using a finite element (FE) software or a FE script developed in code editor, depending on the complexity and detail of the problem.

The next step is to identify the discontinuity and continuity regions to properly assess and judge the stress field. The stress field can be achieved using the load path method (see section 2.4.2), performing a FE analysis of the member or by scripting FE as well. From the identified stress fields a STM is chosen. This is a critical step which might require several iterations and in depth studying since the engineer does not rely on any standard but heavily on her own intuition and experience.

Once the STM is established, the forces in the compressive and tensile members can be calculated from which the reinforcement (ties) are designed to ensure a safe design.

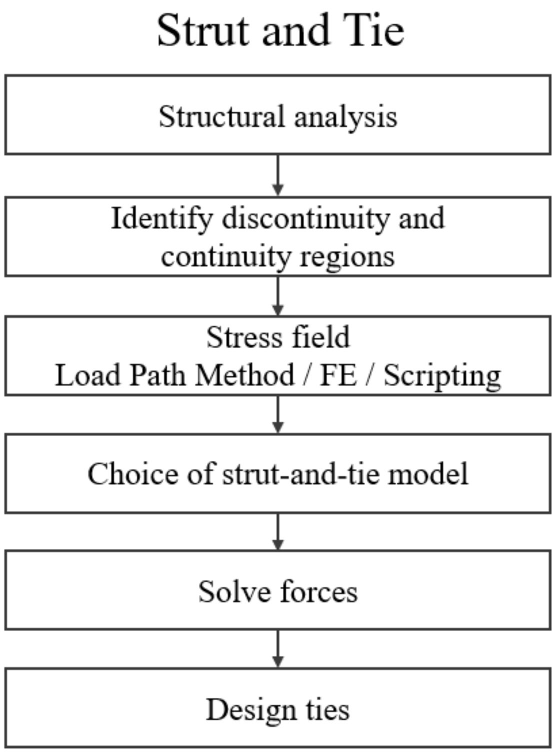

Figure 2.8: Schematic for the Strut and Tie Method.

2.4.1 Stress Distribution in Deep Slabs

Stress fields within reinforced concrete structures are categorized into continuity regions (B-regions) and discontinuity regions (D-regions). The identification is fundamental for selecting the appropriate design methodology of the element and region.

2.4.1.1 B-regions and D-regions

Continuity regions (B-regions) are defined as a region where the strain distribution is linear, resulting in a uniform stress. The Bernoulli hypothesis of plane strain distribution is valid within B-regions and is true for beams in general, with the exception of deep beams (Engström, 2015, p.3).

Discontinuity regions (D-regions) are sometimes referred to as disturbed or dispersed zones due to its nature of having a nonuniform strain distribution. D-regions are usually located close to geometric discontinuities or loading points such as supports, see Figure 2.9 (Engström, 2015, p.1-3). D-region design is not as well developed as the design practice for B-regions, and is commonly based on the engineer's experience and intuition (Leu et al., 2006).

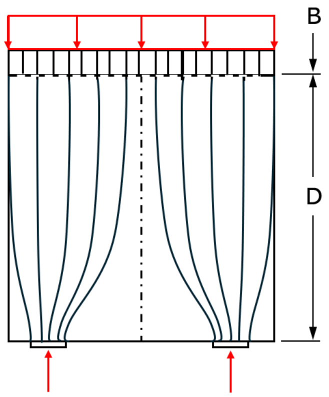

Figure 2.9: Stress field for concrete block with discontinuity (D) and continuity (B) regions.

2.4.1.2 Deep Slabs and Pile Caps

Members with spans $\mathbf{L/h < 2}$ are generally classified as deep beams or deep slabs. The stress distribution for a deep slab will vary depending on the height of the specimen, see Figure 2.10. With an increased height, the stress deviates more from the linear distribution predicted by Bernoulli. This results in the whole slab acting as a D-region.

The stress distributions in Figure 2.10 illustrate the nonlinear distribution for different height to span ratios as proposed by Park and Paulay, 1975. The linear distribution according to Euler-Bernoulli beam theory is true for case $\mathbf{h = L/4}$ and is shown as dotted lines, to illustrate that the stress distribution is not only non-linear but also increases and decreases in the top and bottom ends of the slab.

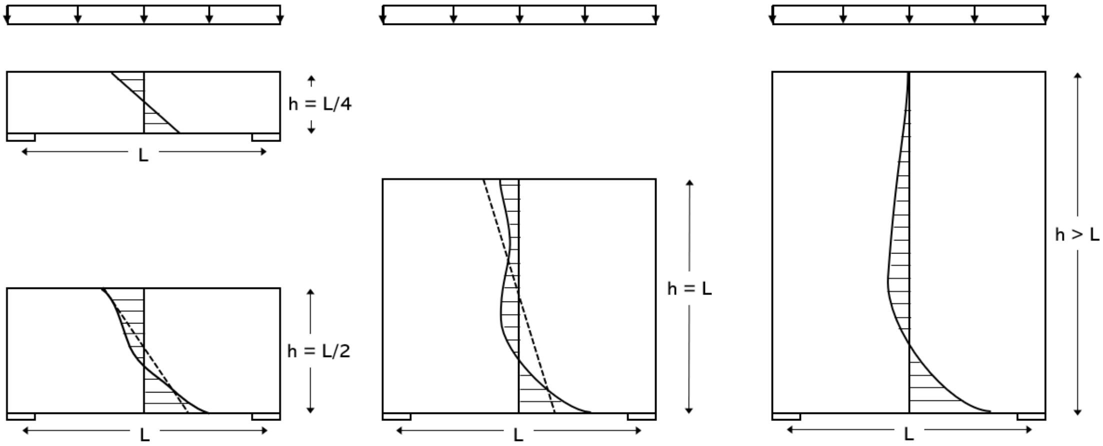

Figure 2.10: Stress distribution for different slab heights (Park and Paulay, 1975, p.702).

2.4.1.3 Influence of Embedded Supports

For the case of a pile cap, it is of interest to develop a FE model for the concrete slab. In the pile cap, the supports (piles and anchors) act within the structure as in Figure 2.11. The piles and anchors are both inclined and demand full surface contact, hence the pile at the bottom of the slab needs to be embedded. The purpose of the anchors is to resist uplift and they need to pull down the structure. The depth of the anchor affects the length and inclination of the struts and the resilience to punching shear. These supports will furthermore impact the stress distribution due to its downward-extending load carrying structure compared to the deep beams in Figure 2.10.

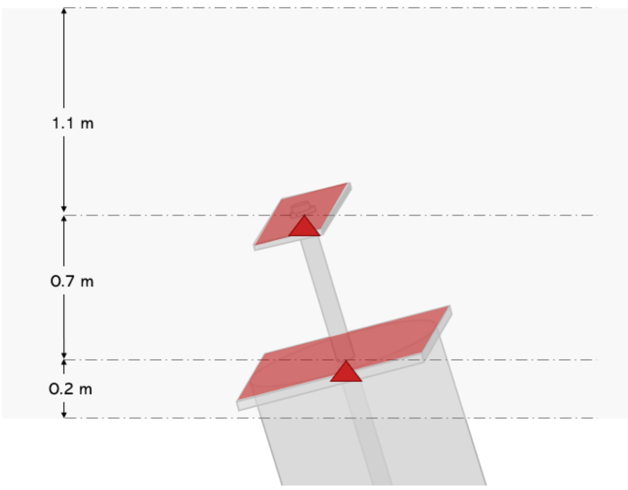

Figure 2.11: Possible pile cap cross section with supports within the structure.

2.4.2 Load Path Method

The load path method (LPM) is a highly influential step within the strut-and-tie method, see the schematic Figures 2.12 and 2.8. According to B. Engström (Engström, 2015, p.17), the primary role of the LPM is to identify the load dividers. These are theoretical boundaries that determine the distribution of internal forces to their respective support.

The load paths aims to, in a simplified manner, mimic the stress field. This is a critical step within the STM, as the simplification may deviate too far from the real behavior. Therefore, it is important to verify the load path and modify them. Leu et al., 2006 refers to the procedure as a "trial-and-error iterative design process", which mainly depends on the engineers' experiences.

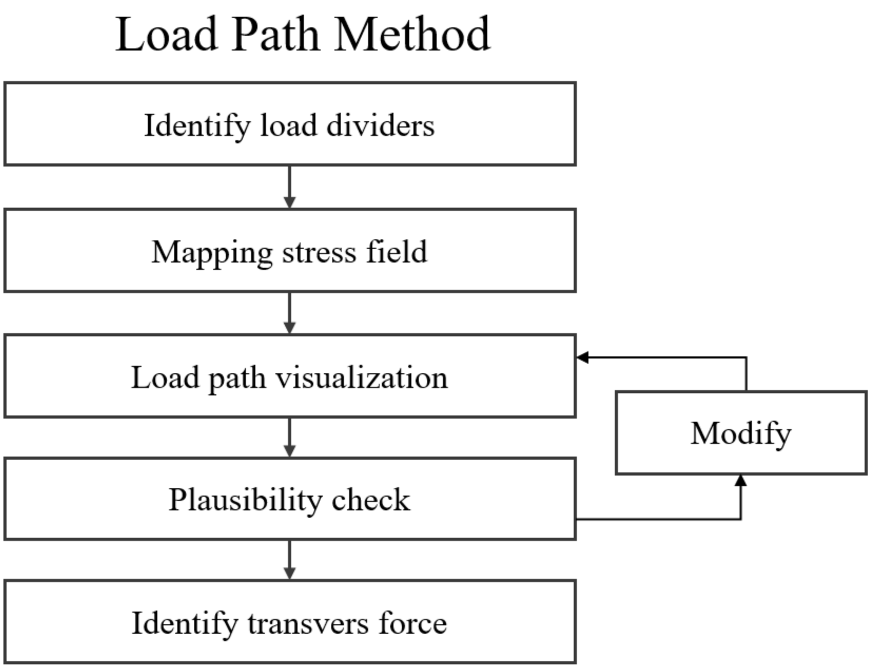

Figure 2.12: Schematic for the Load Path Method.

The sensitivity of the LPM is demonstrated in Figure 2.13 which illustrates how different load dividers for the same slab and stress field, impact the load paths. It highlights the importance of the simplification application and that for identical geometries and loading conditions, it is possible to make different assumptions. This becomes more difficult for structures like mooring dolphins which not only is a three dimensional cross-section, but also incorporates more supports. Note that the dashed lines represent the load dividers to which the force is carried by the nearest support within its section.

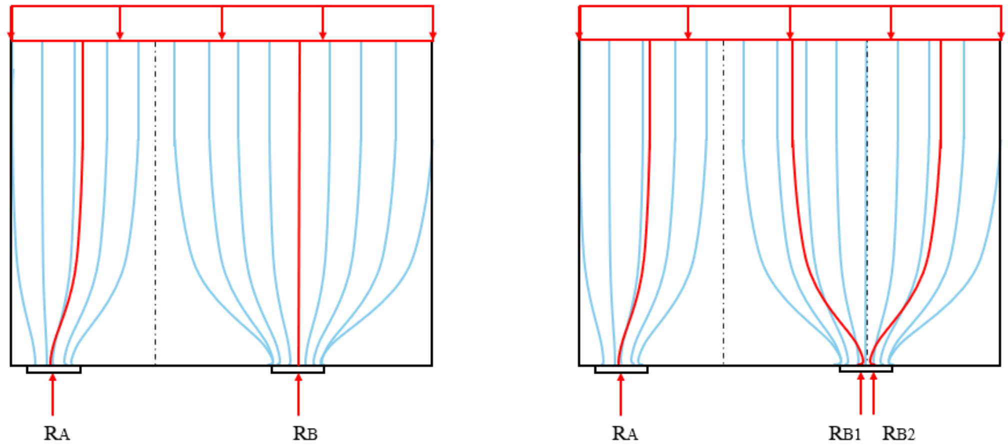

Figure 2.13: Different load paths for the same loaded structure. Red - load path. Blue - stress field. Dotted black - load divider.

Figure 2.14 illustrates how transverse forces are sketched to shape the load path which, depending on the direction, form either struts or ties. The load path is translated into a complete STM with corresponding struts, ties, and nodes. The dashed lines translate into struts, solid lines - ties and circle - nodes. In this STM there are two different nodes, a CCC-node and a CCT-node which indicate how many struts (C) and ties (T) are linked through the node.

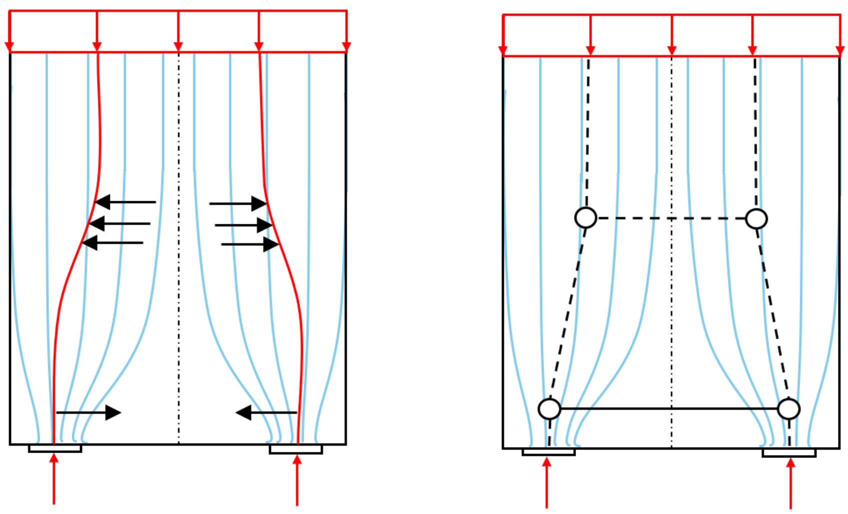

Figure 2.14: Strut-and-Tie Model with load paths. Red - load path. Blue - stress field. Dotted black - load divider. Circle - node. Solid black - tie. Dashed black - strut.

2.4.3 Three Dimensional Strut-and-Tie

Three dimensional strut-and-ties are modeled depending on the geometry of the element. For instance, a member built up by plates may combine multiple two dimensional STMs, one for each plate. For pile caps, a deep slab, the struts and ties stretch in X-, Y- and Z-direction. This is illustrated in Figure 2.15.

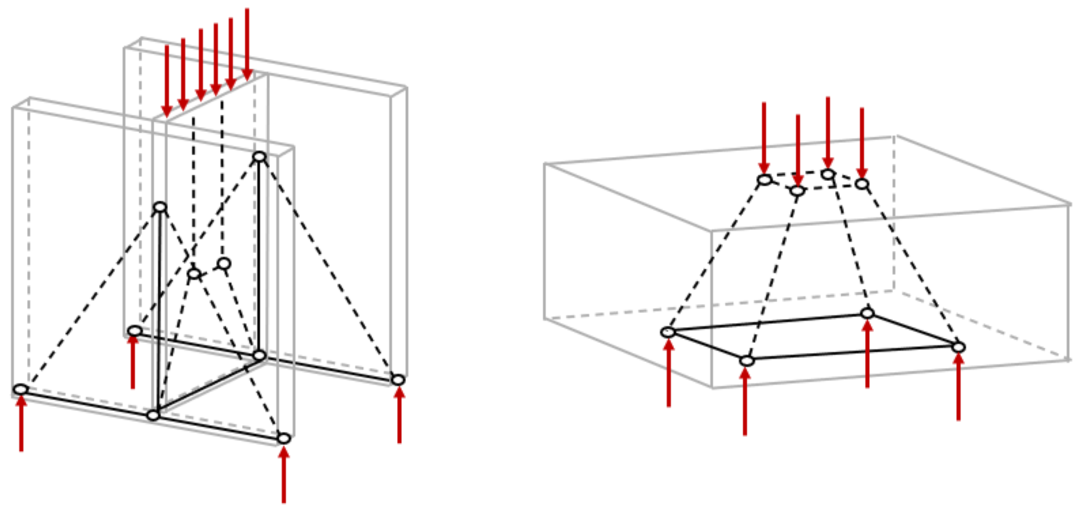

Figure 2.15: 3D STM using two different approaches, a combination of 2D STM and a general 3D STM.

In addition to LPM, one can use finite element software to study the load paths and stress fields within a three dimensional concrete element. In structural models it is practice to position the struts and ties along the principal stresses. Leu et al. Leu et al., 2006 report difficulties by using stress trajectories from three-dimensional finite element analysis for design, since in complex structures it is difficult to establish a model fitting for the tortuous stress field. An example of a complex area is the regions close to the pile and bollard of a mooring dolphin, where the loads are highly concentrated while having geometric stress field variations.

Principal Stress Analysis

There are three principal stresses, all of which act along its respective principal axis, which must not correspond to the global coordinate system. The principal stresses are sorted according to magnitude so that $\sigma_1 \geq \sigma_2 \geq \sigma_3$ with σ_1 being the largest normal stress acting in any direction (Dowling, 2013, p.245). By plotting different principal stresses and altering the tolerance of the stresses to be viewed, ties and struts can be withdrawn from the three dimensional model.

SOFiSTiK BRIC cut
It can be difficult to visualize the stresses within a three-dimensional model since FE software may only show stresses for the outer shell of the model. In the FEA software SOFiSTiK it is possible to make BRIC cuts when designing in three-dimensional solid volume elements called BRIC elements. This makes it possible for the engineer to analyze the internal stresses in the cross-sections where the cut is performed. (SOFiSTiK AG, 2026b).

Evolutionary Structural Optimization
In "Strut-and-Tie Design Methodology for Three-Dimensional Reinforced Concrete Structures", Leu et al., 2006 describes a method called RESO which stands for refined evolutionary structural optimization. To help with the problem previously described, the RESO method filters out elements that do not carry critical stress by rejecting any element where the strain energy density is below the decided rejection ratio **RR**. It is important to not reduce too many elements at once, since it may result in a model that fails in producing the optimum topology. It is therefore an iterative process where **RR** increases with each run and is also limited by a maximum removal fraction of the elements. This continues until the defined stop criterion is reached, which is determined by the engineer.

2.4.4 Struts, Ties and Nodes

Struts, ties and nodes are designed according to Eurocode which states that struts and ties are dimensioned based on dimensioning strength in respective compression and tension. Nodes are designed based on equilibrium with an additional focus on detailing which depends on the kind of node, the incoming angles, and the stress magnitudes. (Swedish Institute for Standards, 2005, p.104-108).

2.4.4.1 Shape of Concrete Struts and Ties

The shape of struts can vary depending on the force path within the structure. Shown in Figure 2.16, the three types are prismatic, bottle and fan (Schlaich and Schäfer, 1991). Ties, on the other hand, are often defined as reinforcement and preferred in design as horizontal or vertical going lines. Although they could take the form of the shapes in Figure 2.16.

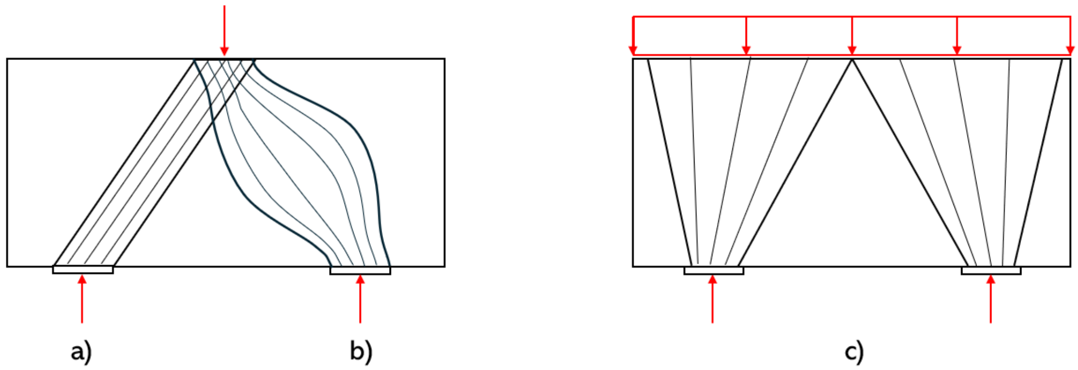

Figure 2.16: Strut shapes: a) Prismatic, b) Bottle, c) Fan.

2.4.4.2 Strength of Concrete Struts and Ties

Concrete is stronger in compression compared to tension. For concrete class C35 the characteristic compression capacity is equal to 35 MPa, compared to 2.2 MPa in tension, a capacity of approximately 6.3%. (Al-Emrani et al., 2013, p.B36-B41)

The effective concrete strut strength is given by Eurocode (Swedish Institute for Standards, 2005), and is based on a uniaxial cylinder compressive strength test. The stress limit proposed in Eurocode is defined as $f_{cs} = \alpha_e f_{cd}$ where $\alpha_e = 0.6(1 - f_{ck}/250)$ for struts subjected to transverse tensile stresses to the struts. Otherwise $\alpha_e = 1$. Other similar equations are proposed by fib, ACI and Canadian standards (Yun and Ramirez, 2016).

2.4.4.3 Strength of Concrete Struts - Experimental Study

In a research project by Yun and Ramirez, 2016, a new equation is proposed that advocates for a larger capacity of the struts than previously proposed by mentioned standards. This proposed method takes into account three-dimensional stress behavior of the pile caps along with impact from the reinforcement. The research included 115 reinforced concrete pile caps that were tested until failure, which was then compared and evaluated against the proposed equations from Eurocode among others. It was concluded that Eurocode was over-dimensioned by an average of 64% while the proposed method only 8%. The coefficient of variation for the proposed method was 24.8% and Eurocode 51.3%, both mainly deviate towards larger capacities. This entails possible large differences when designing with FEs, compared to hand calculations using STM depending on the definition of the struts ultimate strength.

2.5 The Finite Element Method

The Finite Element Method (FEM) is a powerful tool that emerged in the early 1960s (Ottosen and Petersson, 1992, p.4). It is a numerical approach that can be used to solve complex solid mechanics problems. Finite element analysis (FEA) is employed in this thesis to investigate the structural behavior of deep slabs and provide insights for their design.

2.5.1 Finite Elements

According to Ottosen and Petersson, 1992 (p.223), the first step of FEA is to choose suitable element types for the model. Note that element types can be combined and that it is important to choose the right type for the purpose of the analysis and to choose what best represents the real behavior of what is to be studied. Therefore, there is a large variety of elements.

Shell Elements
Shell elements are plane surface elements (SOFiSTiK AG, 2026a, p.2-18), that captures both membrane and bending structural behavior (see Figure 2.17). The membrane behavior is considered under plane stress conditions, where in-plane forces dominate.

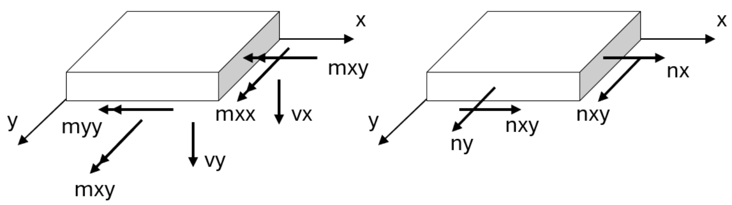

Figure 2.17: Internal forces and moments in shell elements

The theory of plates is a two-dimensional problem in three-dimensional space, an engineering approximation that is especially applicable for thin plates (Ottosen and Petersson, 1992, p.335). A single layer of shell elements can be computationally sufficient to capture the in-plane condition (Fagerström and Ekh, 2025, p.154). However, since the thesis shall conduct an analysis for a deep slab, higher-order elements such as solid volume elements are of better choice.

Solid Elements
Solid elements are three-dimensional finite elements used in structural analysis. They can be categorized into different types according to Ottosen and Petersson, 1992(p.137), such as a tetrahedral, a four-faced solid element with either four nodes or ten nodes. Or a hexahedral (see Figure 2.18), a six-faced solid with either eight nodes, or twenty nodes with additional nodes placed along the edges.

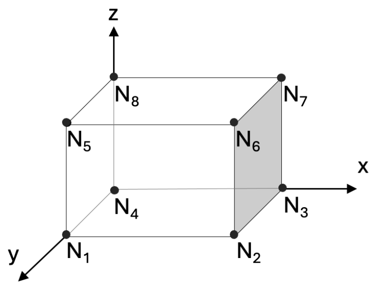

Figure 2.18: Eight-node hexahedral element

Eight-node hexahedral elements are considered low-order elements and behave analogously to their two-dimensional counterparts (Oñate, 2009, p.308). According to Oñate (2009, p.250), a three-dimensional elastic analysis is not conceptually difficult in practice compared to the two-dimensional analysis, as it can be treated as an extension of lower-dimensional theory. However, it is more computationally demanding, and it is rare to obtain exact solutions.

Beam Elements
Plane beam element consists of two nodes and is formulated according to the assumptions of Euler–Bernoulli beam theory (Oñate, 2013, p.1). Each node possesses translational and rotational degrees of freedom, typically comprising axial displacement, transverse displacement, and rotation (Oñate, 2013, p.3). The element can transmit axial forces, bending moments, and shear forces between nodes. Unlike Timoshenko beam elements, which explicitly account for transverse shear deformation, the Euler–Bernoulli beam element neglects shear deformation while still transmitting and calculating shear forces as internal force resultants required to satisfy equilibrium.

Rod Elements
Rod elements are elements in between two nodes. They are only able to transfer axial forces directly but when in larger systems they can transfer transverse forces and shear indirectly (Ottosen and Petersson, 1992, p.37). Meaning that within an element only tension or compression can occur at a time. Two subtypes to rod are truss and cable elements.

2.5.2 Pile Head Connection - FE Modeling Recommendations

In Pacoste et al., 2012 *Recommendations for finite element analysis for the design of reinforced concrete slabs*, they provide guidelines on what to include in a slab FE model and how to design the slab and its supports. The following is concluded:

- Edge and corner columns that are cast together with the slab, like all piles for the mooring dolphin, are recommended to model in the FE software.
- For modeling of supports at single points, similar to the connection between pile/anchor and slab, the recommendation is that the supports are designed as pinned with stiff couplings.

2.5.3 Shell Model - How it Worked

Figure 2.19 illustrates an approach that employs lower-order elements for the FE-modeling of a mooring dolphin. In this model, the pile cap is represented by shell elements, while the piles are modeled as beam elements.

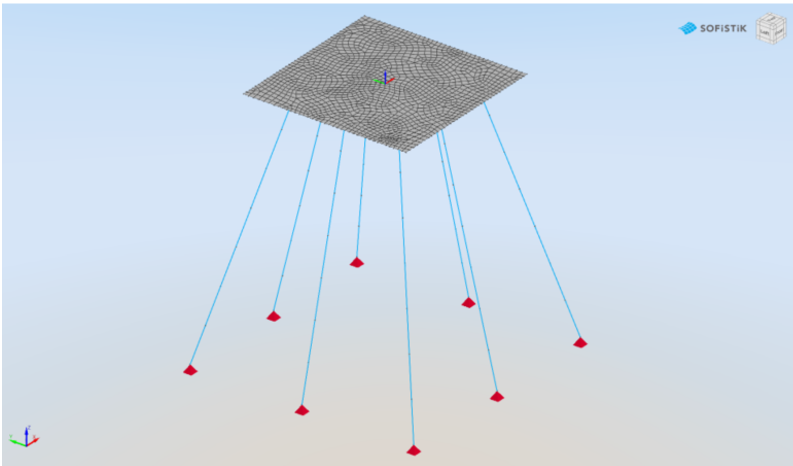

Figure 2.19: FE model of mooring dolphin using lower order elements.

The cap is assumed to behave as a rigid body, exhibiting only in-plane deformation. The piles are modeled as beam elements rigidly connected to the pile cap, while the pile toes are pinned at the bedrock level and therefore do not resist bending moments.

The primary focus of this model is on pile response, since shell elements cannot capture through-thickness stress variations. The reaction forces in the piles are evaluated under various loading conditions applied to the shell. The reinforcement is then designed separately using a two-dimensional STM.

2.6 Nonlinearity

A pile cap consists of several components that interact to transfer complex load paths and maintain structural equilibrium. Certain elements are active only in compression or tension, resulting in a nonlinear structural behavior. The following section introduces four common types of nonlinearity in solid mechanics (Kim, 2018, p.91).

Geometric nonlinearity
Geometric nonlinear effects arise from nonlinear kinematic relationships, such as strain–displacement and rotation relations. This become significant in problems involving large deformations (Kim, 2018, p.91) which could arise from heavy mooring loading.

Material nonlinearity
Refers to cases in which the constitutive relation is nonlinear, such as in visco-elasticity and elasto-plasticity (Kim, 2018, p.92). This aspect is especially important to consider when designing pile caps, as concrete cracking affects both stiffness and load distribution.

Kinematic nonlinearity
Arises when the displacement boundary conditions depend on the deformation of the structure. It is also referred to as boundary nonlinearity, with contact problems being a common example (Kim, 2018, p.95). Such a connection could be that a pile is allowed to lift, allowing positive deformation in Z (opposite the gravity direction), but is restricted to dig deeper in to the ground, negative deformation in Z.

Force nonlinearity
Force nonlinearity usually arises in addition to geometric nonlinearity, when external forces depend on the deformation of the structure. A typical example is pressure loads of fluids (Kim, 2018, p.95-96), that marine structures are subjected to.

2.6.1 Modified Newton-Raphson Method

A common approach for solving nonlinear equations is to use iterative methods. The modified Newton-Raphson method is an effective procedure for handling nonlinear systems with path (history) dependence. Each iteration produces an increment that estimates the solution and results in a residual (Kim, 2018, p.100). When the residual becomes sufficiently small according to a set tolerance limit, convergence is reached.

In this approach, the system of equations is solved using a constant tangent stiffness matrix, which leads to a more stable analysis, although convergence is slower compared to the conventional Newton–Raphson method (Kim, 2018, p.106–107)

2.7 SOFiSTiK FEA

SOFiSTiK is a FEA software with multiple applications, programs and tools. Following programs are used in this thesis to model and analyze the mooring dolphin.

TEDDY is the text editor in which all code to build the FE model is script in.

GRAPHIC is a graphical program which plots the result for the FE analysis.

VIEWER allows visualization of the model and animate the deformed structure.

SYSTEM allows visualization of the model and animate the deformed structure.

RESULT allows tabular result withdrawal from the FE model.

2.7.1 Overview Element Types

Most FE software apply elements mentioned in Section 2.5.1, but it is possible to adjust and further specify the elements. Hereby follows, the elements used within the thesis and their specific properties.

BEAM
The two noded beam element is denoted as BEAM in SOFiSTiK. Its cross section can be defined which governs its capacity to transfer forces (SOFiSTiK AG, 2026c, p.3-37).

BRIC
The solid element is denoted as BRIC in SOFiSTiK and corresponds to a hexahedral with eight nodes (SOFiSTiK AG, 2026c, p.2-5).

CABL
The two noded rod - cable element is denoted as CABL in SOFiSTiK and can be restricted to sustain only tension when implementing a nonlinear analysis (SOFiSTiK AG, 2026c, p.3-35).

TRUS
The two noded rod - truss element is denoted as TRUS in SOFiSTiK and can be assigned to take only compression along its axis by defining a tensile rapture force limit close to zero (SOFiSTiK AG, 2026c, p.(3-33)).

QUAD
The QUAD element involves plane elements such as plates and shells (SOFiSTiK AG, 2026c, p.(3-47)). SOFiSTiK implements Mindlin's plate theory (SOFiSTiK AG, 2026a, p.(2-20)), taking shear deformation into account. The plane element is generalized as a quadrilateral element (SOFiSTiK AG, 2026c, p.(2-3)).

KINEMATIC CONSTRAINTS - COUPLINGS
A coupling is a form of support condition defined by its constraint to a reference node (SOFiSTiK AG, 2026c, p.(3-22)). These provide numerically stable, infinitely stiff elements and boundary conditions, though they are limited to 1st order theory (linear analysis).

SPRI
The spring element is denoted as SPRI in SOFiSTiK, and can function as a coupling element or a support condition (SOFiSTiK AG, 2026c, p.(3-55)-(3-57)). It is defined by a principal direction, and a set of spring constants that describe stiffness in the axial, lateral, and rotational directions.

2.7.2 SOFiSTiK Stress Visualization

Stress analysis is best performed in GRAPHIC (SOFiSTiK AG, 2026b) where it is possible to make "cuts" in the three-dimensional volume model. By making BRIC cuts the stress distribution and paths can be visualized, see Figure 2.14 of a BRIC cut used to establish struts within a three-dimensional model.

3 FE Model

The FEA software SOFiSTiK was used to model and analyze the mooring dolphin. The goal of the FE model was to produce a model that exhibited realistic behavior of the structure. From the FEA, stresses were withdrawn to produce the STM.

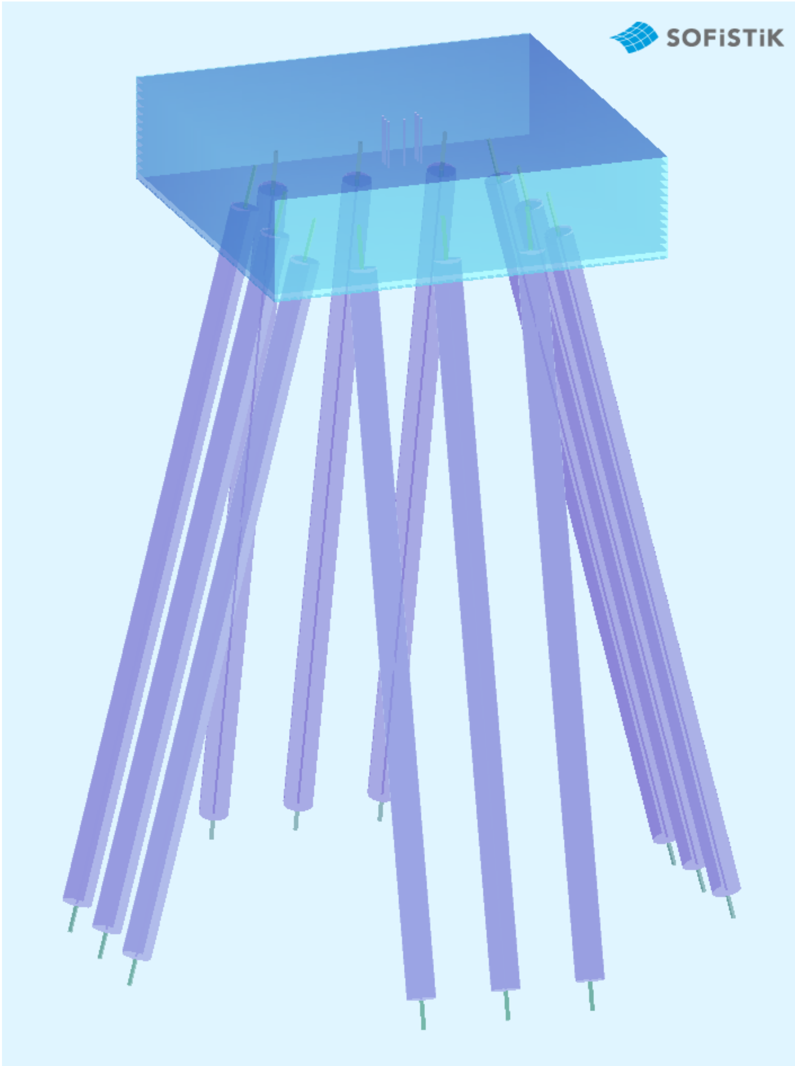

Figure 3.1: Final mooring dolphin FE model.

3.1 FE models' main Structural Elements

The FE model was divided into four different parts: pile cap, piles, anchors, and bollard. See Figure 3.1 for the main structural elements of the mooring dolphin FE model.

Pile Cap
The pile cap is a rectangular concrete slab that connects the bollard to the piles and anchors.

Piles
The purpose of the piles is to transfer compressive forces. They are attached to the bedrock and embedded in the slab. The pile head is produced and modeled with a pile compression plate to ensure that the stress distribution field is spread out onto a compression zone, to avoid stress concentrations.

Anchors
The purpose of the anchors is to transfer the tensile forces. They run from the middle of the pile cap, down to the deep bedrock. The anchor plate is modeled to ensure that the stress distribution field is spread out onto a tensile zone, this to avoid stress concentrations.

Bollard
The attachment consists of one bollard and seven bolts, designed primarily to transfer the mooring load to the pile cap. The mooring line attached to the bollard gives rise to a tensile loading, translating into both bending moments and shear forces.

3.2 Evolution of the FE Model

Developing a functional three-dimensional nonlinear FE model demanded an extensive iterative process throughout the modeling phase of this thesis. The following sections briefly describe the most significant conceptual approaches and model configurations investigated during the modeling phase.

3.2.1 Pile Cap

The pile cap was defined as a quadratic concrete slab, symmetric in X and Y to limit the possible alternative load paths from different mooring directions. The concrete material was modeled as linear elastic. Linear material behavior for the concrete was assumed to be sufficient for the objective of the thesis since a STMs truss system is recommended to follow the elastic stress field. A nonlinear concrete analysis would have required reinforcement design and modeling of the slab, as well as a significantly longer analysis run time.

Two Part Slab

In conventional pile cap modeling, the concrete beneath the pile head connection is typically neglected. In this approach, the surrounding concrete was included to analyze its influence on load transfer and potential effects on the internal stress field as mentioned in Section 2.4.1.3. The model was executed in two parts:

- The top part, involved the pile and anchor plates, and bollard attachment.
- The bottom part with holes for the piles, captured the structural behavior beneath and around the pile plate (see Figure 3.2).

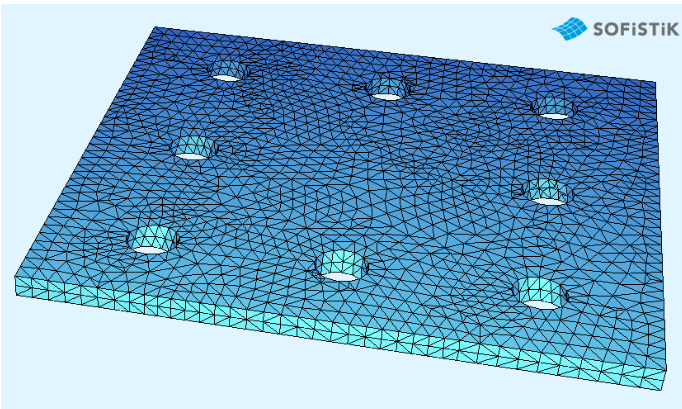

Figure 3.2: Bottom slab with holes for pile insertion.

To model a bottom slab with circular holes inclined at an angle, the meshing was done automatically by the software. The top slab, on the other hand, was meshed with systematic noding to enable identification of the nodes within the slab needed to specify where the bollard bolt, anchors and piles were connected to. Unfortunately, no manageable way to connect the slabs while maintaining each mesh was found, even after discussing the problem with the SOFiSTiK team (personal communication, 2026, 27 Mars).

One Part Slab
The one part slab is the pile cap model used for the final FEA of the mooring dolphin. The pile attachment is on the bottom side of the slab instead of 20 cm in through the bottom. Since the analysis assumes linear elastic concrete behavior, the contribution that would otherwise be provided by reinforcement in the bottom layer of the lower slab was not included. However, this was not expected to have a significant influence on the overall results. Furthermore, this modeling approach is commonly used in practice.

3.2.2 Piles and Anchors

The piles and anchors were the elements that undergone the most amount of iterations. They are two critical structural components in describing the behavior of a mooring dolphin, each assumed only to be able to carry either tension or compression and have hinged ends. To capture this behavior of the components multiple methods were executed until the final design was achieved. The first evolutions were done with an 8 pile configuration, which was the intended model for the thesis, but later on it was altered to 12, see the following *Pile Configurations and Hinged Connections* and Figure 3.3 for both pile configurations.

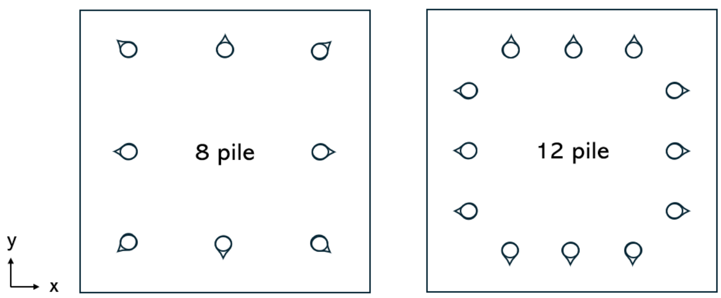

Figure 3.3: Intended 8 pile, and final 12 pile configuration.

Nonlinear Material
Since the pile and anchor should only work in compression or tension, the materials for each were defined accordingly. The material curve for the BEAM pile was designed such that it had zero capacity in tension but with strength in compression. The same was defined for the anchor BEAM but opposite, only allowing tension. BEAM were used to account for moment and shear transfer within the components.

When running the nonlinear FE analysis, the elements continued to carry both compression and tension, regardless of the defined nonlinear material properties. See

Figure 3.4 where the left side piles and anchors are both blue (in tension) while the right side piles and anchors are in red (compression). Consequently, this approach was abandoned.

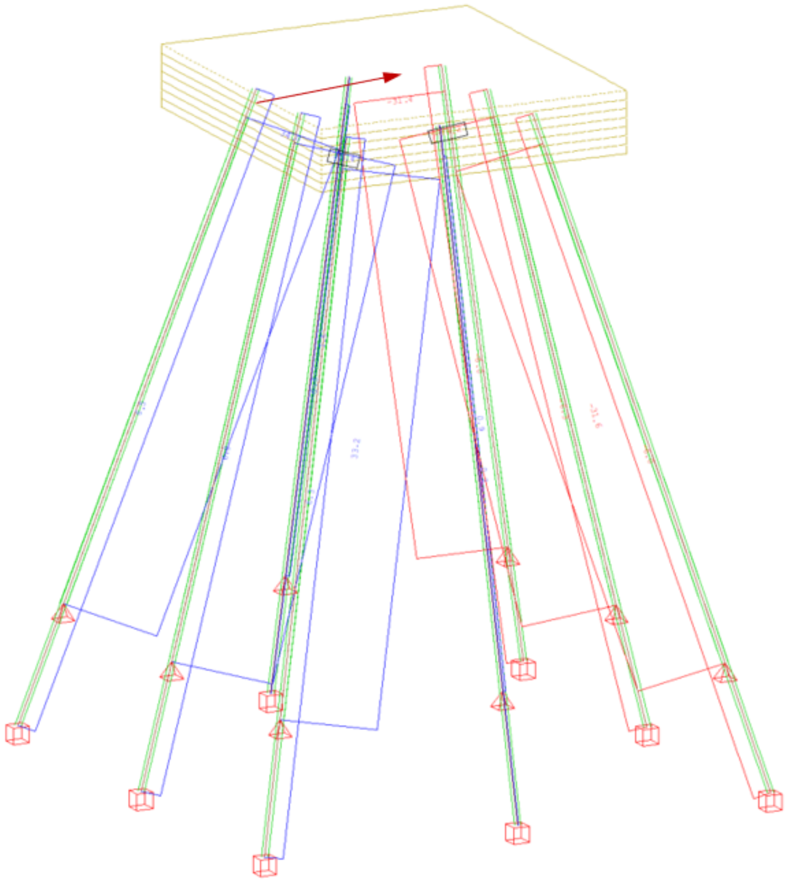

Figure 3.4: Resulting normal force in the elements from a horizontal load.

See Appendix A.1 for the specified material curves for the model in Figure 3.4.

Nonlinear Spring Elements

The second approach involved nonlinear SPRI pile elements instead of BEAM piles. The nonlinear behavior was defined by a force displacement relationship, similar to the nonlinear material, which successfully got implemented by the springs.

Figure 3.5 shows a simplified FE model of a concrete cube with a spring pile and a spring anchor.The model illustrates that the pile, represented by the shorter spring, carries compression, while the anchor carries tension as intended.

However, the application of the springs to the actual model did not succeed properly and equilibrium was not achieved. The approach also presented difficulties related to stiffness definition. In particular, it was challenging to define stiffness in directions other than the springs' axial direction, as both the piles and anchors were inclined and needed to resist global horizontal forces.

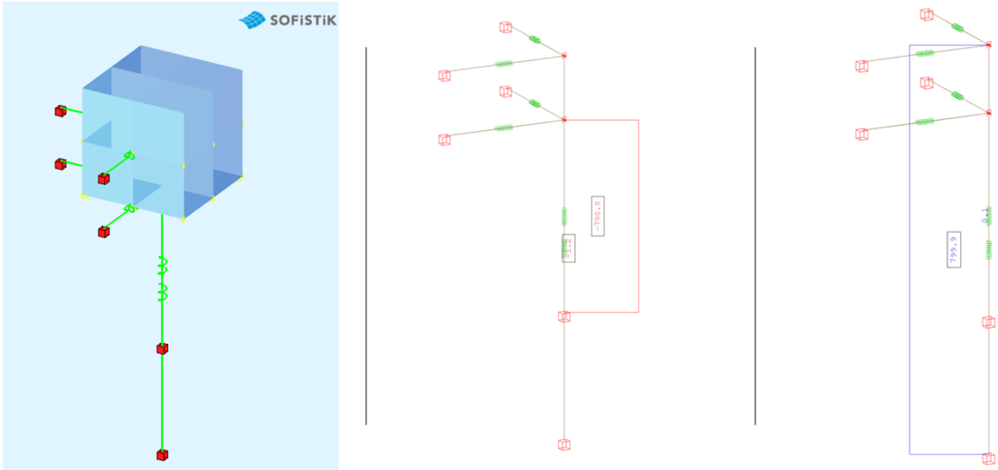

Figure 3.5: Simple geometry with nonlinear spring elements. Left: FE model. Middle: Spring under self-weight - pile spring in compression. Right: Spring under negative self-weight - anchor spring in tension.

Nonlinear Spring Boundaries
Since the components in the model include both compression and tension elements, the supports were represented using nonlinear boundary conditions. These conditions influence and regulate the kinematic behavior of the restrained elements.

To capture moment and shear transfer to the piles under self-weight, the beam elements were kept in the model. Nonlinear springs were introduced at the interfaces between the pile compression plate and the pile head, as well as between the anchor tension plate and anchor head, to control which stresses that could be transferred.

The idea of nonlinear spring boundaries was later implemented as a support condition at the pile bedrock foundation. This configuration permitted slight penetration into the bedrock while allowing for vertical uplift and limited horizontal movements. By lifting the pile and removing its property of anchorage into the bedrock, the objective was that it would ensure zero tension response in the pile from the mooring load. Although this solution worked better than previous iterations, it still showed transfer of tensile stresses, presumably as a result from the horizontal effects.

The implementations of spring boundaries were many, with up to six springs for each pile (both ends, all directions), but the desired behavior could not be replicated.

Cable Element for Anchorage
CABL elements when running a nonlinear analysis, only allow for transfer of tensile forces. This is the desired behavior of the anchors, by the defined model. Cables were kept in the model from then on for the anchorage of the pile cap.

Truss - Beam Elements for Pile
TRUS elements compared to BEAM elements are not capable of transferring moments or shear forces. With SOFiSTiKs function CRAC, a maximum allowed tensile rapture force could be defined for the TRUS elements. When set to near zero the element only works in compression, meaning that the element does not allow any tensile forces. This is only valid for nonlinear analysis.

Upon assigning the specified cross section for a TRUS or BEAM element, SOFiSTiK automatically calculates and defines all the geometrical parameters for the element, including moment of inertia and sectional areas. It was possible to manually override the cross section area to a value approaching zero. Consequently, the axial response dependent on the area was significantly reduced and left were the axial, shear and moment behavior rather than reaction magnitudes. For the mooring load case, the reactions should be zero since the load transfer in the hinged connection should in theory only translate into axial force.

For the self-weight load case, the moment and shear are dependent on the pile elements self-weight, and the model no longer needed the property CRAC since all piles would be compressed with no acting horizontal or uplift force. Additionally, the BEAM was reset to its original area and the TRUS elements could be turned off.

Pile Configurations and Hinged Connections
The 8-pile model with truss - beam piles was thought to be sufficient, but after further analyzing the internal stresses under self-weight loading, it showed signs of fixed behavior at the pile heads, see Figure 3.6. The rigid links over the pile head in both tension and compression indicate that the connection is stiff and transfer moments due to bending in the piles.

By applying SOFiSTiK condition AHIN and EHIN to the BEAM elements, one could force the ends to work as hinged connections, where AHIN and EHIN control the different ends of the beam (SOFiSTiK AG, 2026c, p.(3-38)). Subsequently, the model was unable to run and the reason was later found to be that the pile configuration was unable to fulfill the system equilibrium. This led to the final 12-pile configuration seen in 3.1, compared to the 8-pile configuration in 3.4.

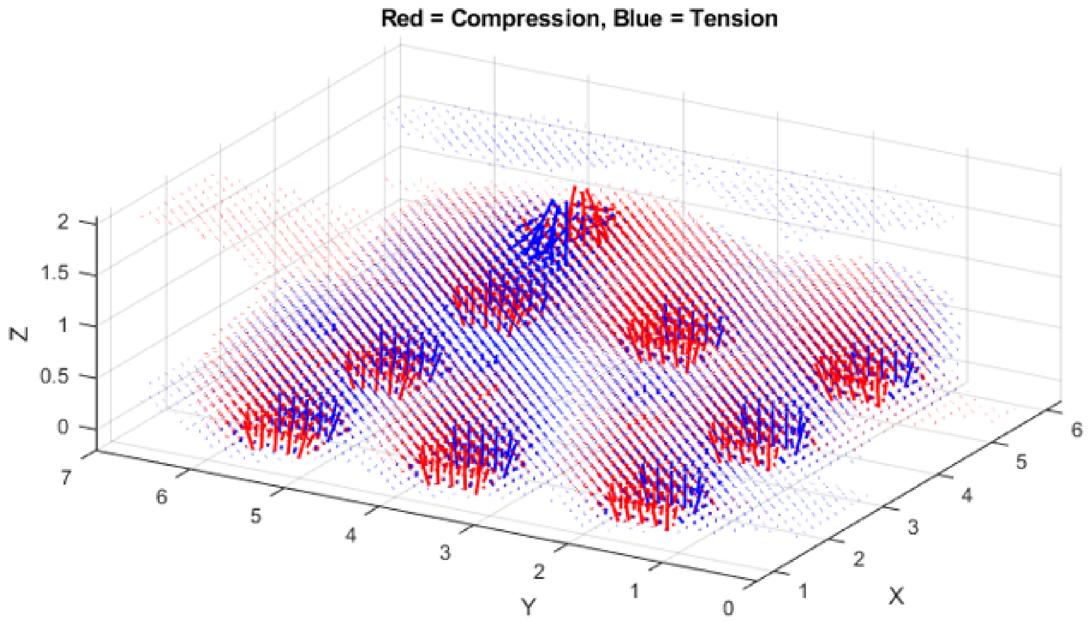

Figure 3.6: Tension and compression over the pile heads in the rigid links for load case self-weight

Truss Elements for Pile

Upon further analysis of the beam elements' capacity to transfer moment and shear forces, it was determined that their influence on the global behavior of the pile cap was negligible. Consequently, the model was reduced from Truss - Beam piles to Truss only piles. See Appendix A.2, A.3 for beam pile shear forces and moments, and A.4 for a principal stress section over the pile heads for truss only contra beam only FE models.

Pile Plate and Anchor Plate

The pile plate and anchor plate were modeled using rigid links to distribute the support force and to simulate the plates. This approach was sufficient when the connecting node (the master node) was located on another level compared to the other nodes (multiple slave nodes). For instance, the pile head, the master node is located at the pile head coordinate placed 0.1 mm below the slab underside. The links go from the master node to the slave nodes in the BRIC elements of the slab. The modeling of these connection was done with Section 2.5.2, *Pile Head Connection - FE Modeling Recommendations*, in mind.

Another approach considered during the study was the development of a bedding material. Nonlinear properties could be achieved by assigning a defined bedding material to a structural area. By controlling the directional stiffness, an area can be designed to act either in tension or compression. This approach is commonly used in foundation modeling, as it allows structural areas to be reused while introducing nonlinear properties for more advanced analyses. (Altersberger, 2019)

3.2.3 Bollard Attachment

The attachment was idealized into three main components: a bollard lever arm, seven bolts, and a connecting plate. According to Eurocode (**sve** SS-EN 1992-4:2018, p.36-37), the bolts are ineffective in the compression zone, see Figure 3.7. However, this effect was neglected in the FE model, as the primary focus of the analysis is on the global behavior of the pile cap.

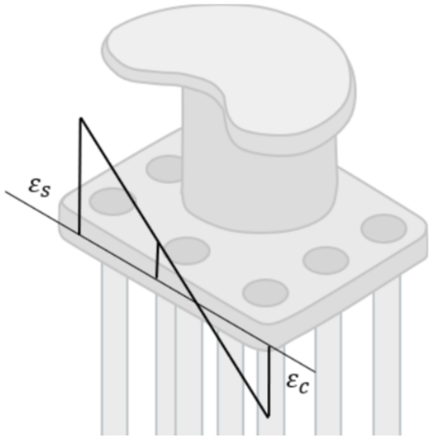

Figure 3.7: Illustration of strain distribution in the connection plate.

Since the main objective of the bollard attachment is to transfer the mooring load as pure compression or tension, the bolts were modeled using truss elements. Figure 3.8 shows the evolution of the model.

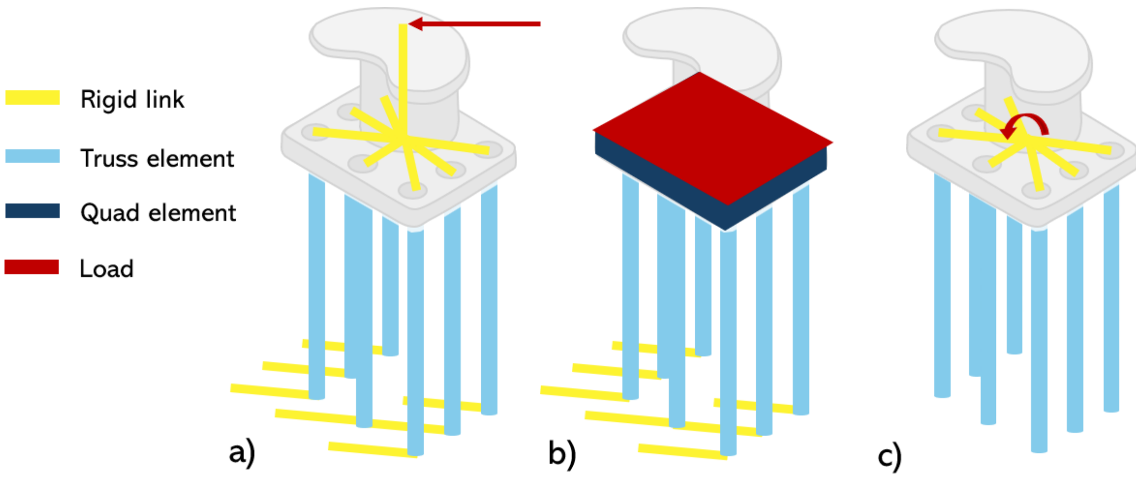

Figure 3.8: Evolution of the bollard attachment for the mooring dolphin FE model.

Bollard with Rigid Link and Lever Arm
In the first bollard version (a), the plate and the lever arm were modeled using rigid links. The TRUS elements were connected to the BRIC nodes via rigid links at their ends. However, the load transfer was not achieved as the bond between the TRUS and BRIC elements was insufficient.

Bollard with Plate
In the second iteration (b), the plate was modeled using QUAD elements, with its thickness extending down into the top BRIC layer of the pile cap. The load was applied as a moment over the entire surface area of the plate. The TRUS elements were connected to nodes within the QUAD's and had rigid links to the BRIC in the bottom end of the TRUS bolts. Despite this, the bond between the bollard attachment and the volume elements remained insufficient.

Bollard with Rigid Link and Moment - TRUS in BRIC nodes
For the final bollard attachment version (c), the connection between the bolt and load application was modeled using rigid links, centered at a separate node. The TRUS elements were directly connected to the BRIC nodes, see Figure 3.9. Although this approach had to alter the geometry of the bollard attachment, the bond was sufficient. Under horizontal loading and moment, the TRUS elements developed a tension–compression force couple, transferring the load primarily through axial tension and compression.

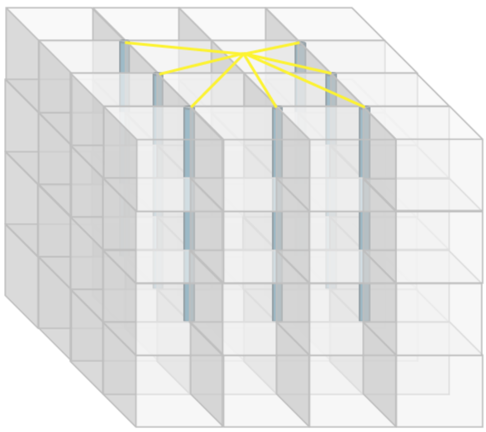

Figure 3.9: Bollard FE design connecting TRUS bolt to BRIC node

3.3 Final FE Model

The final FE model is a combination of truss, cable and solid volume elements along with support conditions and rigid links. These elements were used to model the four main structural elements mentioned in Section 3.1.

Pile Cap
The top plate is modeled solely with solid volume BRIC elements in three dimensions. It is meshed with systematic noding, allowing easy identification of nodes.

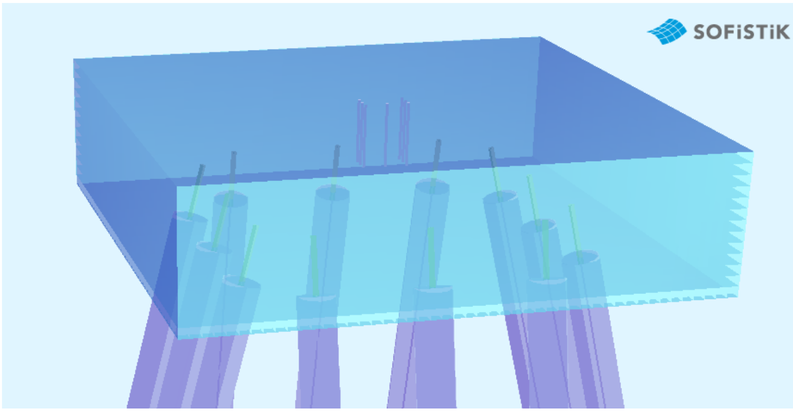

Figure 3.10: Transparent pile cap of final FE mooring dolphin model.

Bollard
This mooring dolphin has one bollard attachment consisting of seven bolts as truss element, embedded in the volume elements. The top nodes of the trusses are provided with rigid links connected to a separate middle node where the mooring load is applied as a horizontal load and a moment.

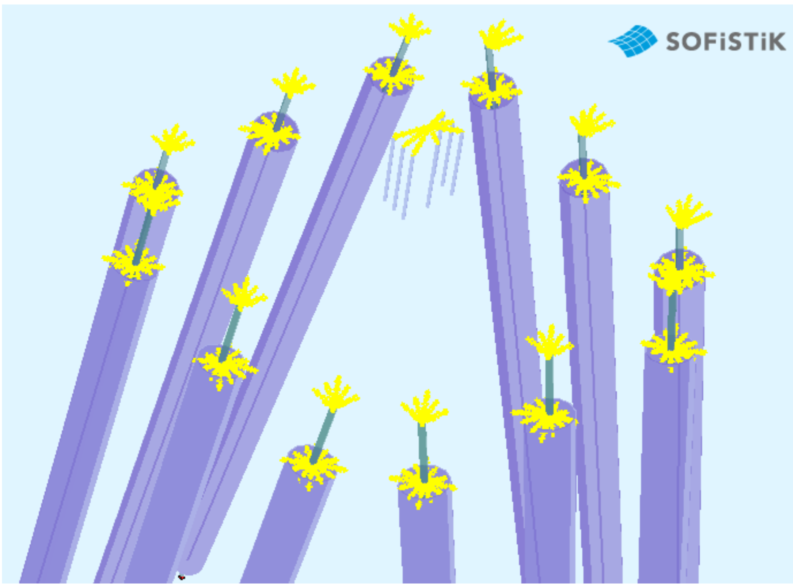

Figure 3.11: Pile cap attachments showing pile head, anchor plate and bollard plate as yellow rigid links.

Piles
There are a total of 12 piles in a symmetric configuration, modeled as compression only elements using truss elements responsible for the axial compressive response of the piles. For more information, see Section 3.2.2 part *Pile Configurations and Hinged Connections" and "Truss elements for Pile.*

The pile plate was designed with rigid links, extended from the middle of the pile head to all nodes within a range corresponding to the pile radius. This process was mesh-dependent, and the resulting distribution was therefore transformed into a quadratic pattern in the X and Y directions. The rigid link radius was rounded down for all mesh sizes which resulted in a more concentrated compression zone at the pile head. This was considered a conservative assumption as it localizes the strut forces. Furthermore, by this approach, it was hoped that the struts and ties would be more visually clear due to the higher concentrations at the pile and anchor plate nodes.

Anchors
The anchor rods are modeled as tension only elements using cable elements. For more information see Section 3.2.2 part *Cable element for Anchorage*. The anchor tension plate was modeled by the same means as the pile plate, discussed in the previous paragraph.

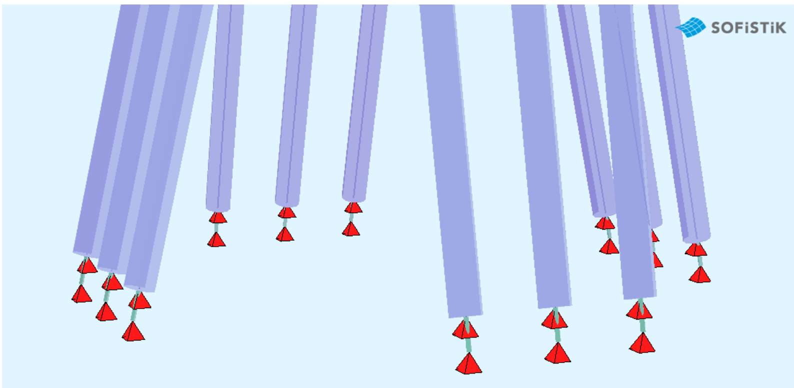

Figure 3.12: Pile and anchor hinged supports.

3.3.1 Properties

The properties of the final FE model are listed below divided into three categories: Structural component data, model plan and section, and boundary conditions. Some properties are affected by the parametric study, see Section 3.3.2.

Structural component data
The assigned properties for the FE structural elements are compiled in Table 3.1. The model is symmetric in X and Y, disregarding the bollard and mesh irregularities. All steel components were assigned a density of 7850 kg/m^3 and a E-modulus of 210 GPa which is standard of structural steel components. According to SIS (Swedish Institute for Standards, 2005, p.36), the same can be assumed for steel fasteners, and was therefore applied to the bollard bolts as well.

Structural component	Dimensions [mm]	Material
Concrete Slab	7000×7000×Note 1	C35
Pile	∅ 508, t 14.2, L 12 700	f_y 235, f_t 360 [MPa]
Pile head	approx. 508×508	-
Anchor rod	∅ 76, t 32, L Note 2	f_y 630, f_t 790 [MPa]
Anchor plate	approx. 225×225	-
Bollard bolt M42	∅ 38, L approx 800	-

Table 3.1: Material and geometry properties

Note 1: Slab height parameter varying between: 1300 mm, 1800 mm and 2300 mm.

Note 2: The anchor rod length is modeled as 12 700 mm up to the bottom part of the concrete slab. The length inside the slab depends on the parametric case: 400, 700 or 1000 mm. The rigid links (anchor head) attach to the nodes located closest to the anchor rod end, meaning that it deviates from the inner rod length depending on the mesh size.

The kidney bollard design is set to withstand the SWL of 100 tons. The mooring line has an inclination ranging from 0° to +45° and an orientation of 180° as in Figure 3.13.

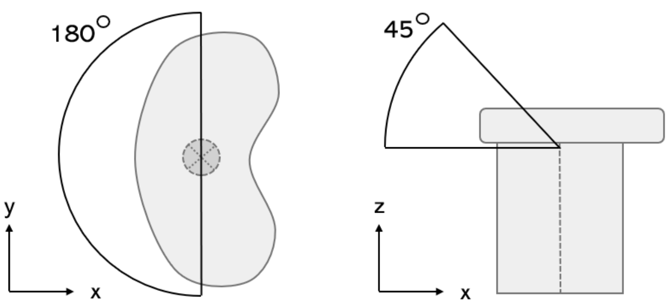

Figure 3.13: Bollard range - orientation and inclination

Model Plan and Section

In Figure 3.14 the plan shows the pile distances for the connection pile - slab, and the direction of the pile rake.

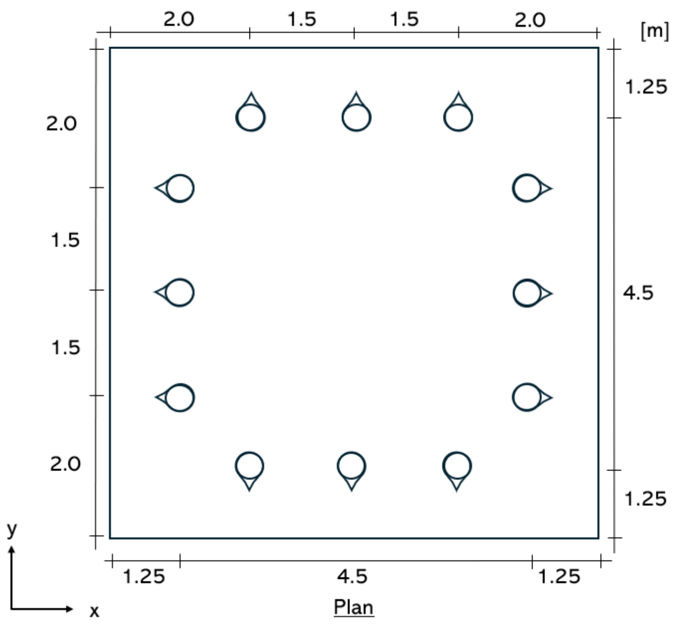

Figure 3.14: Plan for mooring dolphin model.

In Figure 3.15 the section shows the inclination of the mooring dolphin pile in addition to the load application point and the point of the neutral axis with the opposite mirrored pile. A total of six mirrored pile couples exist within the model, all with the neutral axis over the centerline.

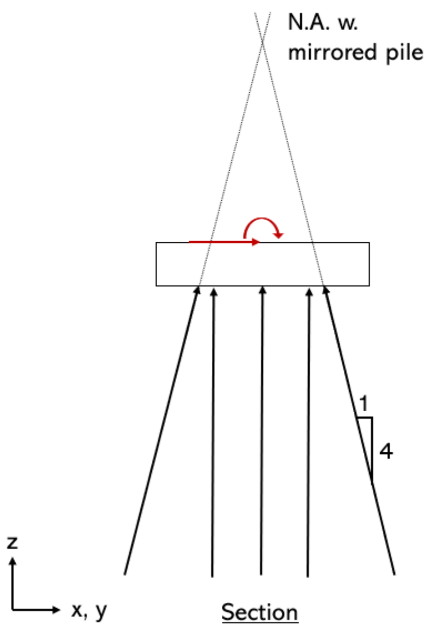

Figure 3.15: Section for mooring dolphin model.

Boundary Conditions
The support conditions have a significant influence on the analysis, as they must accurately represent the boundary conditions required to establish equilibrium and prevent rigid body motion while still describing the real behavior of the structure. Supports can provide stiffness through both translational and rotational constraints (Pacoste et al., 2012, p.9,). Boundary conditions are compiled in Table 3.2.

Connection	Structural element	First end	Second end
	Pile	Concrete Slab: Pinned	Bedrock: Pinned
	Anchor rod	Concrete Slab: Pinned	Bedrock: Pinned
Coupling	**Rigid link group**	**Element**	
	Pile Head	Pinned	
	Anchor Plate	Pinned	
	Bollard	Pinned	

Table 3.2: Boundary conditions for mooring dolphin FE-model

3.3.2 Parameters

Two parameters were studied in the thesis which are visualized in Figure 3.16 and collected in Table 3.3. These were selected due to their influence on the stress field, the strut-and-tie design, and the possibility to make the dimensioning choices in mooring dolphin design.

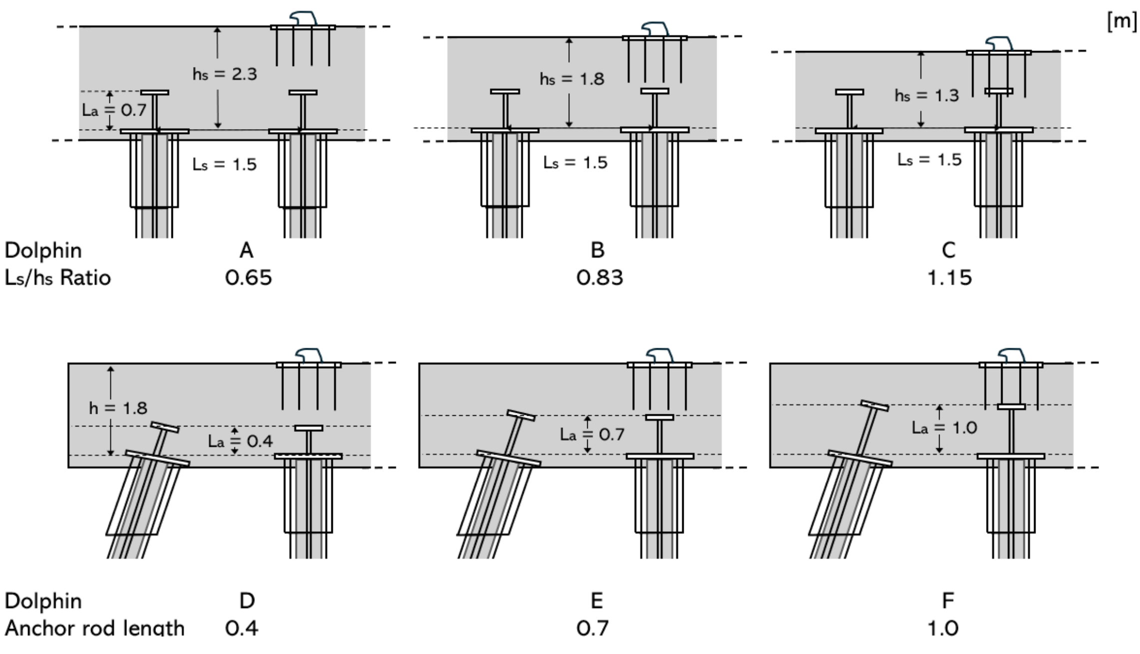

Figure 3.16: Parametric models A-F to be studied in the thesis.

Parameter			
Slab thickness	Model	L_s [m]	L_s/h_s
	A	2.3	0.65
	B	1.8	0.83
	C	1.3	1.15
Anchor rod length	Model	L_a [m]	
	D	0.4	
	E	0.7	
	F	1.0	

Table 3.3: Parametric values for Models A-F.

The L_s/h_s ratio is the depth - span ratio of the pile cap in between the piles and is directly dependent on the slab height h_s. This ratio is a decisive factor in the formation of D-regions and the internal stress distribution. In this thesis the ratio was directly controlled by altering the slab thickness L_s. This is further described in Section 2.4.1.2.

The anchor rod length L_a is of interest due to its direct impact on the length and angle of the compression struts, as the struts and ties are assumed to terminate at the anchor plate located at the head of the rod.

3.4 Pile Cap Mesh

The mesh is predefined as symmetric with hexahedron 8-node elements of the same size. This decision was based on the possibility to locate the nodes and elements and the mesh is therefore generated with a loop and not automated by the software. An automated mesh or a more refined meshing method could produce a denser mesh at regions where the stress varies more significantly, which could improve the representation of the true behavior. However, this is more important for local analysis, and the scope of the thesis is limited to the global structural behavior of the mooring dolphin.

The mesh size was selected based on three criteria: convergence, analysis run time, and the ability to visualize the stress field. The convergence analysis ensures that the mesh accurately represents the stresses in the FE model. The time factor ensures that the analyses do not disturb the workflow. Finally, the ability to visualize the stress field ensures the possibility for the data to be of use for the strut-and-tie modeling.

The analysis checked is nonlinear with 10 iterations and a tolerance of 0.001 for the self-weight of the concrete pile cap.

3.4.1 Convergence Analysis

The convergence requirement was defined by (Ottosen and Petersson, 1992, p.91) as when the approximated FEA solution approaches the exact solution. In other words, a FE model with an infinite number of elements. Six different mesh sizes (see Table 3.4) were evaluated for two cases: using all BRÌC nodes in the model and using a nodal strip of the model. This approach was adopted to reduce the influence of stress singularities near load application points and supports, which could otherwise introduce variability into the results.

Table 3.4: Structured mesh sizes and corresponding total number of nodes

$n_x \times n_y \times n_z$	Number of Nodes
19×19×5	1805
29×29×8	6728
39×39×11	16731
49×49×14	33614
69×69×20	95220
99×99×25	245025

Von Mises Stress Convergence
The stress used in the convergence analysis is the average nodal von Mises stress. Von Mises stress is a common choice for this analysis (Dowling, 2013, p.298) since it only measures the stress magnitude and is non dependent of direction. The stresses were withdrawn in Pa to reduce risk of rounding errors when transferring larger prefixes, since the sum is used to calculate the average nodal stress.

The average stress was calculated both globally for all nodes in the concrete slab (Figure 3.17) and for a strip (Figure 3.20) in the top of the slab between the edge and the bollard to avoid areas of high stress sensitivity. In the global case for all BRIC nodes, it was assumed that the mesh converged at 16 731 nodes and converged/oscillated around 60.5 kPa.

However, when analyzing the von Mises stress for all nodes, stress peaks appeared at nodes corresponding to the initial Z-layers, see Figure 3.18. Since these peaks deviate significantly from the remaining stress values, they strongly influence the calculated average. Consequently, a convergence analysis based solely on the average von Mises stress was not sufficient.

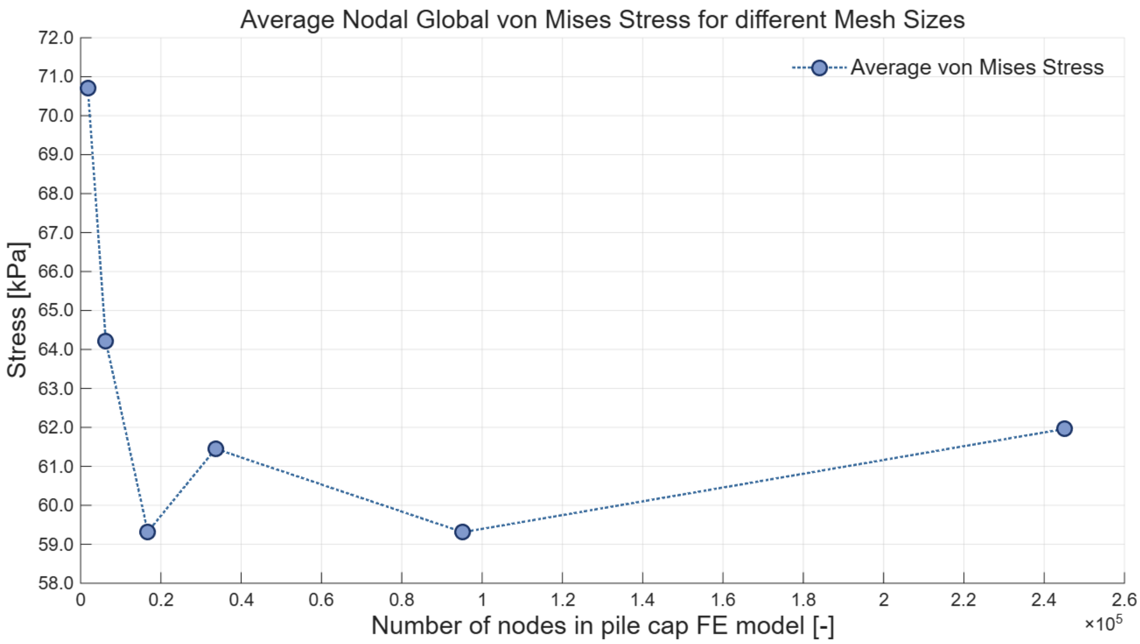

Figure 3.17: Average von Mises stress for all BRIC nodes for the self-weight analysis with different mesh sizes

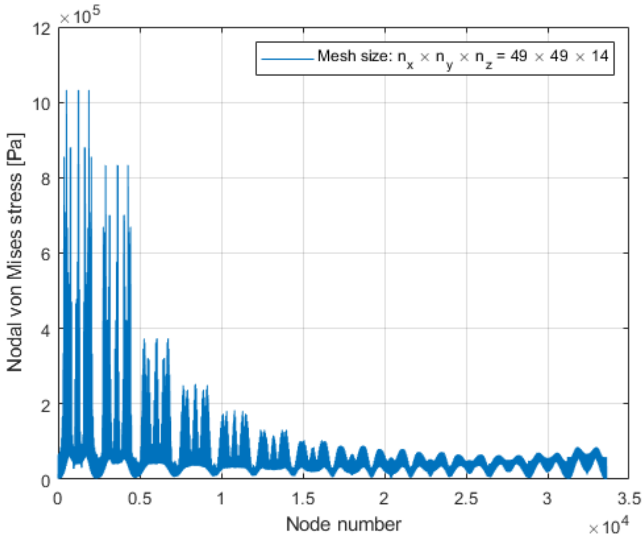

Figure 3.18: Nodal von Mises stress for a mesh size of 49×49×14

The deviation in stress is strongly influenced by the boundary conditions of the cross section, leading to stress localization around the piles where rigid links are present. Higher stress values were there for observed at the initial Z-levels, recognized for six different mesh sizes (see illustrations in Appendix A.3).

An alternative measure that complemented the global convergence analysis was the evaluation of a nodal strip. This approach was based on a suggestion by C. Pacoste et al. (Pacoste et al., 2012, p.9), who recommends assessing a more stable region such as an area away from the supports. As shown in Figure 3.18, the values appeared to stabilize at the top of the pile cap. This led to the selection of a nodal strip located at the top of the pile cap along the X-axis, running between the supports and away from the bollard (see Figure 3.19).

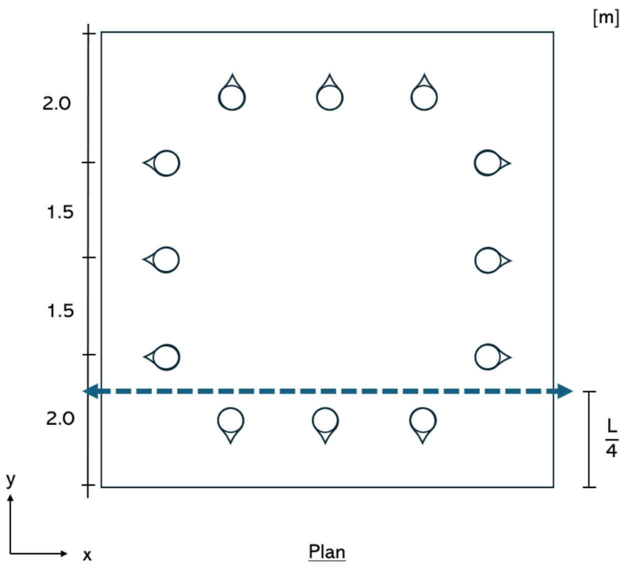

Figure 3.19: Location of nodal strip in top BRIC nodal layer, see dashed blue line

For strip analysis multiple meshes are checked with equal numbers of nodes in X and Y, and about 27% of that in Z due to the geometry, achieving close to cubic elements. Figure 3.20 for the strip analysis confirms the global analysis that the mesh converges around 20 000 elements. Similarly to the global analysis, the resulting average stress oscillates, but for a value of 67 kPa.

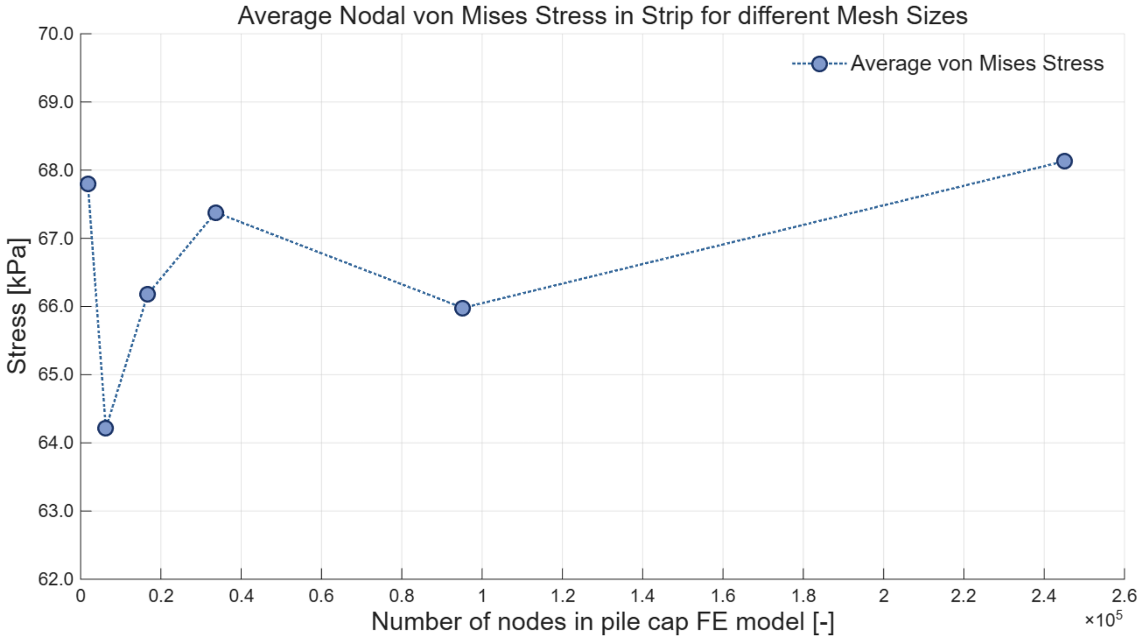

Figure 3.20: Average BRIC nodal von Mises stress for a nodal strip for the self-weight analysis with different mesh sizes

From Figures 3.17 and 3.20 it was concluded that the mesh is not hyper sensitive to the tested mesh sizes since all, except 19×19×5 and 29×29×10, remained within a reasonable range. The remaining mesh sizes were determined as converged.

3.4.2 Analysis Run Time

Time was an important factor for the analysis since it heavily impacts the workflow.

When the FEA was simulated, the computer was set aside to solely focus on the analysis, ensuring equal conditions. The analysis was performed multiple times for the same FEA to examine if time deviated from run to run. It was discovered that the analysis time was very similar and therefore no average run time was calculated.

Figure 3.21 shows that the run time increased exponentially to the number of nodes for the BRIC pile cap, with the most dense mesh reaching a run time of 3.5 h, while the coarsest mesh only took 4 s.

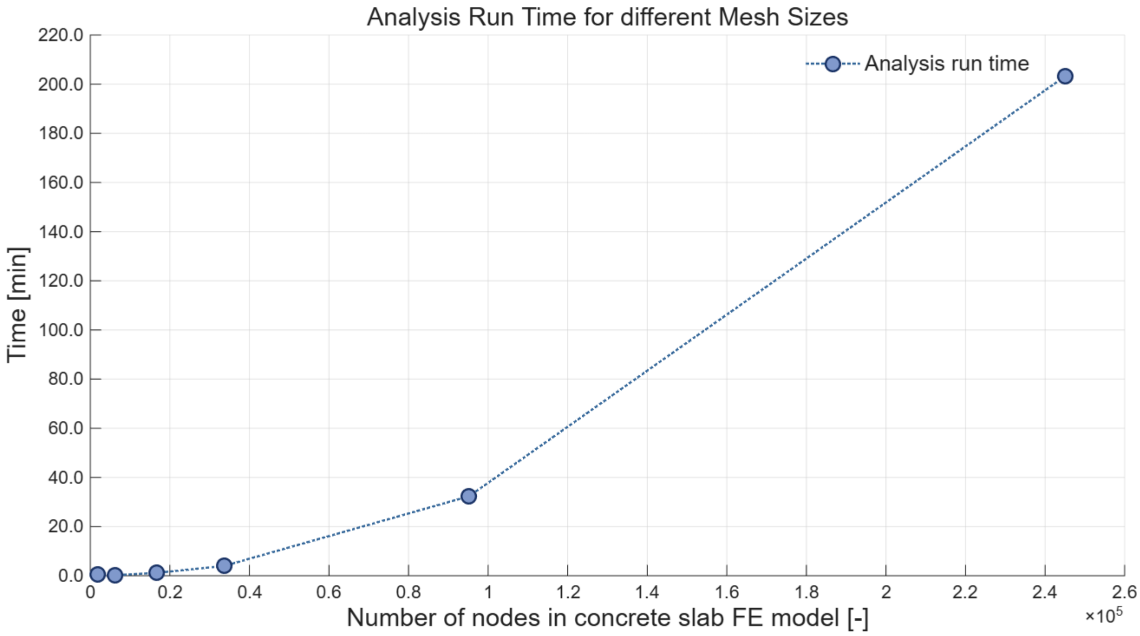

Figure 3.21: Run time for self-weight analysis with different mesh sizes

The run time for meshes 99×99×25 and 69×69×20 both exceeded 30 min which was deemed too long and a disturbance risk to the workflow. Note that for the parametric analysis, multiple load cases and models were analyzed, resulting in a much longer total analysis time. The analysis time of the mooring load cases combined with self-weight also exceeded that of the self-weight load case which was assessed in the run time analysis.

3.4.3 Stress Field Visualization

Accurate representation of the stress field was essential, as the thesis objective relied on determining the load paths and force magnitudes required to establish the STMs. The three-dimensional stress field visualizations were generated in MATLAB as stress field plots, which enabled the identification and configuration of the struts and ties.

Three plots were generated to o conduct a visual plausibility study, each showing the minimum principal nodal stresses (σ_3) for the self-weight load case. The results were compared for coarse, intermediate, and dense mesh discretizations, characterized by $n_x \times n_y \times n_z$.

- 19×19×5 (Figure 3.22)
- 49×49×14 (Figure 3.23)
- 99×99×25 (Figure 3.24)

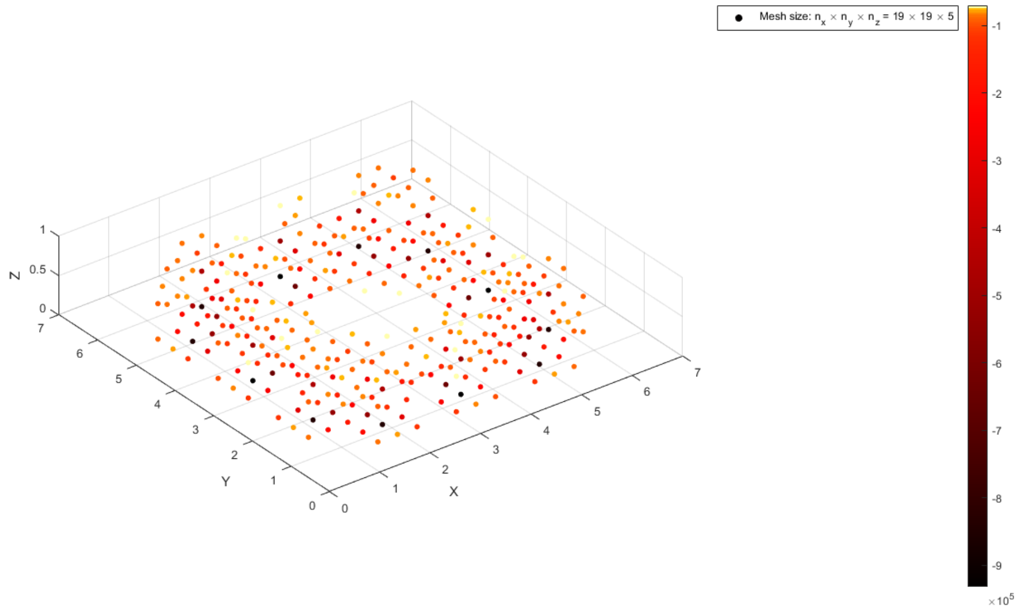

Figure 3.22: Principal nodal stress σ_3 [Pa] for coarse mesh

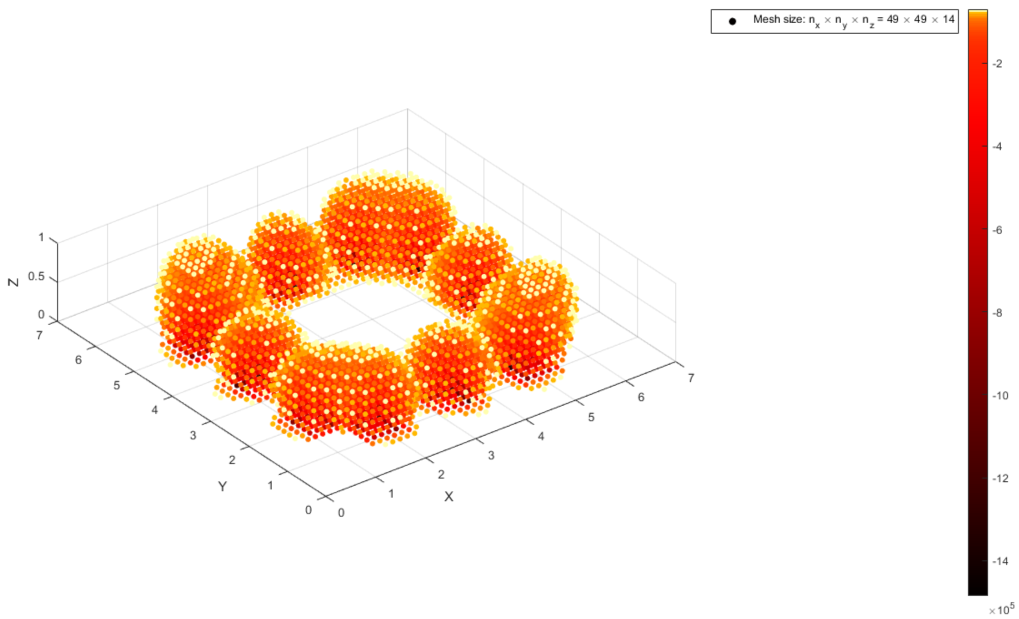

Figure 3.23: Principal nodal stress σ_3 [Pa] for intermediate mesh

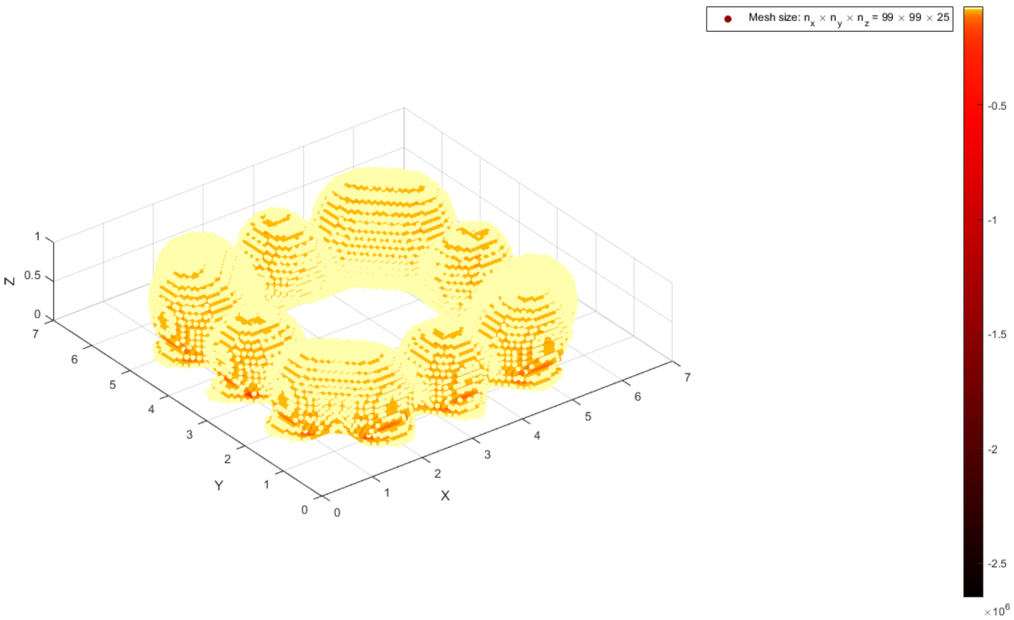

Figure 3.24: Principal nodal stress σ_3 [Pa] for dense mesh

The results showed that both the coarse and dense mesh do not provide optimal visualization. The coarse mesh lacked sufficient resolution while the finer mesh with a larger amounts of nodes tended to obscure the view of each other. The intermediate mesh provided the best result, offering sufficient resolution while maintaining clear identification of the strut-and-tie behavior. However, applications could be applied and utilized for the most dense mesh to either reduce the number of plotted nodes or to filter for specific nodes, allowing the interpreter to study the internal stress field.

3.4.4 Final Mesh Size

The final mesh size was decided to the 49×49×14 with a total number of 33 614 nodes. It is argued that this mesh size was best suited for the thesis based on the three parameters: convergence, analysis run time, and stress field visualization. The 49×49×14 mesh was able to visualize the stress field satisfactorily without taking an excessive amount of time. The average von Mises stress for both the strip and the global analysis was also close to the densest mesh for both analysis, and to the oscillated values.

3.5 Verification

To use the model, it had to be verified. Since it is difficult to predict how stresses and loads act and transfer within the slab, the verification was heavily based on engineering intuition and plausibility assessments of the model.

Support reactions for the self-weight load case should equal the applied self-weight and the piles should contribute symmetrically to the configuration. The reaction forces were calculated and compared to the FE-result (see Appendix A.8). Table 3.5 shows that the reaction force (see Figure 3.25) corresponds to the dead load of the structure and indicates that the model behaves as expected.

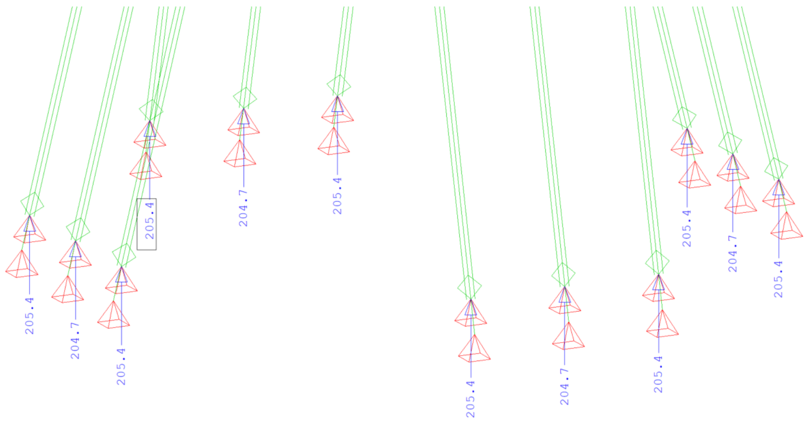

Figure 3.25: Reaction forces, global Z, in piles for slab thickness 1.8m.

	FE result	Hand calculation	*Comment*
Support reaction per pile	205 kN	-	
Dead load for 1/12 of slab	-	185 kN	
Dead load for one pile	-	22 kN	
Total	205 kN	207 kN	*OK!*

Table 3.5: Reaction force verification for slab thickness 1.8 m

Structural engineers H. Mazaheripour and H. von Kraemer (personal communication, 2026, 24 Mars) with knowledge in mooring dolphin design, assessed the global displacement of the pile cap when loaded by a mooring load of 1000 kN (load case a). It reached a displacement of approximately 67 mm (see Appendix A.4) which was deemed reasonable compared to similar dolphins under the same type of loading.

The mooring dolphin's global behavior was analyzed for multiple different load cases. With the structural behavior amplification turned up, the aim was to see expected bending, deflection, and displacement of the structure as a whole. All models analyzed were deemed to act in a realistic and expected way.

3.6 Load Cases

A mooring dolphin is subjected to various loads, see Section 2.3.4 of which two are included in the study: mooring load and self-weight.

The mooring load was applied to the bollard at the connection point of the rigid links. Four different load directions were analyzed, see Table 3.6 and Figure 3.26.

Load Type			
Mooring load	Magnitude	Inclination	Orientation
a	1000 kN	0°	0°
b	1000 kN	0°	45°
c	1000 kN	45°	45°
d	1000 kN	45°	0°

Table 3.6: Mooring load cases applied in SOFiSTiK

Self-weight was applied for all elements within the FE model and combined with the mooring load cases a-d.

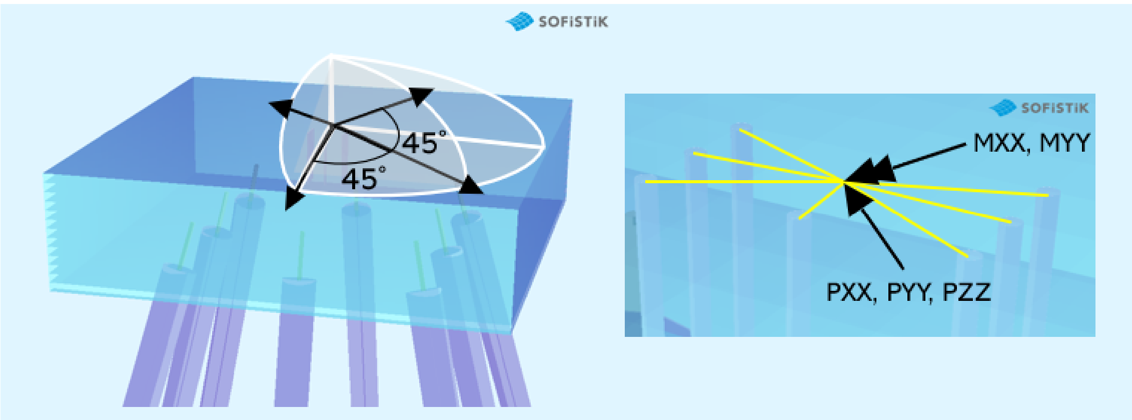

Figure 3.26: Mooring load application.

3.7 Principle Stress FE Analysis

The analysis was performed in the program "general static analysis ASE" available in TEDDY. The analysis was executed as nonlinear through NONL which considers nonlinear springs, cables, and truss elements. It allows cables to fail in compression, trusses to fail in tension through CRAC and worklaw for springs, allowing lift in pile while remaining the compression strength.

Geometric nonlinearity, and thus second-order effects arising from deformations, were not included. These modeling assumptions were considered appropriate for achieving a reasonable representation of the physical behavior of the mooring dolphin in the finite element model.

The analysis produced a result file in RESULT which enabled the withdrawal of principal stresses. These were transferred to Excel and MATLAB for processing and evaluation. In addition to providing result files, the program enabled the results to be studied directly within the model using SOFiSTiK programs, mainly GRAPHIC.

4 Strut-and-Tie Modeling

The strut-and-tie modeling was done with a custom computational script in MATLAB which allows the engineer to adjust which principal stresses to be visualized within the structural model. From the internal principal stress tensors, struts and ties could be determined.

The script was used to analyze the six different parametric cases seen in Section 3.3.2. Each case was further analyzed for four different mooring load cases combined with self-weight, see Section 3.6.

With the stress field as the basis, struts and ties were sketched in the three-dimensional model. The field was simplified into red dashed lines for compressive struts, and blue solid lines for ties. These aim to describe and visualize the general stress field and how the STM configuration could be established. Note that the proposed ties follow the tensile load path and are not placed strictly in the vertical or horizontal direction.

4.1 Stress Field in 3D

The following six stresses, $\sigma_x, \sigma_y, \sigma_z, \tau_{xy}, \tau_{xz}, \tau_{yz}$, were extracted from the tabular RESULT application to calculate the principal stresses for all nodes in the model. Compared to the convergence analysis, the principal stress was used for the stress field visualization and strut-and-tie identification to enable analysis of both the magnitude and direction of the internal stress tensors.

The principal stress field has three stresses in each node, $\sigma_1, \sigma_2, \sigma_3$, all perpendicular to each other. Consequently, the stress field is hard do interpret and therefore in need of processing. This was achieved by applications within the custom computational script, referred to as the "stress visualization tools".

4.1.1 Stress Visualization Tools

Different tools were implemented into the custom computational script to make the internal stress field more accessible for the interpreter.

Tension or Compression

σ_1 is the largest principal stress in the node, usually positive and plotted for tensile stresses. σ_3 is the lowest, usually negative, and plotted for the compressive stresses. Since the principal stresses are sorted from the highest to the lowest value, it is possible for σ_3 to include tensile forces, if a node is completely in tension in all three local directions. Therefore, the stresses were sorted to ensure either only negative (compression) or positive (tension) values.

As mentioned previously, a node could experience compression or tension in multiple directions, therefore σ_2 was also studied to see the possible impact on the direction and magnitude of the resultant stress. It was noted after sorting σ_2 by compression or tension, that it had little impact on the behavior of the global stress field. σ_2 appeared more around supports and the bollard, where the stress magnitude and concentrations were higher, even so for σ_1 and σ_3.

Stress Threshold

The stress threshold was not set to a specific value, but was altered depending on the area of interest. Some struts were more prone to be visualized for a set tolerance, while other minor struts weren't visible at all.

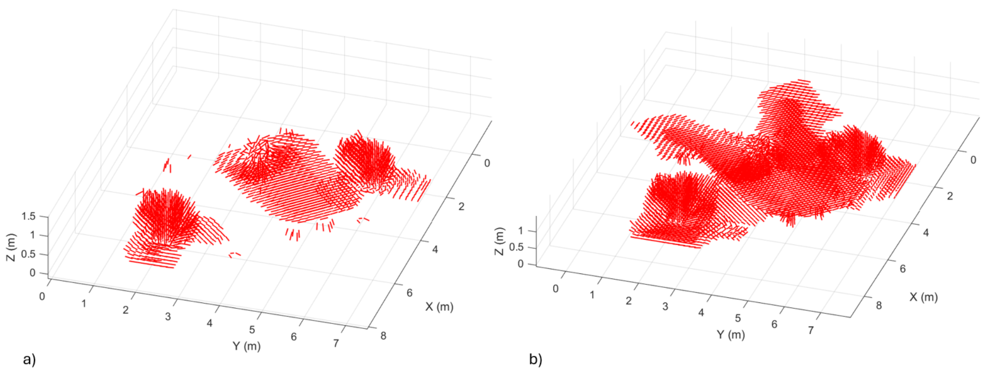

Figure 4.1: Different stress thresholds for the same parametric and load case - tensor plot. a) Threshold 8e5 Pa, b) Threshold 6e5 Pa.

Due to stress tolerance being a tool used to work with the model rather than a set limit, it was important to be consistent in deciding which stresses were to be neglected. Some struts or ties were needed to fulfill node equilibrium and could therefore not be ignored, consequently lowering the threshold value. It is important to include struts and ties of the same magnitude elsewhere in the current model to avoid biasing certain stress paths.

Cut and Skip

Two other tools that were used to visualize the internal stress field are cut and skip. Cut was used to display specific sections or parts of the model, removing stresses, which otherwise obscured the view of the interior model. Examples could be that the bottom half of the stress field was plotted or a strip in the middle of the pile cap. Skip was used to dilute the mesh, by plotting every second or forth nodal stress, etc.

Plot Type

Three different plot types were used to interpret the stress field: The tensor plot, the magnitude tensor plot and the magnitude plot, see Figure 4.2 where they are all plotted with the same threshold.

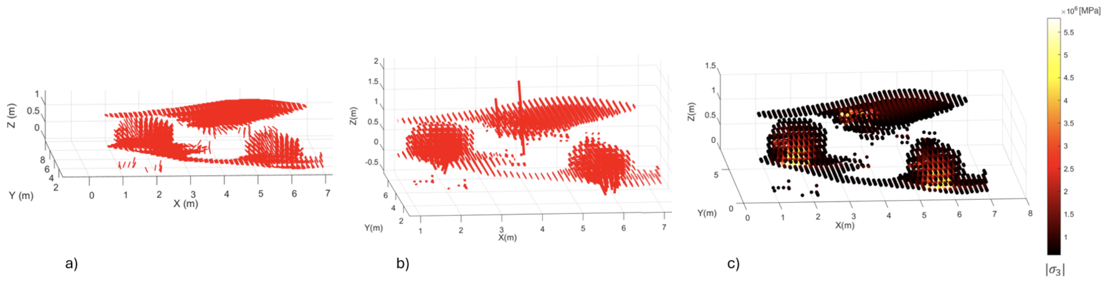

Figure 4.2: Plot types: a) Tensor plot, b) Magnitude tensor plot, c) Magnitude plot.

The tensor plot (a) shows the direction of σ_1 or σ_3, depending on the chosen principal stress. It is independent of stress magnitude, meaning that each principal direction is represented by a line segment of constant length. This makes it a useful tool for visualizing the stress flow and the orientation of the principal stress field within the pile cap. The main advantage of this representation is that all tensors are given equal visual weight, which allows the overall stress direction field to be interpreted clearly without being influenced by variations in magnitude.

The magnitude tensor plot (b) also represents the direction of σ_1 or σ_3, but in this case the vector length is scaled according to the magnitude of the corresponding principal stress. This provides additional information compared to the pure tensor plot, as it highlights not only the stress directions, but also where higher or lower stress magnitudes occur. As a result, it is an effective way to visualize both stress concentrations and stress flow paths simultaneously.

The magnitude plot (c) visualizes scalar principal stress fields, such as σ_1, σ_3, $|\sigma_3|$, at nodal points within the structure. Unlike the tensor-based plots, it contains no directional information and is therefore independent of stress orientation. Instead, stress values are represented through a color-mapped distribution, which enables clear identification of stress concentrations within the stress field.

4.2 Interpretation of the Stress Field

The interpretation of the stress field was carried out through an iterative process involving the use of stress visualization tools, the identification of nodal locations, assessment of equilibrium conditions, and discussions with experts within the subject. It is important to work consistently with the stress tolerance threshold to ensure that the designing engineer is consistent in what struts and ties are represented in the STM.

As stated in Section 2.4.4.2, according to Eurocode, the concrete capacity should decrease when subjected to transverse tensile stresses, a stress behavior that frequently occurs in the mooring dolphin stress fields. What the study by Yun and Ramirez, 2016 suggests is that the reduction in concrete strength is not as pronounced in pile caps as assumed by Eurocode and other design standards. Note that even with the strength reduction that of Eurocode, the tensile capacity is still far below that of compressive capacity, which is why the tensile stresses are of the utmost importance when analyzing the stress field and mapping the STMs.

The nodes, when not located in a pile head, anchor head or bollard, are placed depending on the following: change in direction of the stress tensors, equilibrium in nearby connected nodes, and zonal stress peaks. Note that the model is meant to understand the general stress flow, still the integrity of the model is important, therefore, equilibrium in nodes is prioritized over the exact representation of tensor direction or stress magnitude.

4.2.1 Expert Input

As already mentioned, STM design is heavily based on experience and intuition of the assessing engineer. Therefore, the model was discussed with experts in the subject. Hadi Mazaheripour, doctor of engineering and experienced in mooring dolphin pile cap design and Karin Lundgren, professor in Concrete Structure at Chalmers University of Technology. When discussing the stress fields with the experts it was ensured that they were both provided with the same information about the model and stress field, and they were asked the same questions, to reduce the risk of influencing their answers.

H. Mazaheripour (personal communication, 2026, 12 May) emphasizes that the tensile strains are of most importance since concrete is weaker in tension. Meaning that these areas need to be reinforced for the structure not to fail under heavy loading. Therefore when identifying the struts and ties, ties will be of high importance to identify. Consequently, the ability to visualize the ties could govern which stress tolerance to apply.

H. Mazaheripour also expected to see struts forming between the anchor tension plate and the pile compression plate. These could be identified in the stress field plots, see Figure 6.2 and 6.3. What H. Mazaheripour did not expect was that the struts and ties took the shape of roof trusses, to the upper side of the pile cap from the heads of the piles and anchors.

Prof. Lundgren (personal communication, 2026, 29 April) on the other hand, expected that something similar to roof trusses could appear before seeing the actual stress field. The theory could be confirmed by analyzing the stress tensor plots, see Figure 6.2. In discussion with Prof. Lundgren it was also decided to ignore the local stress concentrations under the anchor plates, assuming that these stresses could reach equilibrium independently from other struts and ties in the system, and since the focus is on the global behavior of the mooring dolphin.

4.2.2 Strut-and-Tie Representation

The compressive and tensile stresses when identified, were represented by struts and ties, respectively. These are simplified and follow the global general stress field. Struts are represented by dashed red lines while ties by solid blue lines. Two different line widths were used to highlight the magnitude/size of the stresses, and/or to visualize which load direction is dominant for a certain node. The wider line widths are more dominant struts or ties and the process of deciding which strut/tie to widen was done through analyzing the stress field and discussing what needed to be highlighted in the STM. In order to understand the strut-and-tie magnitudes it is recommended to look at the stress tensors in the live plots to better grasp the intention of the line width.

The piles and anchors are also a part of the STM as load application points where the pile are acting on, towards the slab like struts and are therefore represented by a darker shade of red. The anchors are acting away from the slab, acting as ties, and therefore represented by a darker blue. The supports are sized depending on the pile-, anchor reaction forces showing which are under the highest normal force magnitude. Reaction forces for all models A-F and load cases a-d can be found in Appendix A.5

5 STM Result

The following 10 STMs were configured for parameters in Section 3.3.2 and load cases in Section 3.6. Note that parametric models B and E are the same and that for all models the STM was identical between load cases a and d, and b and c, resulting in a total of 10 models. Therefore, only figures for load cases a and b are included in Chapter 5 with the remaining STMs in Appendixes A.6 and A.7. All models can be found in our GITHUB folder as live plots, where it is possible to rotate and inspect the MATLAB figures of the three-dimensional STMs and alter the stress field.

As mentioned in Chapter 4, the struts and ties are represented by lines. Note that by the lines alone one cannot judge the magnitude or shape of the struts but one must look at the tensor plot and magnitude plot for the case of interest. In some cases a strut is represented by one line and sometimes two if needed to fulfill equilibrium in nearby node. It should not be assumed that the magnitude of that strut is necessarily larger, but that the additional lines still represent the direction of the stresses. On the other hand, if a strut or tie is made thick it signals that it is a major stress path.

As mentioned previously, mooring dolphins are exposed to numerous loads from all directions. This entails that the pile cap can deform, strain, and crack possibly everywhere. Therefore, reinforcement is placed along all sides of the rectangular concrete block to reduce the widths of the cracks. These are not necessarily represented by struts or ties within the STMs but note that they are taken into consideration and that they are of great significance.

5.1 Load case a & d

Note that a and d have the same configuration with altering inclinations due to the different anchor length and slab height. The models A-F remain similar with identical node linkage for models B, C, D, E. With model A having additional struts from the bollard to the compressive piles and model F additional struts from the back end middle pile plate towards the two closest active pile plates. See following Figures 5.1, 5.2, 5.3, 5.4 and 5.5 for STM for models A-F and load cases a and d.

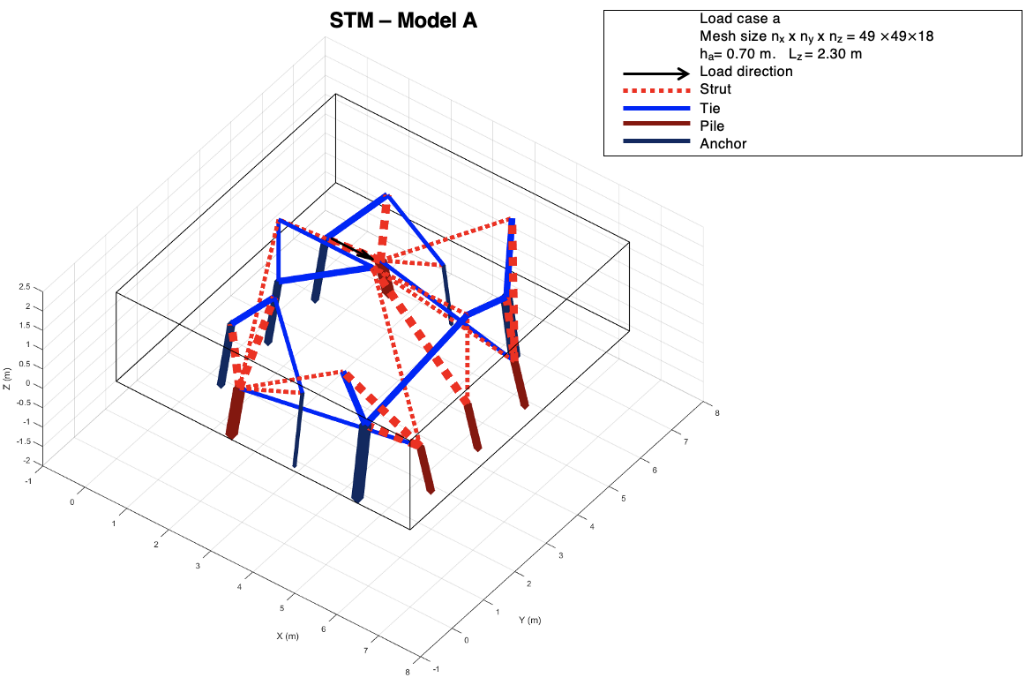

Figure 5.1: STM for model A, load case a.

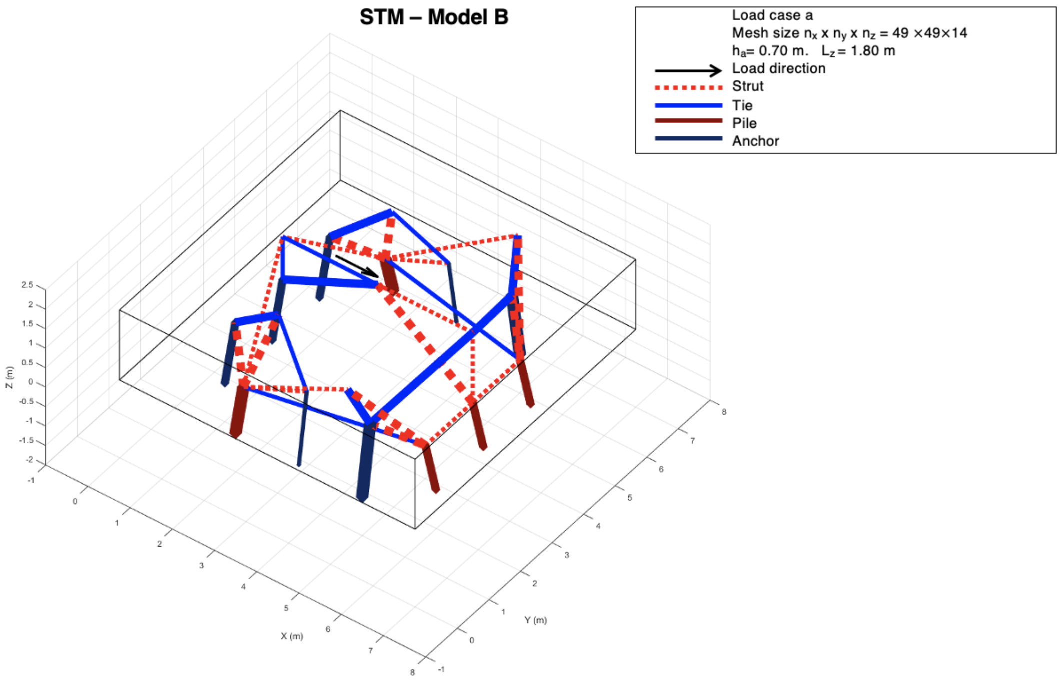

Figure 5.2: STM for model B & E, load case a.

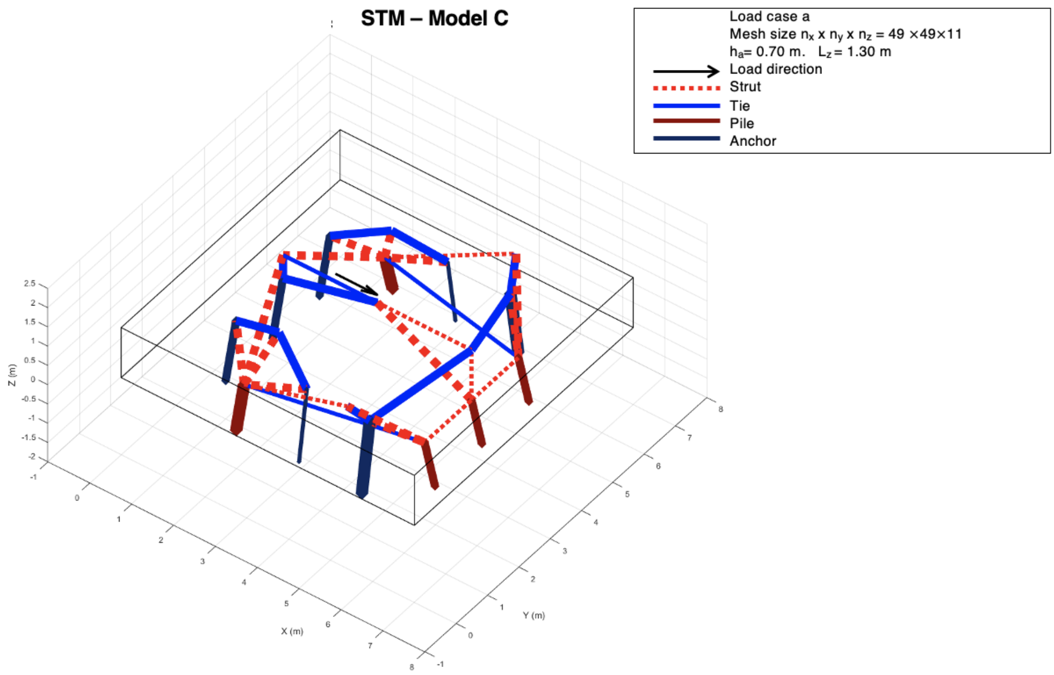

Figure 5.3: STM for model C, load case a.

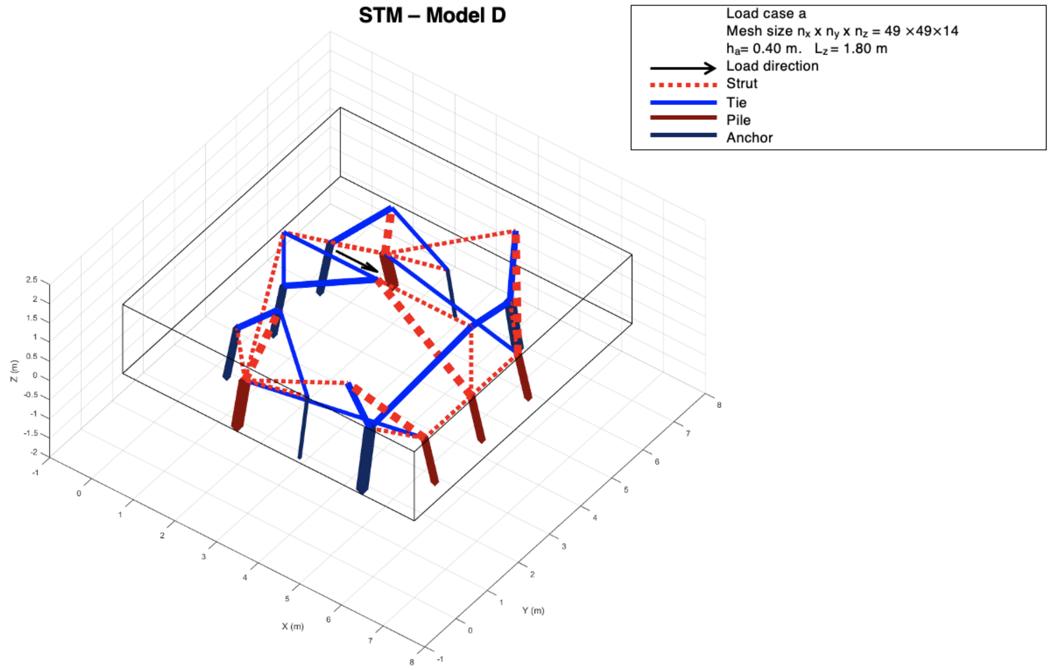

Figure 5.4: STM for model D, load case a.

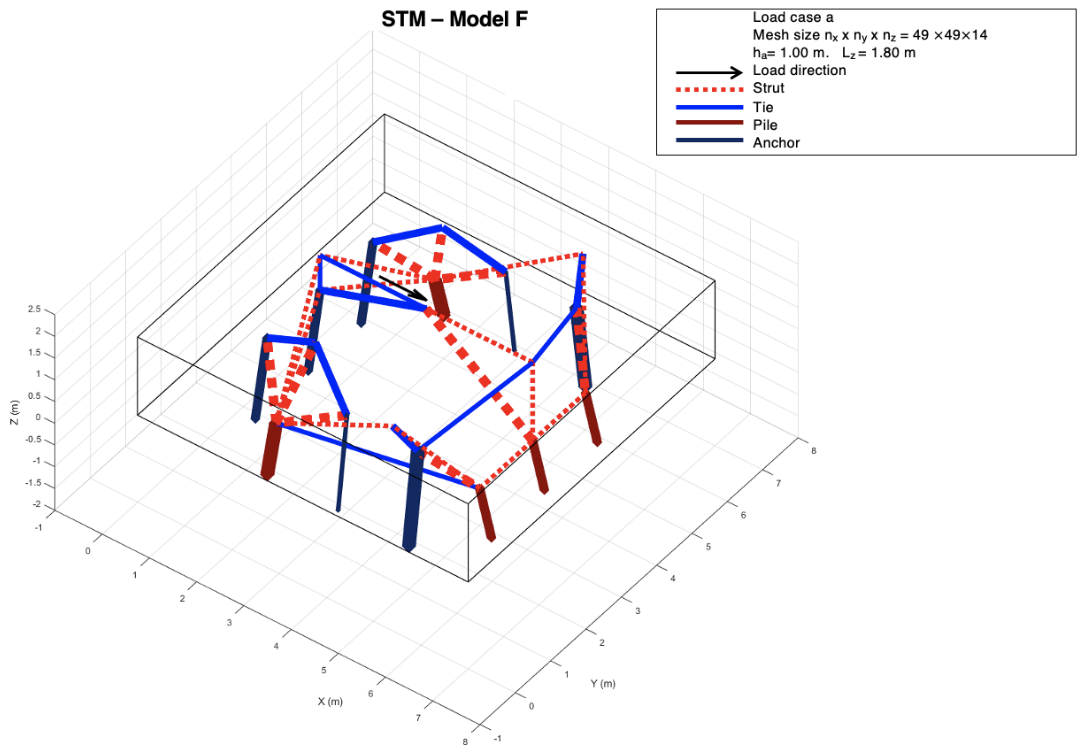

Figure 5.5: STM for model F, load case a.

5.2 Load case b & c

Note that b and c have the same configuration with altering inclinations due to the different anchor length and slab height. The models A-F remain similar with identical node linkage for models A, B, C, E, F. Model D has additional struts in the lower part of the STM. See following Figures 5.6, 5.7, 5.8, 5.9 and 5.10 for STM for models A-F and load cases a and d.

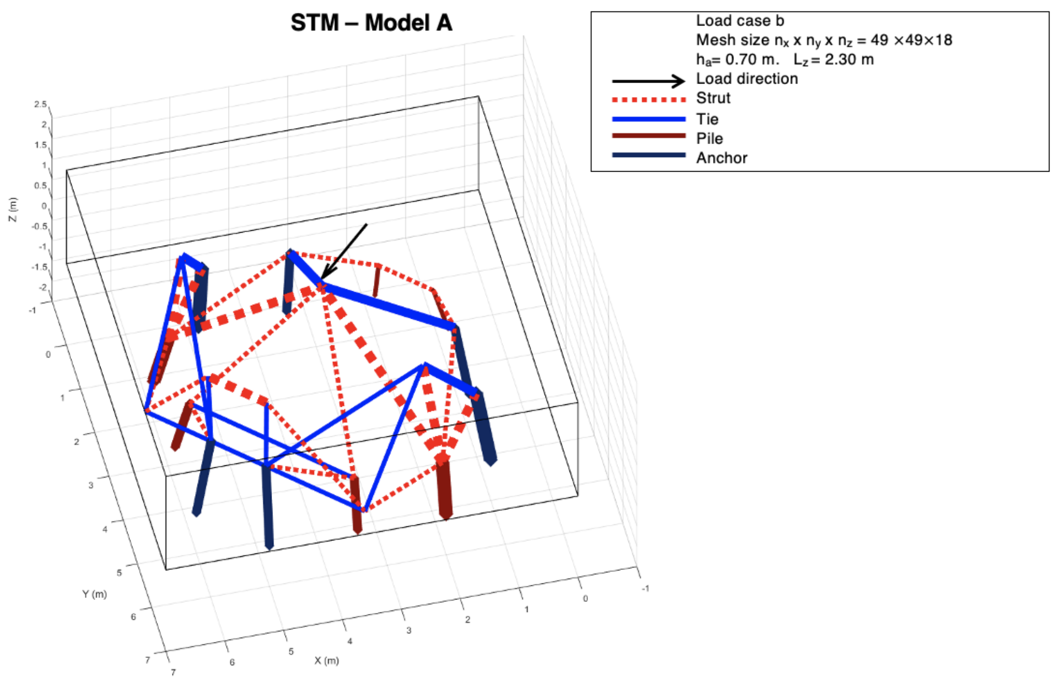

Figure 5.6: STM for model A, load case b.

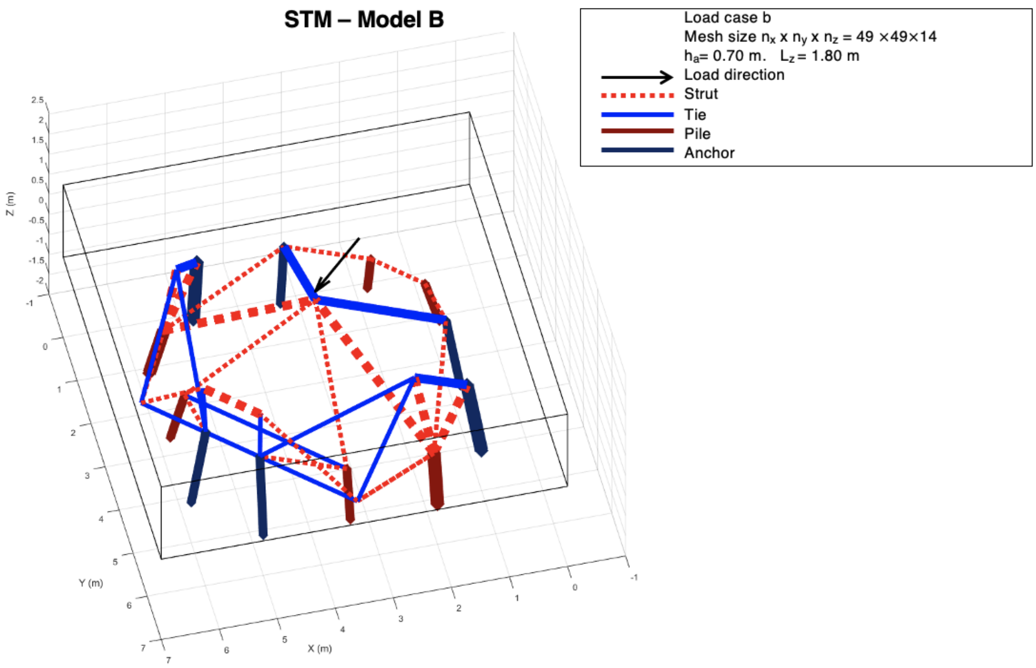

Figure 5.7: STM for model B & E, load case b.

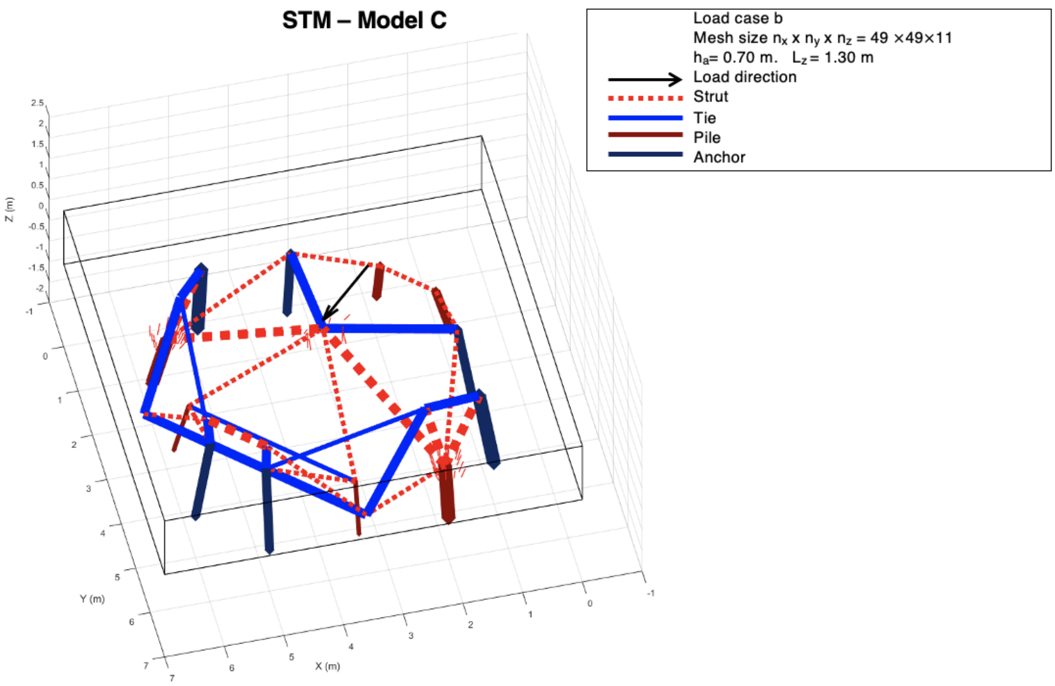

Figure 5.8: STM for model C, load case b.

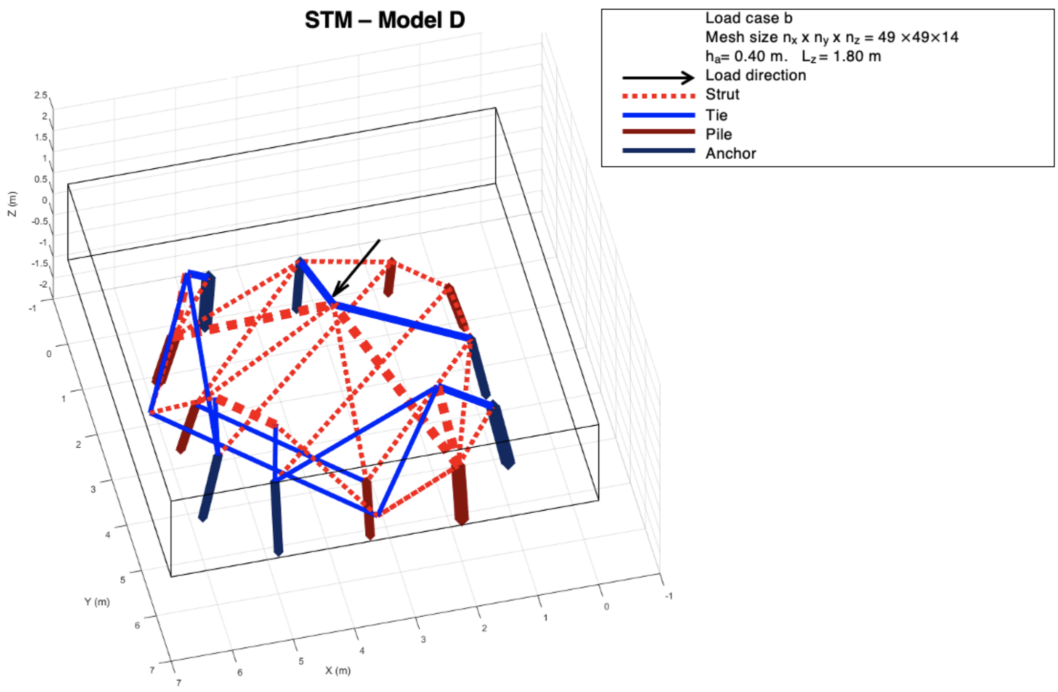

Figure 5.9: STM for model D, load case b.

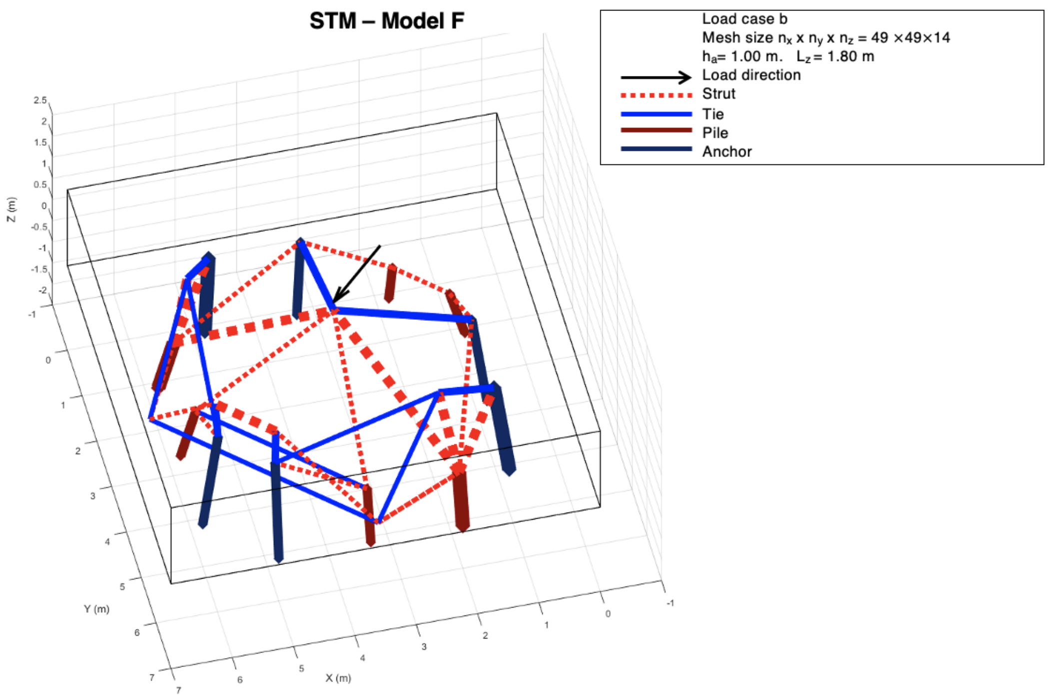

Figure 5.10: STM for model F, load case b.

6 Discussion

In this chapter, the resulting stress fields and STMs are discussed, the method evaluated, and further comments on discoveries made in the work. In Section 6.1, regarding the stress field analysis and STMs, the discussion focuses on the general structural behaviors found in the internal stress fields rather than individual models or struts/ties. Section 6.2 evaluates the method applied in the thesis, addressing other modeling possibilities and, advantages and disadvantages with the chosen approach. Finally, Section 6.3 highlights two additional findings in the thesis with the possibility to optimize the mooring dolphin design.

6.1 Stress Patterns

The main differences between the stress fields of load cases a and d, and c and b, are the magnitude of the struts and ties and the stress concentrations along the sides of the cap. This is due to the inclination of the load, as a more inclined load reduces the reactions in the piles and anchors. Additionally, there is a similar effect from the different slab heights, models A-C. Since model A is thicker and thereby heavier, the reactions in the piles are larger, and the reaction forces in the anchors are smaller than those in model C. See Appendix A.5 for pile and anchor reaction forces for the parametric study.

The overall result from the parametric study was that the configurations remained very similar with only one or two strut/tie differences. More varied results might have been obtained if the strut-and-tie model configurations had been evaluated based on the magnitude of the stress distribution, rather than solely on visual arrangement.

Following a previously mentioned recommendation by Prof. Lundgren, the local stress field beneath the active anchor heads was neglected in the model. Here, the tensile stresses and compressive stresses are perpendicular to one another, and since concrete is weaker in tension it is important to reinforce these sections of the pile cap to ensure structural capacity. The tensile stress field in these areas demands both vertical and horizontal ties. See Figure 6.1, how the tensile stresses continue below the anchor head and how some compressive stresses reach above the plate.

As predicted by H. Mazaheripour, struts between the pile compression plate and the anchor tensile plate were included within all the strut-and-tie models, see Figure 6.2 (a). The same is true for the roof trusses predicted by Prof. Lundgren. Roof trusses are defined as going from pile to pile or anchor to anchor, via the top of the slab, see Figure 6.2 (b).

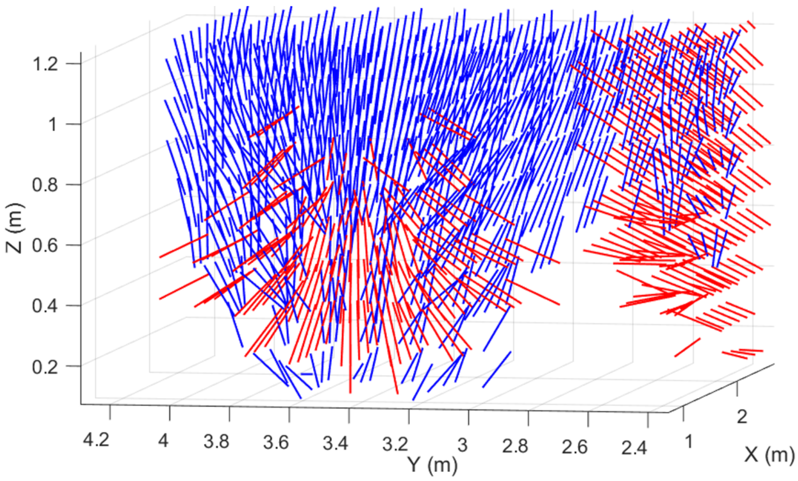

Figure 6.1: Local tensor stress field around active anchor tension plate at height 0.7m. Blue - σ_1, Red - σ_3.

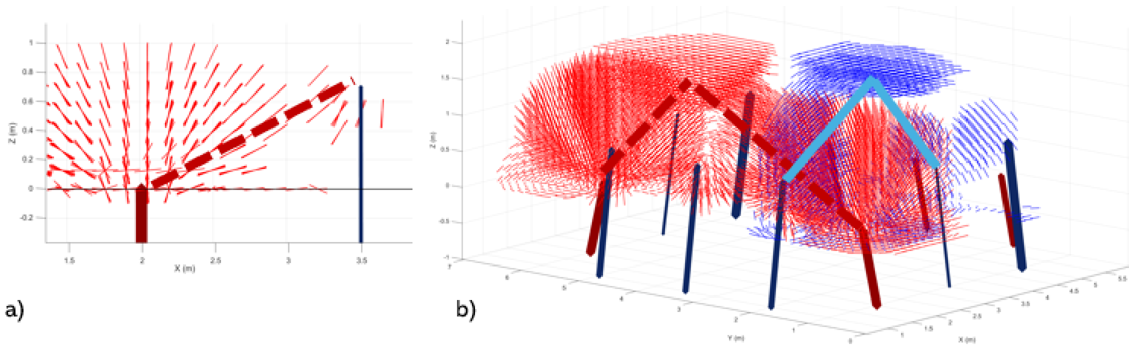

Figure 6.2: a) Pile head - Anchor head strut. b) Roof truss strut and tie. Blue - σ_1, Red - σ_3.

6.1.1 Load case a & d

The strut-and-tie configurations are identical for load cases a and d for all parametric models. The STM differs depending on the anchor height and slab thickness due to preferred load paths and although all models A-F are similar, the magnitudes vary and for certain models struts and/or ties are added.

Pile Head - Anchor Head Strut
As mentioned, struts form in between active anchor- and pile plates. It has been observed that the strut mainly stretch from the anchor tension plate towards its nearest active pile compression plate. For load cases a and d, there are three active anchors in a row. The middle one, being the furthest from any active pile plate, seems to disperse the compressive stresses, resulting in a much smaller stress than for the other two. Therefore, this strut was excluded from all models, except for model F, due to its larger anchor height.

A pattern that can be seen is that struts are more prone to occur where the inclination is larger. This can for example be seen in model F where the anchor height is 1.0 m, allowing a strut to take form from the middle back end anchor plate to the neighboring acting pile plates. This was not seen in model D and E, suspecting that the angle between the plates was too low to clearly see a strut taking form. See Figure 6.3 for the strut on hand for models D ($L_a = 0.4m$) and F ($L_a = 1.0m$) and take note of the extra strut in F.

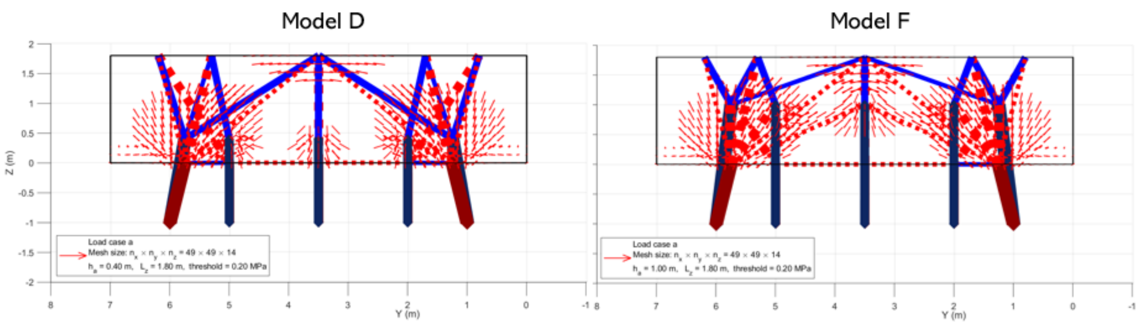

Figure 6.3: Back end strut comparison for models D and F. Blue - σ_1, Red - σ_3.

To get a better understanding on how the stresses from the middle back anchor plate acts, an imperfection angle of 10° was investigated. This was to see if struts would potentially take form and how they would display themselves. It was concluded that if the distance between two active pile heads was equal, the strut would stretch towards a preferred compressed pile plate depending on the load direction and structural behavior. See Figure 6.4 for the compression stress tensor field in the specified area.

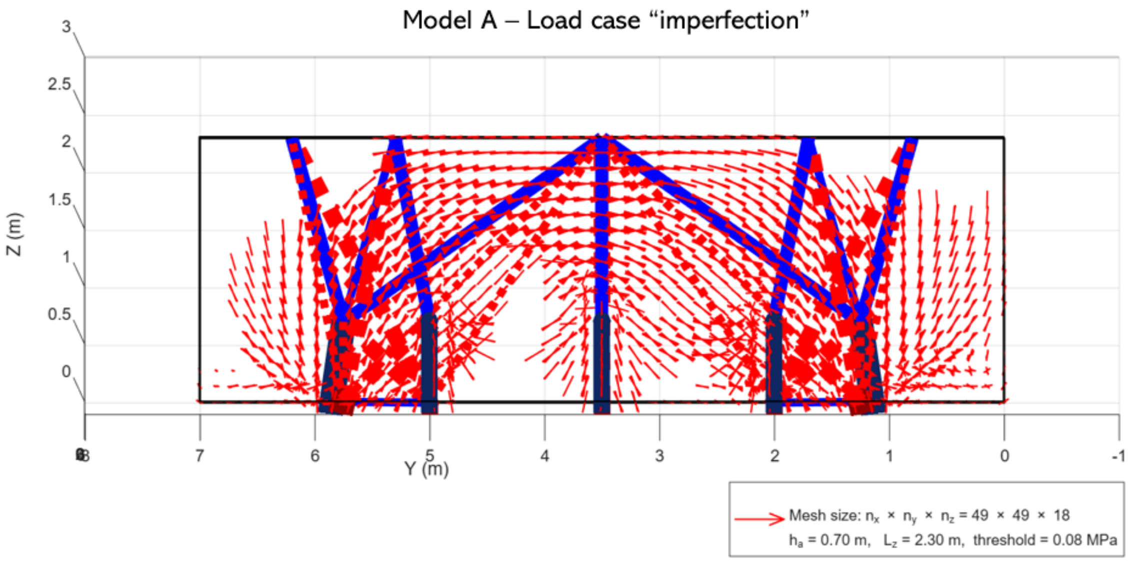

Figure 6.4: Back end stress σ_3 tensor plot for model A, load case "imperfection". Note that no new strut is added to the STM, for the now visible strut on the right side.

Three Main Struts and Ties

A lot of discussion was held regarding the modeling of the front three struts. Intuitively at first glance of the stress field of model A, and after discussing it with H. Mazaheripour (personal communication, 2026, 12 May), it was perceived as a fan strut spreading from the bollard down to the three pile heads. However, upon further analysis of models B and C, more specifically the magnitudes and directions of the stresses, an unexpected behavior was observed. It seemed like only the pile head in the middle was forming a strut to the bollard and that the corner pile heads mainly contributed via the side roof truss struts. See Figure 6.5 and 6.7 for a comparison of the front struts for models A ($h_s = 2.3m$) and C ($h_s = 1.3m$). For model C it is much clearer that the side struts are not reaching towards the bollard compared to model A.

Due to the initial expectation of struts extending from the bollard down to the three pile heads, an assumption based on experience and intuition, it was decided to keep the three frontal struts for model A in addition two the other side going ones which were visible when lowering the threshold, see Figure 6.6. Furthermore, in model A the struts were more fused together compared to models B and C and the decision to keep the fan like strut was also made to highlight the different stress behavior of the slab height parameter. The roof truss strut was also kept since the behavior in models B and C was observed in model A as well, see Section 5.1 for the strut-and-tie models.

Another explanation as to why the fan strut only appears in model A is due to the amount of compressive forces within the model. Since the slab is thicker it also experiences more compressive stress due to increased self-weight, which could contribute to the wider stress field and a more fan like appearance.

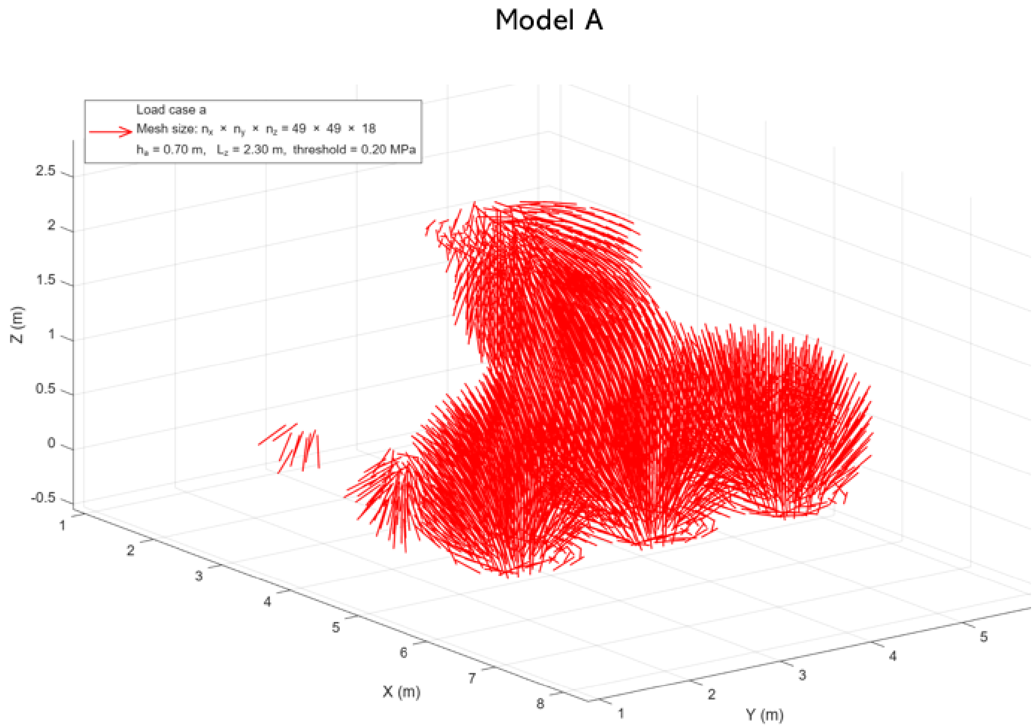

Figure 6.5: Front (x = 3.3-7.0 m) three stress σ_3 struts for model A. Threshold 0.2 MPa.

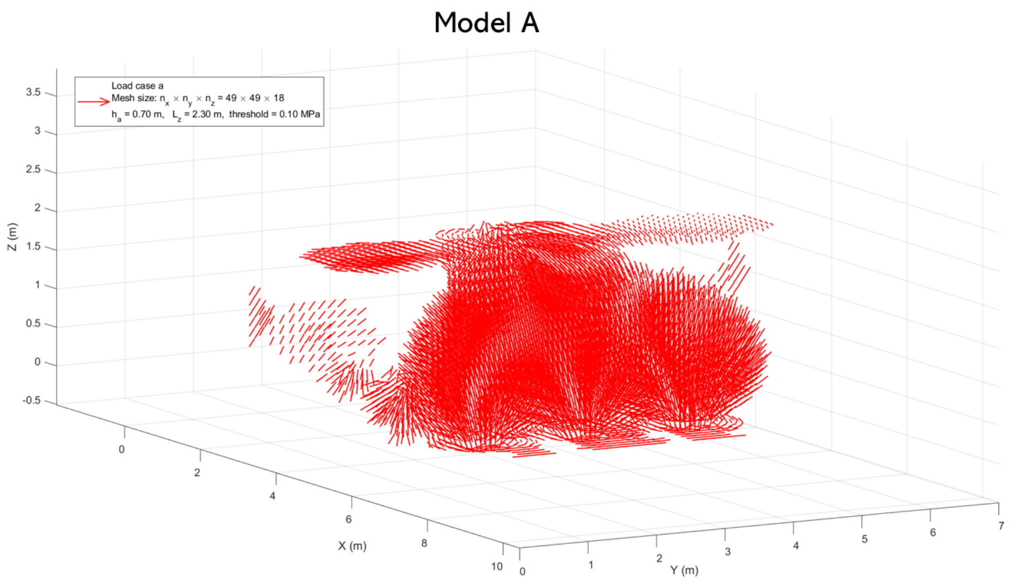

Figure 6.6: Front (x = 3.3-7.0 m) three stress σ_3 struts for model A. Threshold 0.1 MPa.

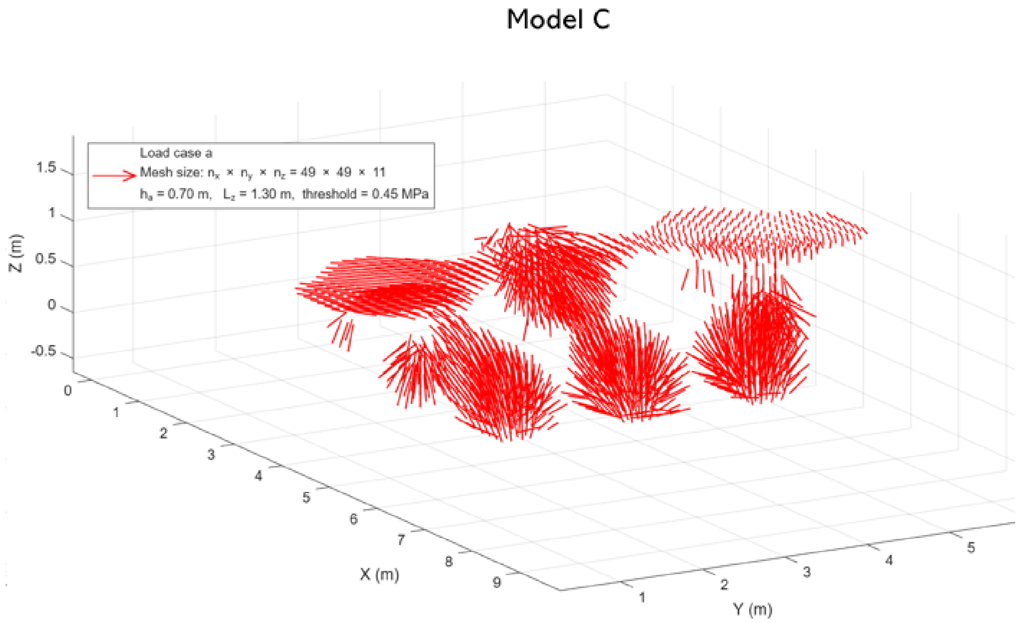

Figure 6.7: Front (x = 3.3-7.0 m) three stress σ_3 struts for model C. Threshold 0.2 MPa.

A similar structural response is observed on the opposite side, but in tension. This was also first anticipated such that three struts would face in the opposite direction of three ties. The maximum vertical distance in Z between the anchor plate and the top of the slab (which directly governs the inclination of the strut or tie) occurs in model A, reaching 1.6 m, see Figure 6.8. The vertical distance between the top side and anchor tension plate of model A is less than the corresponding distance found between the slab top and the pile compression plate in model B (1.8 m).

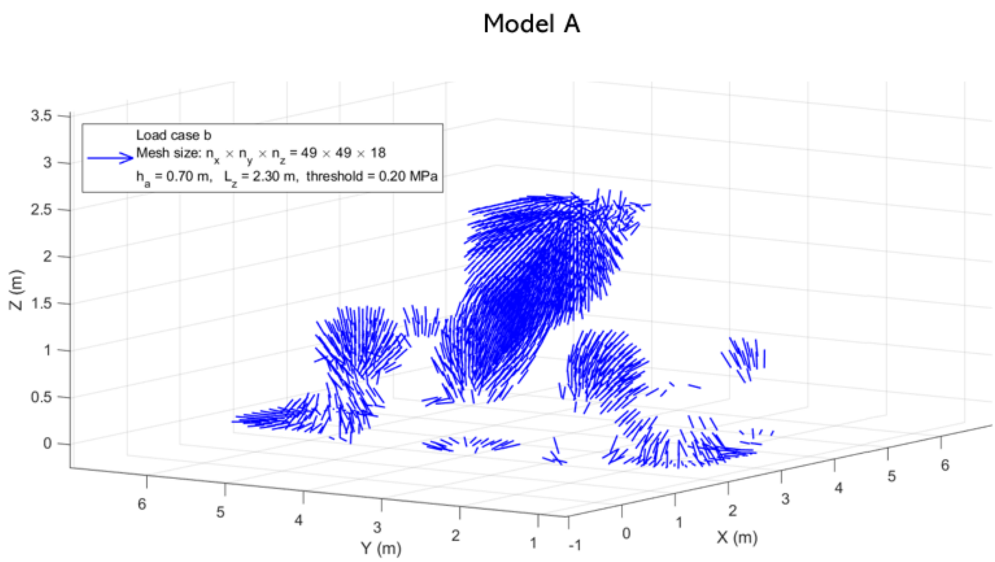

Figure 6.8: Back three (x = 0.0-3.7 m) stress σ_1 ties for model A. Threshold 0.2 MPa.

Notably, there is no fan action detected except for the previously mentioned fan strut in model A. This behavior could be explained by the inclination of the struts and ties, since the fan behavior seems to appear for steeper angles. Note that this is not only true for certain angles, but must fulfill other criteria as well.

Furthermore, Figure 6.5 and 6.7, show that the internal stresses are more prominent along the sides of the pile cap for thinner slabs. This was observed for the other load cases as well.

6.1.2 Load case b & c

The strut-and-tie configurations are identical for load cases b and c for all parametric models. Furthermore, the stresses for load cases b and c varied over a larger span than load cases a and d, demanding higher thresholds for both compression and tension. With the force acting in 45 degrees, the strut-and-tie system is now symmetric over the diagonal. Compared to cases a and d, the system consists of larger pile forces while reaching approximately the same anchorage forces.

Wavy Stress Field

The stress field distribution in b and c is more localized toward the surface of the pile cap since these are larger areas with higher stress magnitudes compared to those in load cases a and d. The stress field within the models A-F, are best described as a combination of traditional bottle and fan struts with an enveloping wavy stress flow. This wavy stress flow does not follow the general strut shapes but bends, see Figure 6.9. Note that in the STMs, all struts and ties are drawn as straight lines between the nodes.

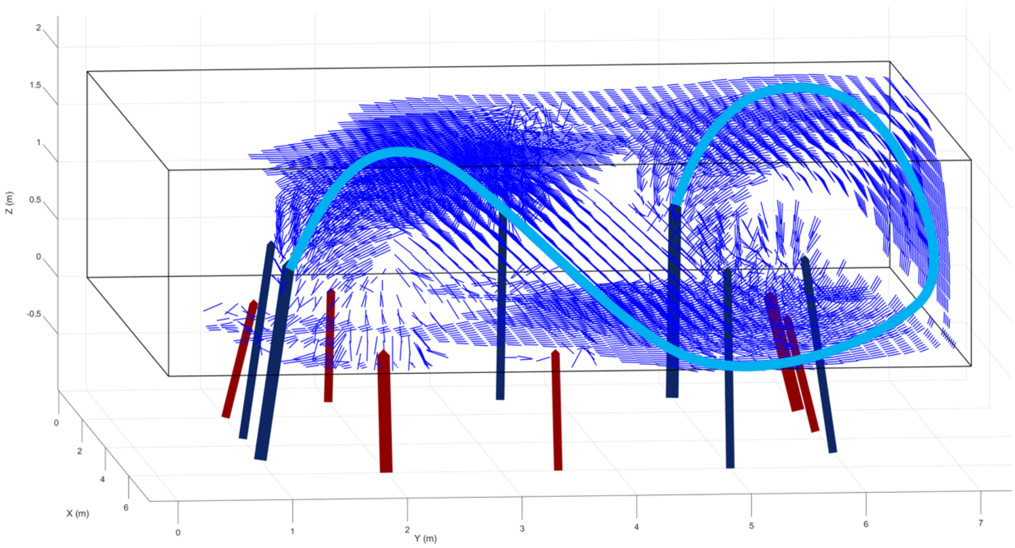

Figure 6.9: Wavy stress (σ_1) flow bends of load cases b and c - Model B, clarified by a light blue line indicating the stress path.

A similar stress flow to the one in Figure 6.9 can be found for compression as well in cases b and c, and furthermore in load cases a and d, although with significantly lower stress magnitudes and therefore not highlighted.

Large Side Stress

The previously mentioned "roof truss" struts and ties, and the "wavy bend" stress fields represent some of the major stresses at the vertical and horizontal sides of the model. For the wavy bend in Figure 6.9, it shows how the stress flow takes shape from the anchor to the top of the slab and later to the side and then the bottom before reaching the symmetry line. It also shows a larger tensile area at the upper side and on the lower side. The same is true for the compressive field which can partly be seen in Figure 6.10 where the transverse compressive bottom stress field to that of Figure 6.9 are plotted. Note that no ties are drawn along the sides of the pile cap, but that there is a demand that should be taken into account when dimensioning the reinforcement accordingly.

In model D where the anchor height is low, additional struts were added in the bottom of the pile cap, representing the general bottom stress field. These struts were only implemented in model D due to the anchor head being located further down within this bottom stress field compared to the other models.

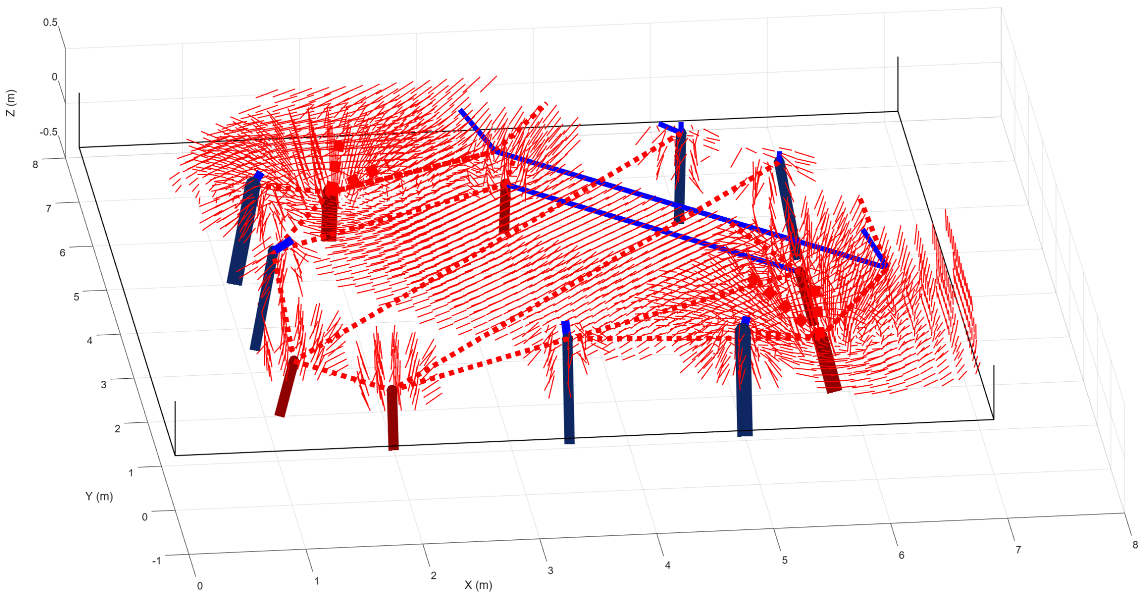

Figure 6.10: Compression bottom stress σ_3 for load case b, model D, with additional bottom struts.

6.2 Method Evaluation

The final FE model using TRUS and CABL elements was successful in describing the tension and compression behavior. However, with the eight-pile configuration and hinged boundary conditions, the system was unable to reach equilibrium. A fixed connection had to be assessed for that pile configuration to work, which resulted in undesirable structural behavior. This suggests that the final pile configuration might have enabled earlier FE-designs, such as the nonlinear spring model, to work. Furthermore, this emphasizes the impact of pile configuration and the sensitivity of finite element models to the selection and implementation of boundary conditions.

Strut-and-tie is generally dependent on experience due to the assumptions of the load paths. We recognize we lack experience in the subject and it was decided to rely on the stress field from the finite element analysis with additional input from the experts in mind when mapping the strut-and-tie models. The decision to write a thesis on a subject where experience is valued can be questioned, but we believe that this could be to our advantage when interpreting the stress field. This is because we decided to fully rely on the paths visible in the tensor plots, rather than assuming paths that might be based on previously wrong interpretations of the load paths and, therefore, remained impartial to some degree.

Some disadvantages of the chosen method include uncertainties associated with the verification of the STMs. One such uncertainty is that the configurations were neither established nor validated through evaluations of the relevant force magnitudes and angles. Such evaluations are necessary to ensure equilibrium and achieve a structurally valid reinforcement design. Closely related to this is the fact that the three-dimensional approach applied in this thesis is highly approximated, as several simplifications were required to make the analysis feasible.

It should also be emphasized that the aim of this thesis was not to provide a definitive design guide, but rather to propose approaches that may support future design choices when establishing STM configurations. The analysis should therefore be regarded as exploratory rather than as a strict validation of a specific method. Consequently, the interpretation and application of the findings remain the responsibility of the engineer.

The chosen method of representing the STM can also be questioned. It was decided to not include struts and ties in certain areas as directly below the anchor plates to display the zone in Figure 6.1 and along the sides of the pile cap where it would form large stress fields. For the different STMs, struts or ties would occasionally be identified as going along one side in order to fulfill a nodal equilibrium or to understand the stress flow. However, doing this could lead to an inconsistent inclusion of struts and ties and make it difficult to understand the STM without the stress fields filling these blanks. Additionally, the width variation describing the dominant struts and ties are based on our visual judgment and exists to aid the interpreter but is recognized as a possible source to confusion as well.

Furthermore a knowledge gap is recognized. Since STM configurations are conventionally established in two dimensions, it may be argued that the results obtained from the three-dimensional model do not directly translate to current engineering practice in mooring dolphin design and could therefore be considered of limited practical relevance. However, the findings of this study indicate that the conventional approach contains limitations for which a three-dimensional analysis may provide additional insight and potentially influence future design practice. The intention is not to replace existing methods, but rather to demonstrate how a higher-dimensional analysis can enhance the engineer's understanding of the structural response and reveal effects that may not be captured through two-dimensional STM approaches.

6.3 Additional Findings

The positive mooring load inclination for load cases c and d resulted in lower stresses and lower reaction forces in both the piles and the anchors. This finding may be considered in future design and production. By lowering the pile cap closer to the water, or by limiting the bollard to larger inclinations of the mooring line, the vertical component of the mooring force increases, which, for the investigated load cases, resulted in lower dimensioning stresses. For the investigated pile cap, this may entail a reduction in material use. However, this is likely to also expose the pile cap to a harsher environment closer to the water. Pile caps subjected to cycles of wetting and drying may subsequently increase the risk of both abrasion and chloride ingress.

An additional finding observed during the analysis was the structural behavior of the connection. When AHIN and EHIN were implemented in the BEAM elements, the response was hinged. But before then it showed signs of fixed behavior, as discussed in Section 3.2, Part: *Pile Configurations and Hinged Connections*. The fixed behavior led consequently to a large reduction of forces in piles and anchors for the investigated load case, and mooring dolphin with its 8-pile configuration. Figure 6.11 displays the global support response in Z, with marked maximum tensile and compressive values for each model. There is a large magnitude difference that could entail the possibility of optimizing the structure by fixing the pile - slab connection, see Table 6.1 for max values for both models. Note that this model has not been evaluated and that one specific case was investigated.

Connection	Max. compression [kN]	Max. tension [kN]
Hinged	879.1	1385.8
Fixed	471.9	599.6

Table 6.1: Global support reaction in the local pile axis for the FE model with truss - beam piles as either hinged or fixed to the pile cap.

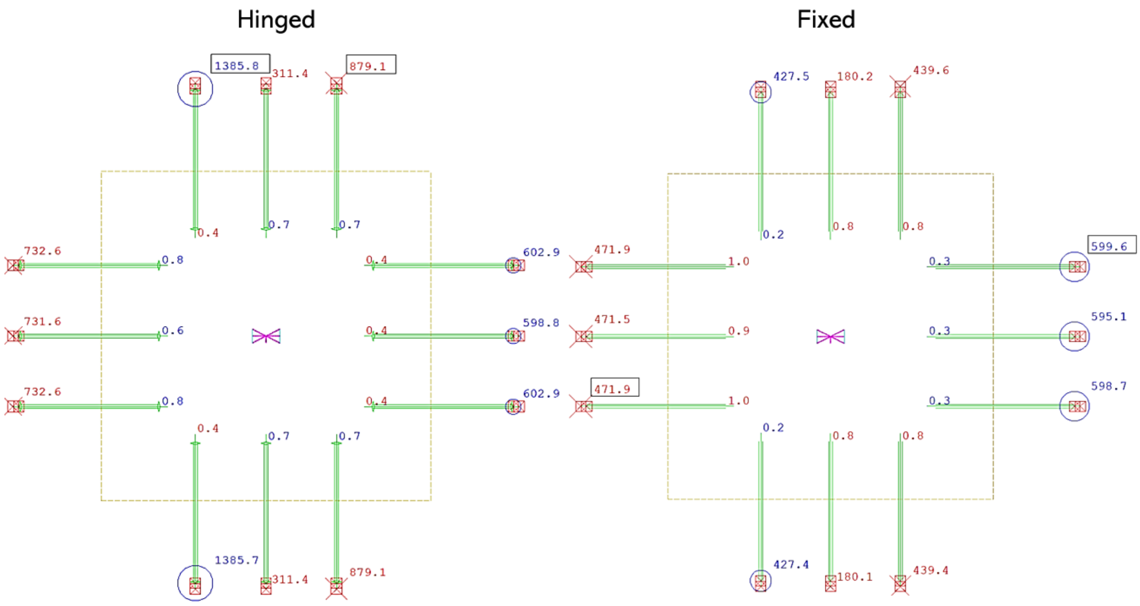

Figure 6.11: Global support reaction [kN] in the local pile axis for the FE model with truss-beam piles, either hinged or fixed to the pile cap. Red indicates compressive force, and blue indicates tensile force.

7 Conclusion

In this thesis, a three-dimensional FE model was established to analyze the internal stress field of a mooring dolphin pile cap for strut-and-tie modeling. A parametric study was conducted for parameters, slab height and anchor rod length, and mooring load of different directions, for a better understanding of how the internal stress field tends to behave. Visualization tools were developed to extract and analyze the stress fields and the STMs were configured accordingly.

It was concluded that the parametric models did not impact the STM configuration on a large scale, other than altering the nodal locations at the anchor plate and top side of the slab, and a couple of additional struts/ties, see Chapter 5. Furthermore, the orientation of the load heavily impacted the response of the piles and anchors, and the STM configurations. The inclination did not alter the STM configurations but affected the magnitude of the reactions and stresses.

The most significant strut-and-tie findings from the analysis of the mooring dolphin FE model were:

- "Pile head - Anchor head" struts
- "Roof truss" struts and ties
- Large side stresses
- "Wave bend" stress flow

The pile head - anchor head struts were confirmed, although not always as straight forward as previously assumed. The struts did not necessarily stretch between the two as prisms or as bottles, but could, due to the impact of surrounding stresses, bend into a bow-like shape between the head plates.

The roof truss strut and ties were also confirmed and correlate to high stress concentration observed on the sides of the pile cap, in this case for the top side.

Since high stresses tend to gather at the sides of the pile cap it indicates that this is a critical design area. Fortunately, the sides are generally reinforced and can be designed based on the stresses from the mooring load.

The wave bend stress flow is important to take into consideration when designing with STM. Surrounding stresses influence the direction of the struts and ties and are therefore important to consider.

Based on the above findings, the following recommendations for the development of STMs are proposed:

- Struts tend to form between the active anchor tension plates and its nearest active pile compression plate.
- Struts and ties tend to form between two active piles and two active anchors, referred to as the "roof truss". Resulting in large stresses in the top of the slab.
- Stresses tend to gather at the sides of the pile cap which needs to be addressed to avoid cracking. It is also recommended to try to utilize the reinforcement in these areas for both STM and surface reinforcement.
- Struts and ties do not follow the stereotypical, general shapes and can bend and flow. It is important to analyze how the stress implication points impact the stress field and how the tensile and compressive tensors interact.

N.B.: These recommendations on strut-and-tie design are strictly based on this mooring dolphin model alone and for the specific load cases specified in the thesis. The analysis is also performed with linear concrete which does not address cracking which impact the stress field.

7.1 Further Research

As concluded in this thesis, the structural behavior and performance of mooring dolphins in the FE-model are highly dependent on the modeled geometry and applied boundary conditions. The results were therefore strongly influenced by the specific pile configuration, load cases, and boundary conditions adopted in this study. Furthermore, the thesis was limited to a linear elastic analysis, without consideration of second-order effects. To further develop and refine design guidelines for dolphins, the following areas are proposed for future research.

Parameters
Throughout the FE modeling phase, multiple iterations were carried out, some of which displayed unexpected but plausible structural behavior. One such variation involved a fixed connection between the pile head and the concrete slab. This resulted in reduced pile response and significant moment transfer within the system.

Additionally, it was discovered that the initial pile configuration could not achieve equilibrium with hinged connections. Further investigation is therefore needed to identify the configurations for which equilibrium can be achieved. Examining such alternative layouts could provide valuable insights into whether the corresponding strut-and-tie systems exhibit behaviors different from those observed in this thesis.

Load cases

The recommendations presented in this thesis are based solely on the effects of self-weight and various mooring load cases. A more comprehensive assessment of the structure's behavior under a wider range of environmental loading conditions would therefore be valuable. This could include ice loading, which may may introduce lateral pressure on the piles and slab, as well as uplift forces generated by wave action beneath the slab. In particular, wave-induced uplift may significantly alter the internal stress distribution within the slab by acting in opposition to its self-weight. Depending on the load case, stresses resulting from gravity loading may be reduced due to bouyancy, while new critical stress states may develop elsewhere in the structure, potentially leading to different structural response.

Cracked State

The finite element analysis presented in this thesis assumes linear-elastic material behavior and is limited to verification in the ultimate limit state. Future research could therefore focus on nonlinear analysis that account for concrete cracking. Such analysis would provide a more realistic representation of the structural response by capturing the stiffness reduction associated with crack development.

Furthermore, the influence of minimum surface reinforcement, which is required for crack control and durability in marine structures, could be investigated through a nonlinear analysis. For example, the finite element model could be extended by adopting a smeared-crack constitutive model for reinforced concrete, or by explicitly representing the reinforcement using separate solid elements (Plos, 2000, p.30). Such approaches would enable a more realistic assessment of cracking behavior and stress redistribution within the pile cap.

It should be noted that the analysis of cracked concrete introduces additional complexity. Crack formation may lead to bifurcation of the structural response, such that equilibrium can be fulfilled in several ways (Plos, 2000, p.41). The equilibrium path predicted by a finite element model may be influenced by factors such as the adopted constitutive model, crack representation, mesh density, and numerical solution procedure. As a result, different crack patterns and internal stress fields may be obtained, and consequently different configurations of the strut-and-tie system.

Additional Stress Analysis Tool

Another direction to continue this study is to analyze how to interpret the struts and ties more effectively. This could include a refined method utilizing the BRIC cuts or applying something similar to the ESO method when designing the mooring dolphins.

Moreover, improved algorithms for sorting and plotting the principal stresses in the three-dimensional field is of need. Suggestively, by applying a stress density condition to the sorting such that lower stresses belonging to larger struts are not neglected, which could lead to missed united action if not careful. It could also allow filtering out and ignore local stress concentration which is not relevant for the global STM analysis.

References

Al-Emrani, M., Engström, B., Johansson, M., & Johansson, P. (2013). *Bärande konstruktioner - Del 1* (tech. rep. No. Report 2013:1). Chalmers University of Technology, Department of Civil and Environmental Engineering, Division of Structural Engineering. Göteborg.

Altersberger, G. (2019, July). Compression-Only Bedding and Uplift Effect. https://sofistikforyou.com/compression-only-bedding-for-structural-areas/

Bredenberg, H., Berglars, B., Rankka, W., Holmberg, G., Eronen, S., & Jokiniemi, H. (2010). *Borrade stålrörspålar, Anvisningar för projektering, dimensionering, utförande och kontroll (rapport 104)* (tech. rep.). Pålkommissionen (Commission on Pile Research). Linköping.

Dowling, N. E. (2013). *Mechanical Behavior of Materials*. Pearson Education.

Engström, B. (2015). *Design and analysis of deep beams, plates and other discontinuity regions* (tech. rep.). Chalmers University of Technology. Göteborg.

Fagerström, M., & Ekh, M. (2025). *TME245 Finite Element Method – Structures* (tech. rep.). Chalmers University of Technology.

Karlsson, H., Håkansson, S., & Sarvell, F. (2024). *Samerkanspålar av stål och betong - Anvisningar för dimensionering och utförande av betongfyllda stålrörspålar (rapport 108)* (tech. rep.). Pålkommissionen (Commission on Pile Research). Stockholm.

Kim, N.-h. (2018). *Introduction to nonlinear finite element analysis*. Springer.

Leu, L.-J., Huang, C.-W., Chen, C.-S., & Liao, Y.-P. (2006). Strut-and-Tie Design Methodology for Three-Dimensional Reinforced Concrete Structures. *Journal of Structural Engineering*, *132*(6), 929–938. https://doi.org/10.1061/(ASCE)0733-9445(2006)132:6(929)

Oñate, E. (2009). *Structural Analysis with the Finite Element Method. Volume 1 Basis and Solids : linear statics* (Vol. 1). Springer.

Oñate, E. (2013). *Structural analysis with the finite element method. Volume 2, Beams, plates and shells : linear statics* (Vol. 2). Springer.

Ottosen, N. S., & Petersson, H. (1992). *Introduction to the Finite Element Method*. Prentice Hall.

Pacoste, C., Plos, M., & Johansson, M. (2012, October). *Recommendations for finite element analysis for the design of reinforced concrete slabs* (tech. rep.). KTH Royal Institute of Technology. Stockholm.

Park, R., & Paulay, T. (1975). *Reinforce Concrete Structures*. John Wiley; Sons.

PIANC. (2026, May). PIANC Members. https://www.pianc.org/members/

PIANC Sverige. (2026, May). PIANC Sverige - linkedin Group. https://www.linkedin.com/groups/10065646/

Plos, M. (2000). *Finite element analysis of reinforced concrete structures* (tech. rep.). Chalmers University of Technology. Göteborg.

Schlaich, J., & Schäfer, K. (1991). Design and Detailing of Structural Concrete using Strut-and-Tie Models. *The Structural Engineer*, *69*(6).

SOFiSTiK AG. (2026a). *ASE - General Static Analysis of FE Structures* (tech. rep.). SOFiSTiK AG.

SOFiSTiK AG. (2026b). *GRAPHIC - Graphical Representation of Finite Elements and Beam Structures* (tech. rep.). SOFiSTiK AG.

SOFiSTiK AG. (2026c). *SOFiMSHA - Import and Export of Finite Elements* (tech. rep.). SOFiSTiK AG.

SSAB. (2025). *RD pile wall - Design and installation manual* (tech. rep.). SSAB.

Swedish Institute for Standards. (2005). *SVENSK STANDARD SS-EN 1992-1-1:2005 - Eurokod 2: Dimensionering av betongkonstruktioner - Del 1-1: Allmänna regler och regler för byggnader* (tech. rep.). Swedish Institute for Standards. Stockholm.

Swedish Institute for Standards. (2026). *SVENSK STANDARD SS-EN 1990-1:2023+A1:2026 Eurokod – Grundläggande dimensioneringsregler – Del 1: Nya byggnadsverk* (tech. rep.). Swedish Institute for Standards. Stockholm.

The British Standards Institution. (2014). *BS 6349-4:2014 Maritime works - Maritime works – Part 4: Code of practice for design of fendering and mooring systems* (tech. rep.). The British Standards Institution.

The British Standards Institution. (2017). *BS 6349-1-2:2016+A1:2017 Maritime works – Part 1-2: General — Code of practice for assessment of actions* (tech. rep.). The British Standards Institution.

The British Standards Institution. (2019). *BS 6349-2:2019 Maritime works Part 2: Code of practice for the design of quay walls, jetties and dolphins* (tech. rep.). The British Standards Institution.

Trafikverket. (2023, July). *TRVINFRA-00227: Bro och broliknande konstruktion, Byggande* (tech. rep.). Trafikverket (Swedish Transport Administration).

UN Trade and Development. (2025, April). Shipping data: UNCTAD releases new seaborne trade statistics. https://unctad.org/news/shipping-data-unctad-releases-new-seaborne-trade-statistics

Yun, Y. M., & Ramirez, J. A. (2016). Strength of Concrete Struts in Three-Dimensional Strut-Tie Models. *Journal of Structural Engineering*, *142*(11). https://doi.org/10.1061/(ASCE)ST.1943-541X.0001584

A Appendix

A.1 Nonlinear Material Curves

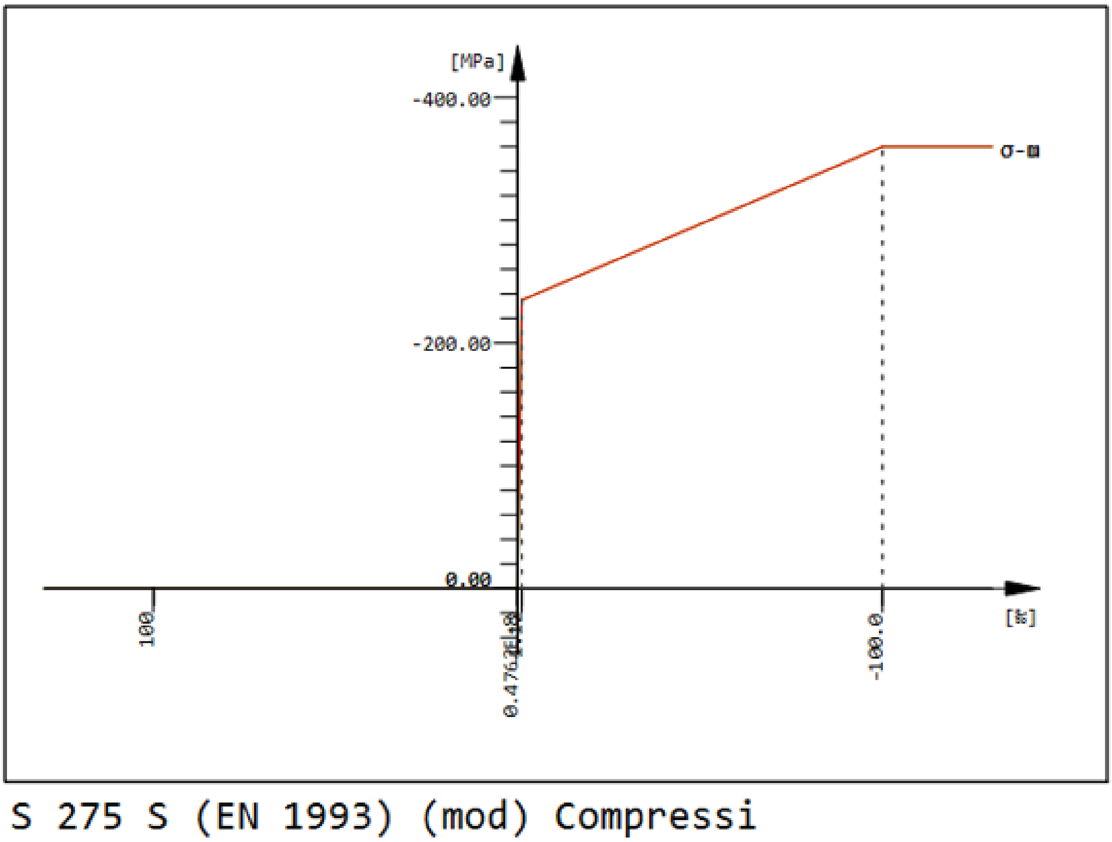

Figure A.1: Nonlinear material curve for compression pile used in nonlinear material evolution of the FE model in SOFiSTiK. Y-axis [MPa] X-axis [‰].

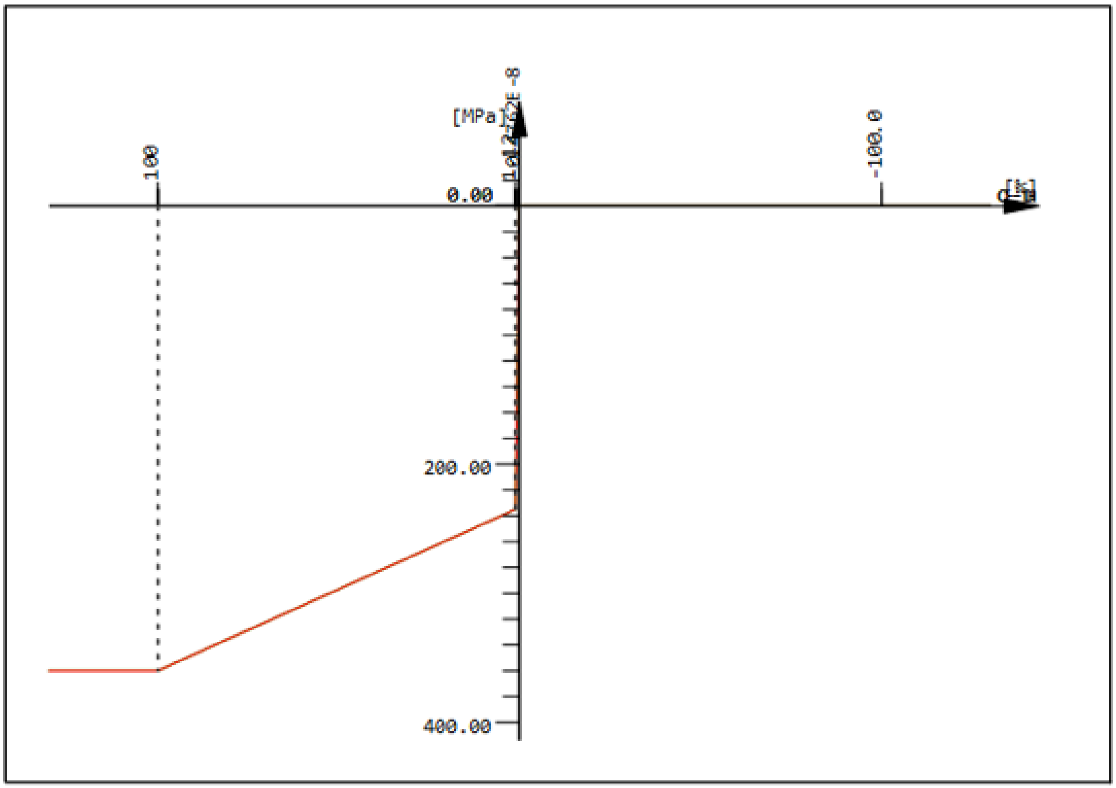

S 275 S (EN 1993) (mod) Tensile S

Figure A.2: Nonlinear material curve for tension anchor used in nonlinear material evolution of the FE model in SOFiSTiK.Y-axis [MPa] X-axis [‰].

A.2 TRUS Pile Reasoning

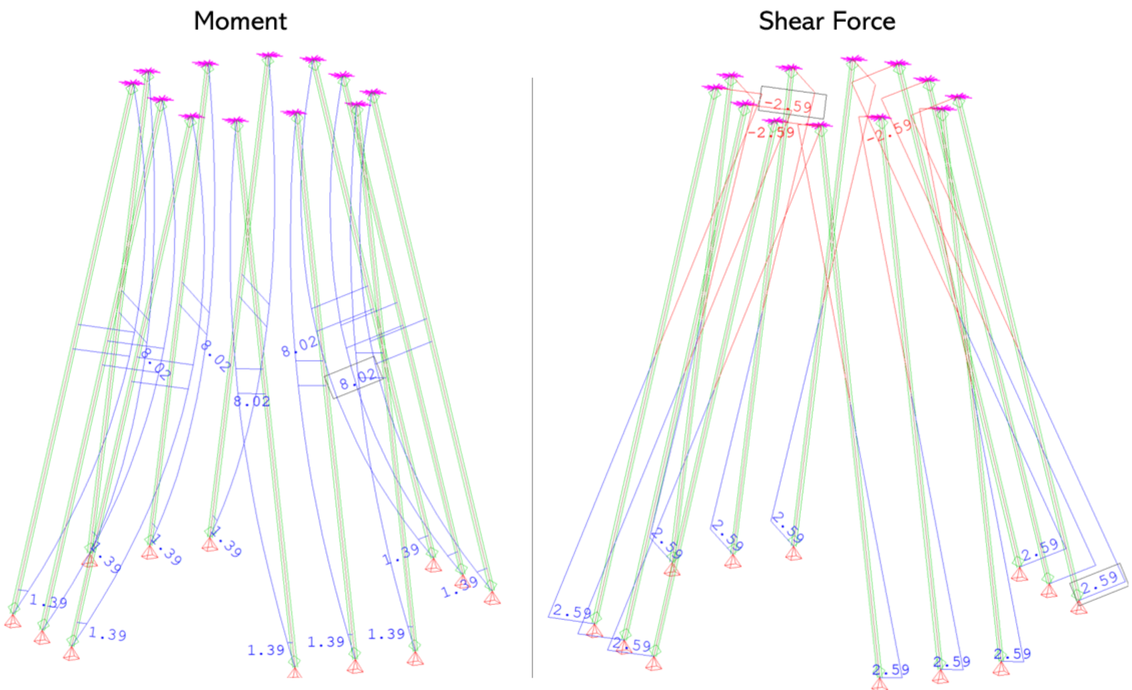

Figure A.3: BEAM pile moment force [kNm] and shear force [kN] for self-weight.

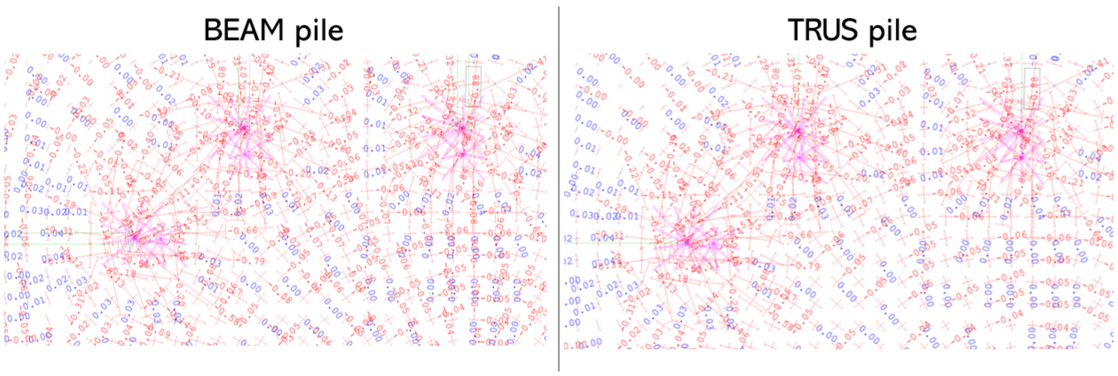

Figure A.4: Pile head principal stress field.

A.3 Nodal von Mises Stress

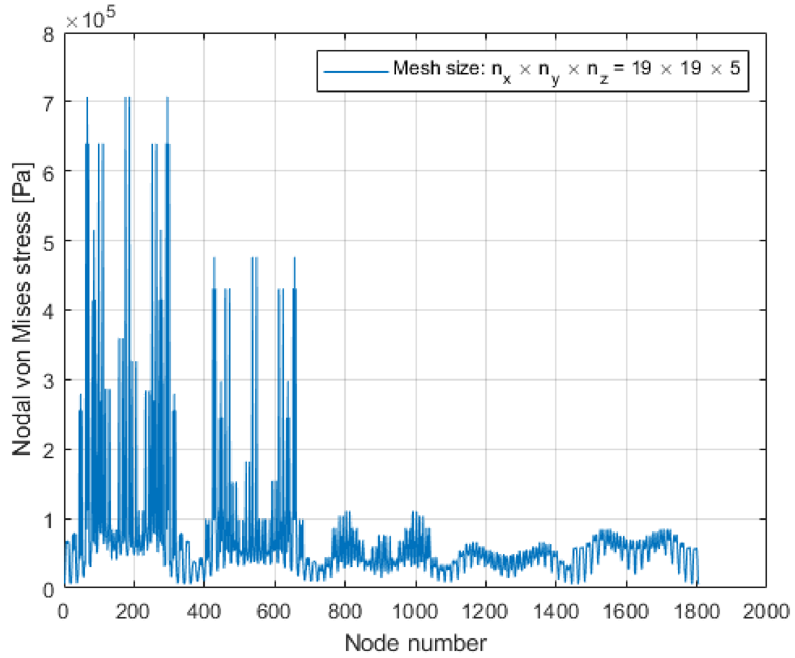

Figure A.5: Nodal von Mises stress for a mesh size of 19×19×5.

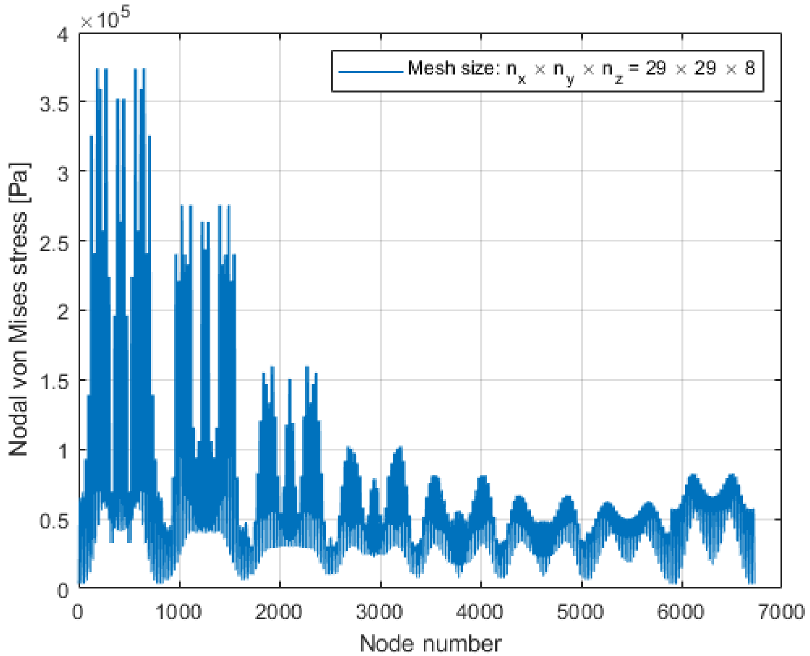

Figure A.6: Nodal von Mises stress for a mesh size of 29×29×8.

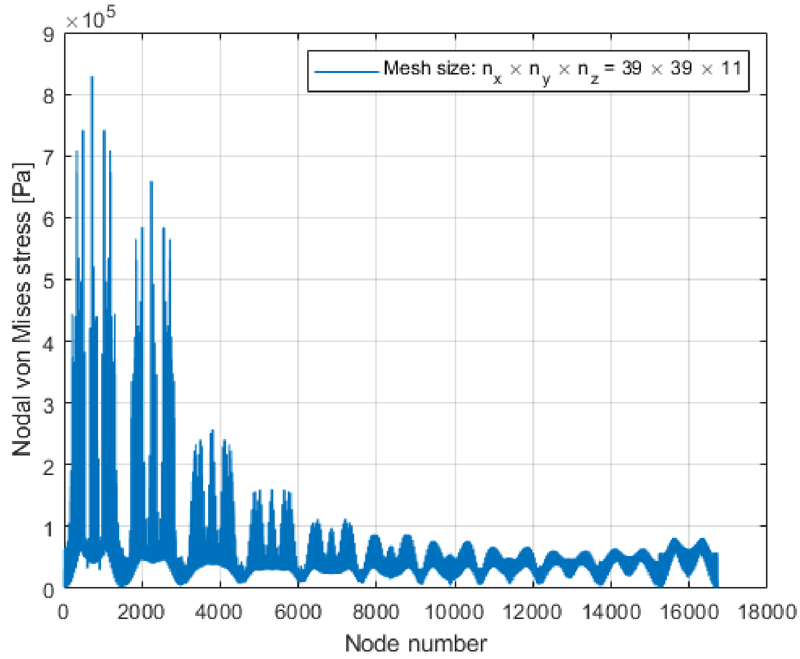

Figure A.7: Nodal von Mises stress for a mesh size of 39×39×11.

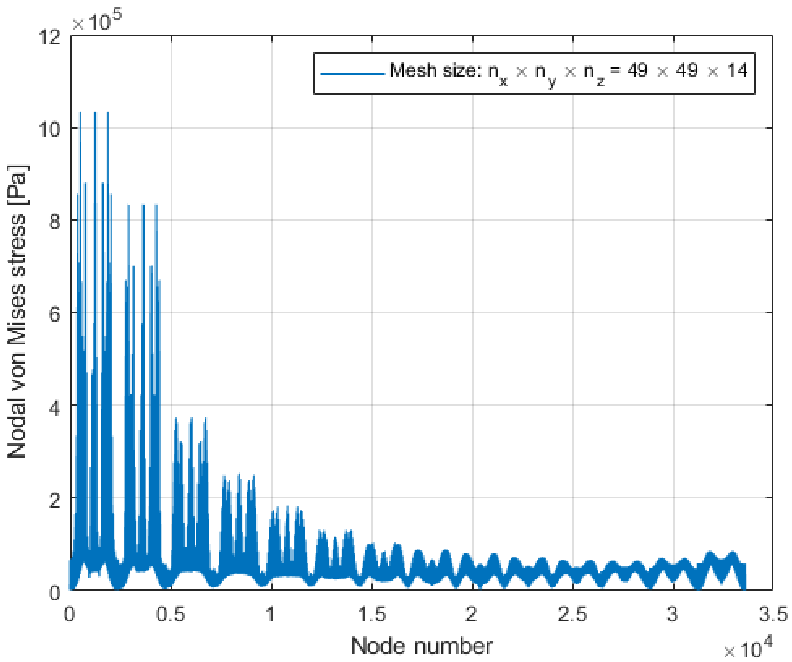

Figure A.8: Nodal von Mises stress for a mesh size of 49×49×14.

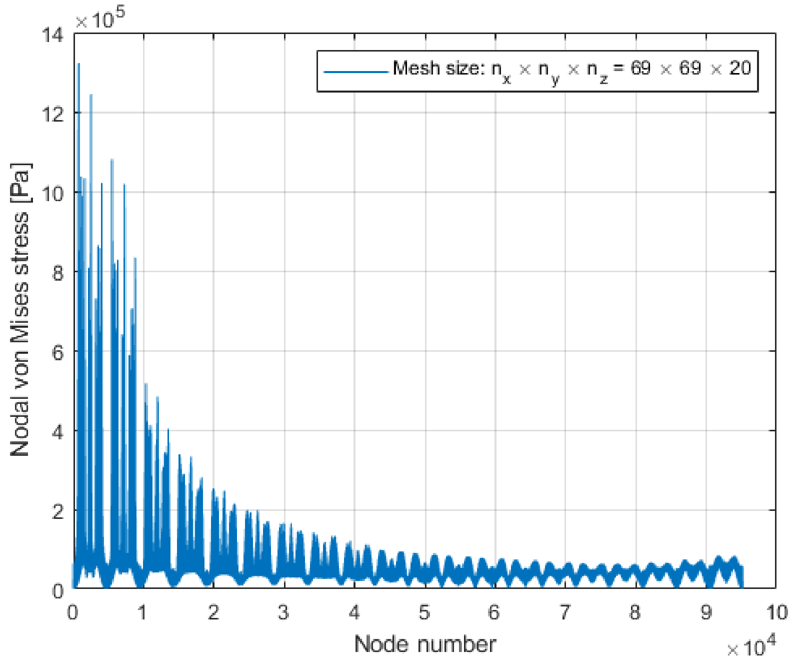

Figure A.9: Nodal von Mises stress for a mesh size of 69×69×20.

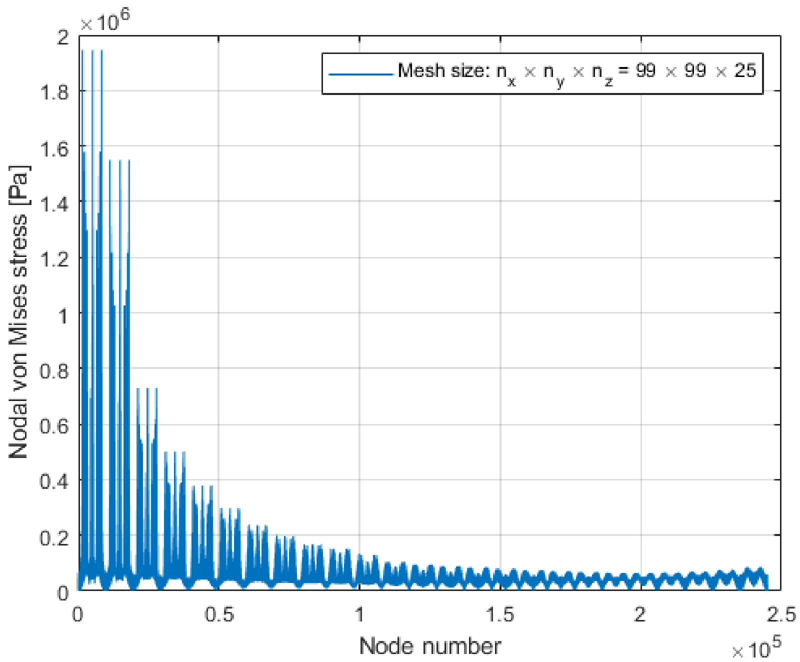

Figure A.10: Nodal von Mises stress for a mesh size of 99×99×25.

A.4 Slab Displacement

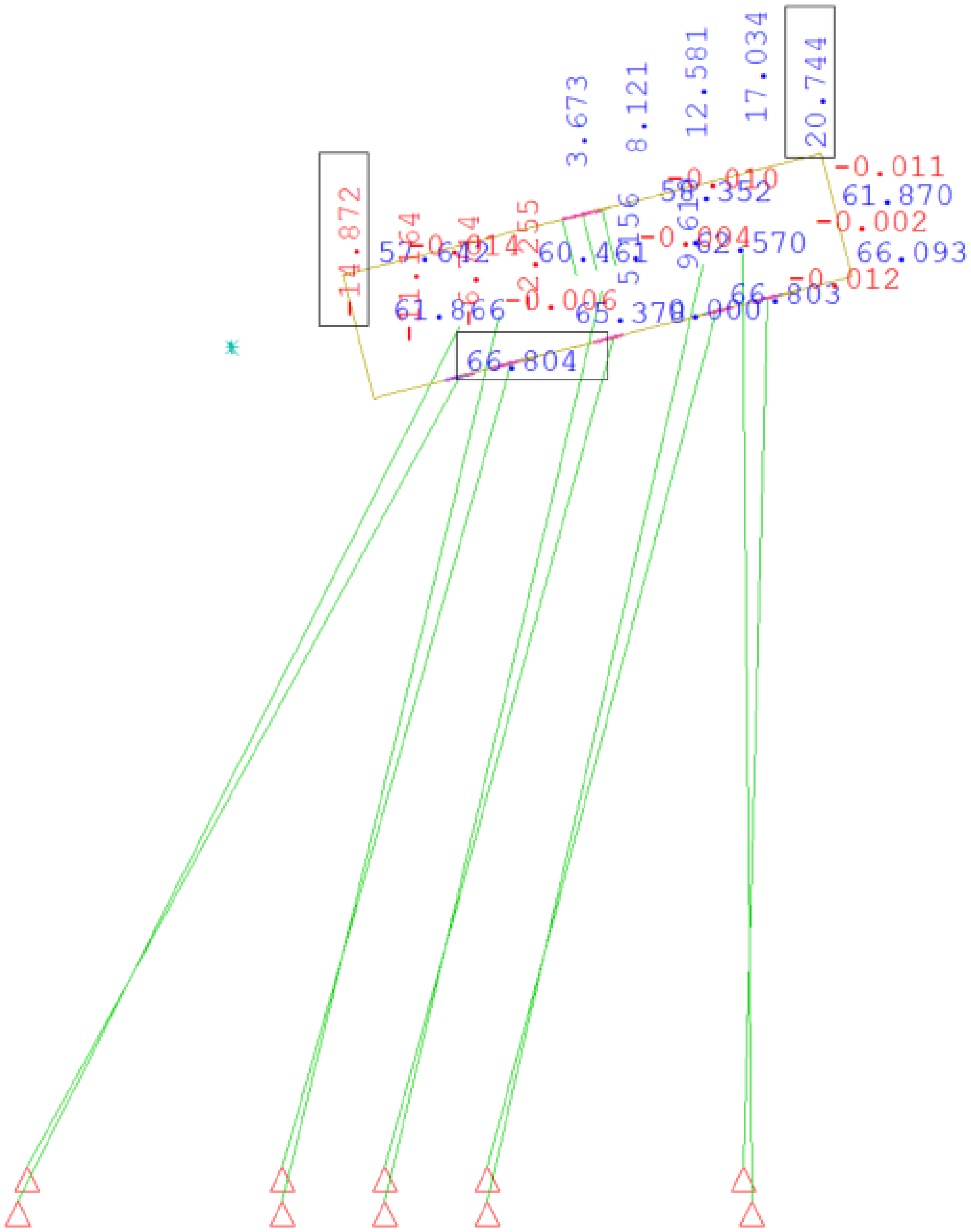

Figure A.11: Model A, pile cap displacement [mm] for mooring load case a.

A.5 Reaction Force

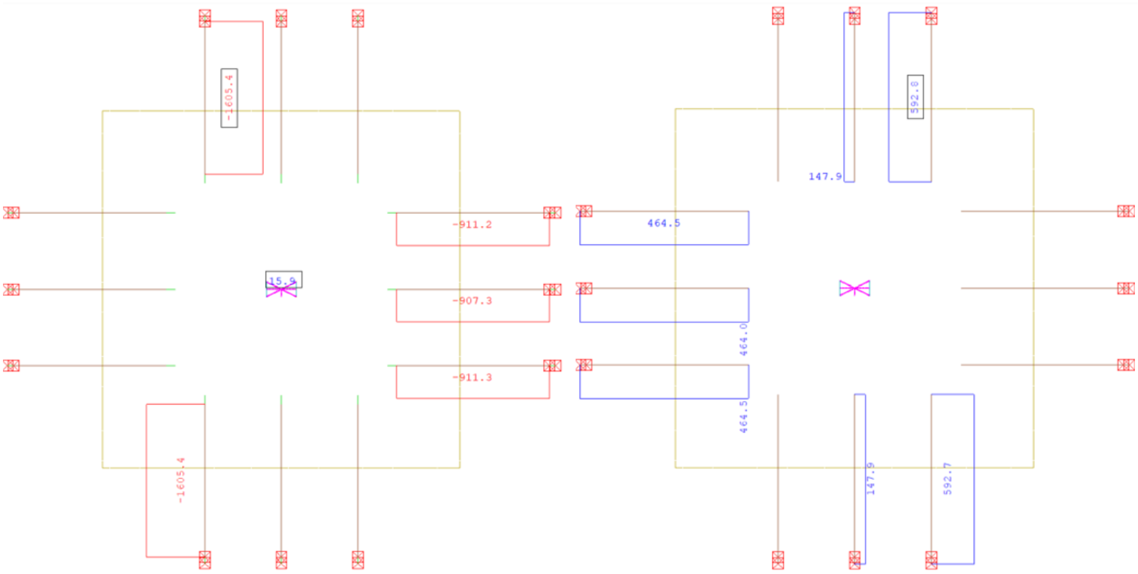

Figure A.12: Reaction force model A, load case a. Red compressive forces represents pile reactions, blue tensile forces represents anchor reactions.

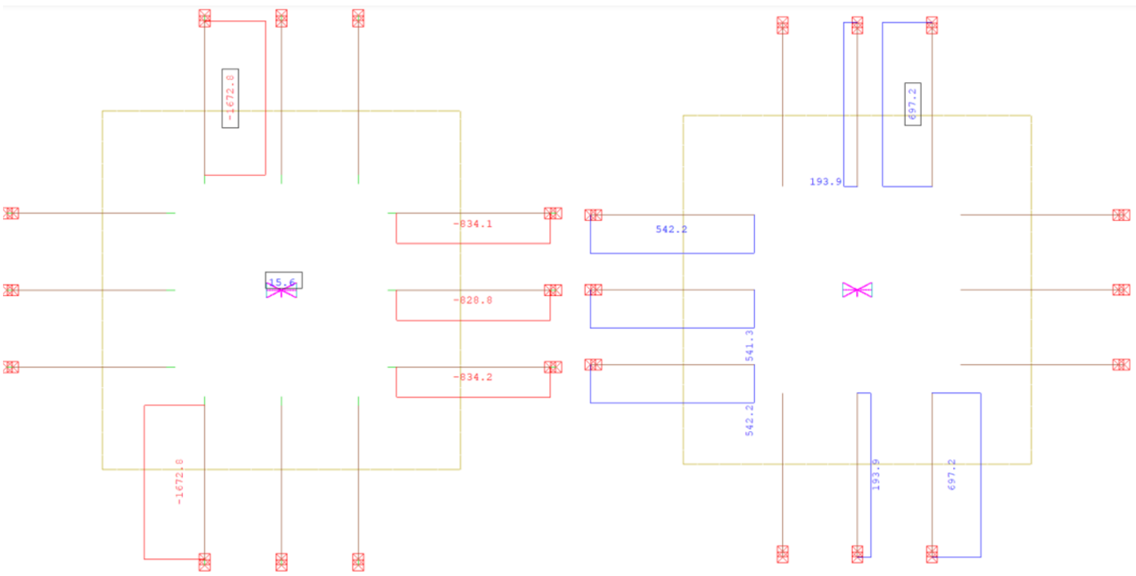

Figure A.13: Reaction force model B & E, load case a. Red compressive forces represents pile reactions, blue tensile forces represents anchor reactions.

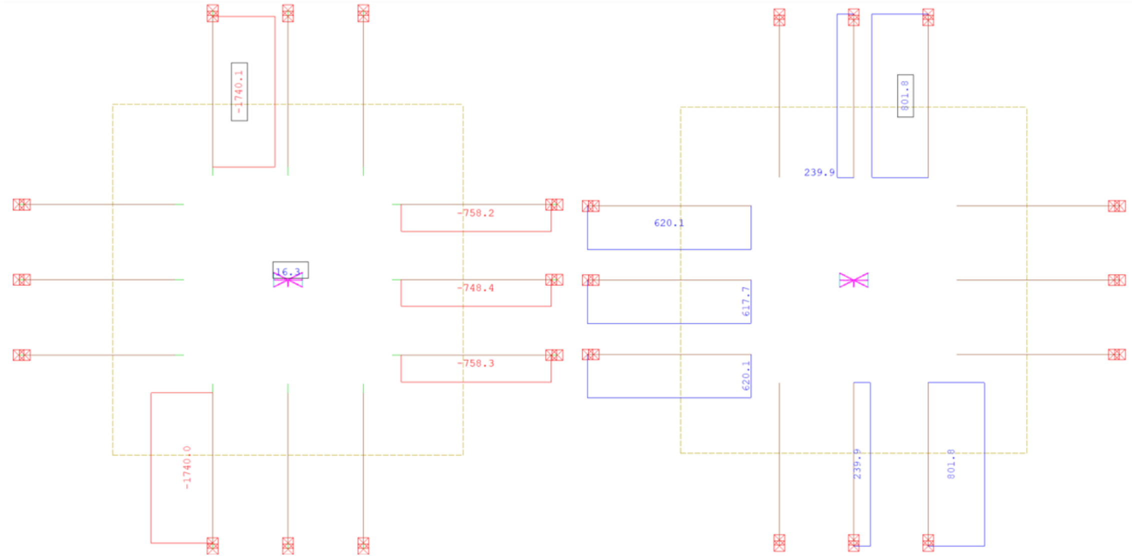

Figure A.14: Reaction force model C, load case a. Red compressive forces represents pile reactions, blue tensile forces represents anchor reactions.

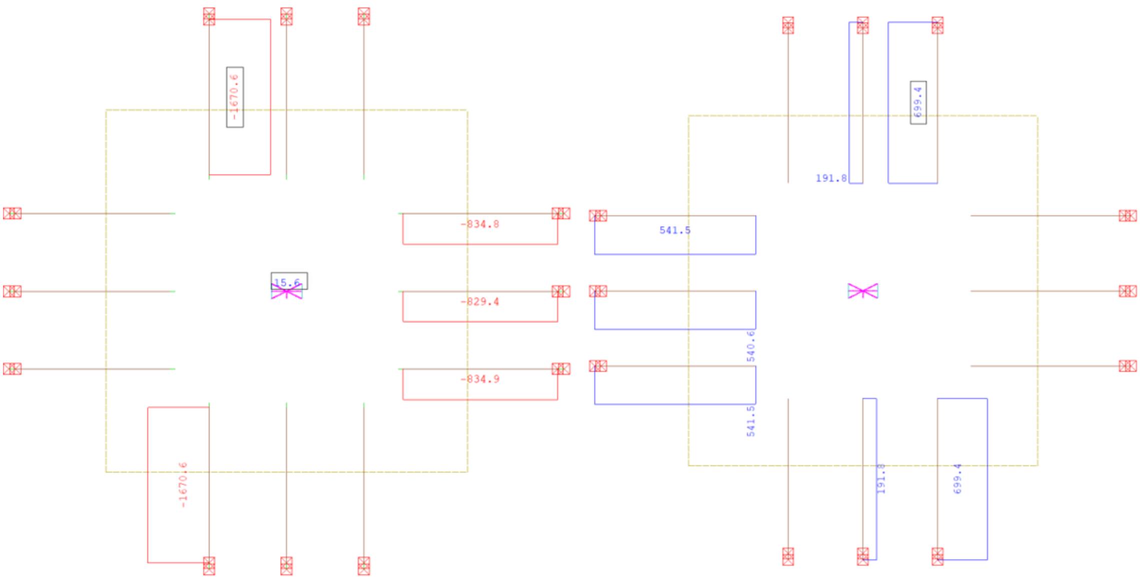

Figure A.15: Reaction force model D, load case a. Red compressive forces represents pile reactions, blue tensile forces represents anchor reactions.

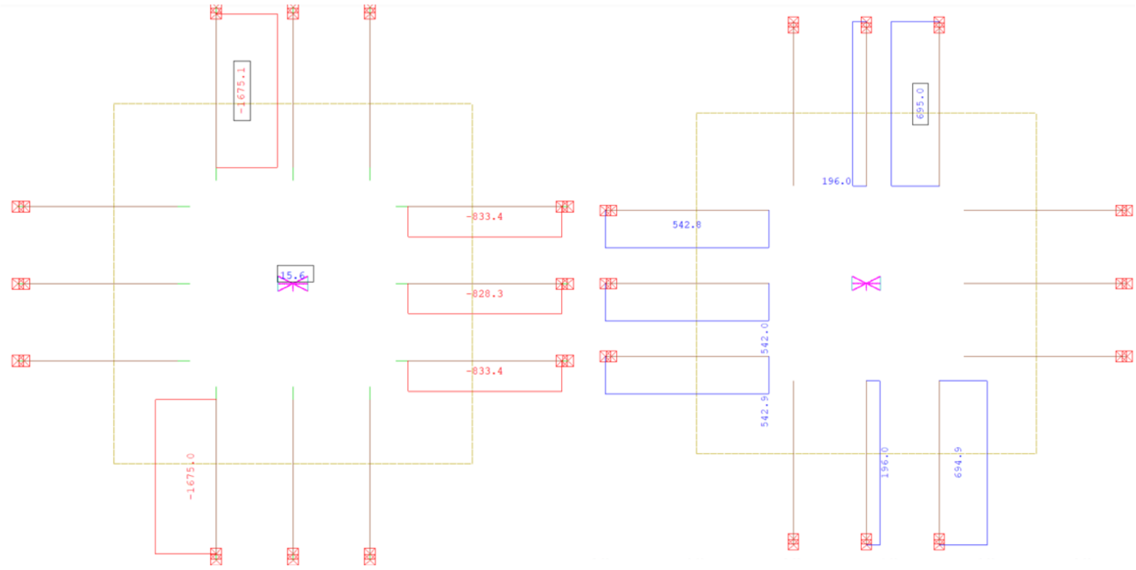

Figure A.16: Reaction force model F, load case a. Red compressive forces represents pile reactions, blue tensile forces represents anchor reactions.

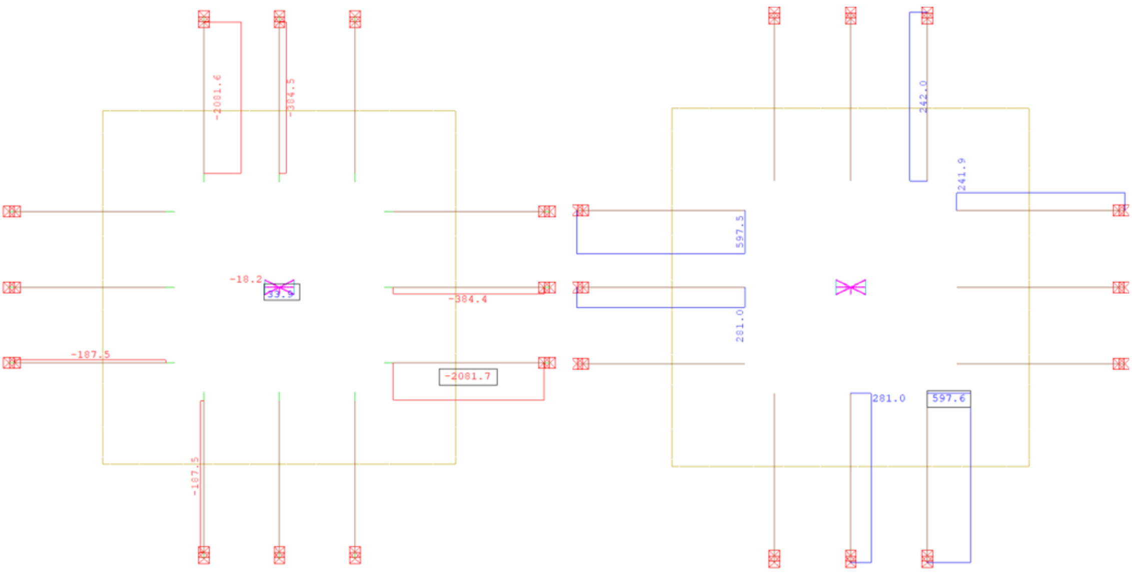

Figure A.17: Reaction force model A, load case b. Red compressive forces represents pile reactions, blue tensile forces represents anchor reactions.

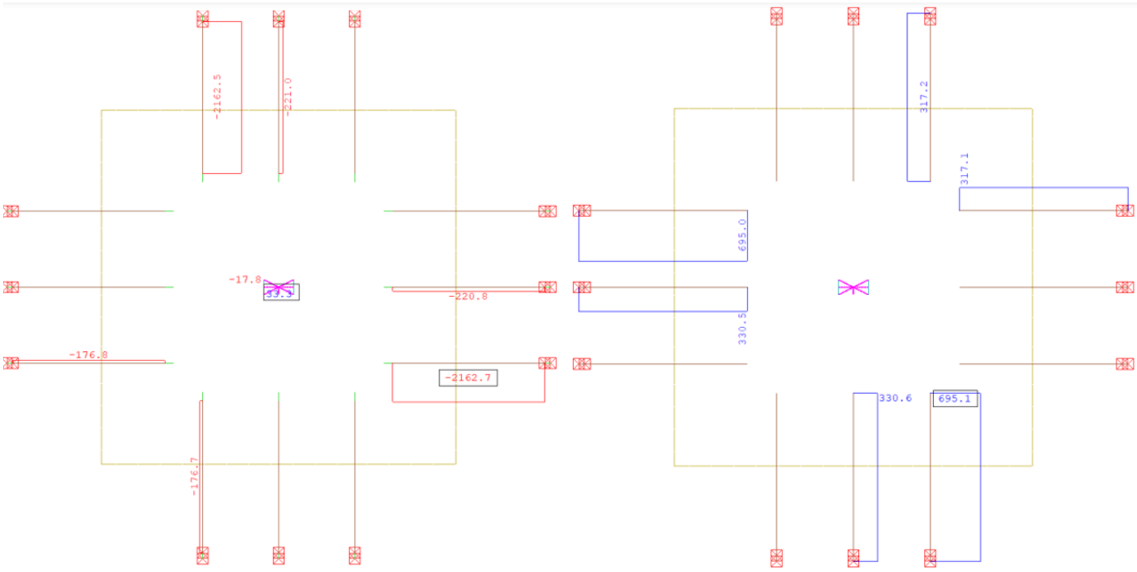

Figure A.18: Reaction force model B & E, load case b. Red compressive forces represents pile reactions, blue tensile forces represents anchor reactions.

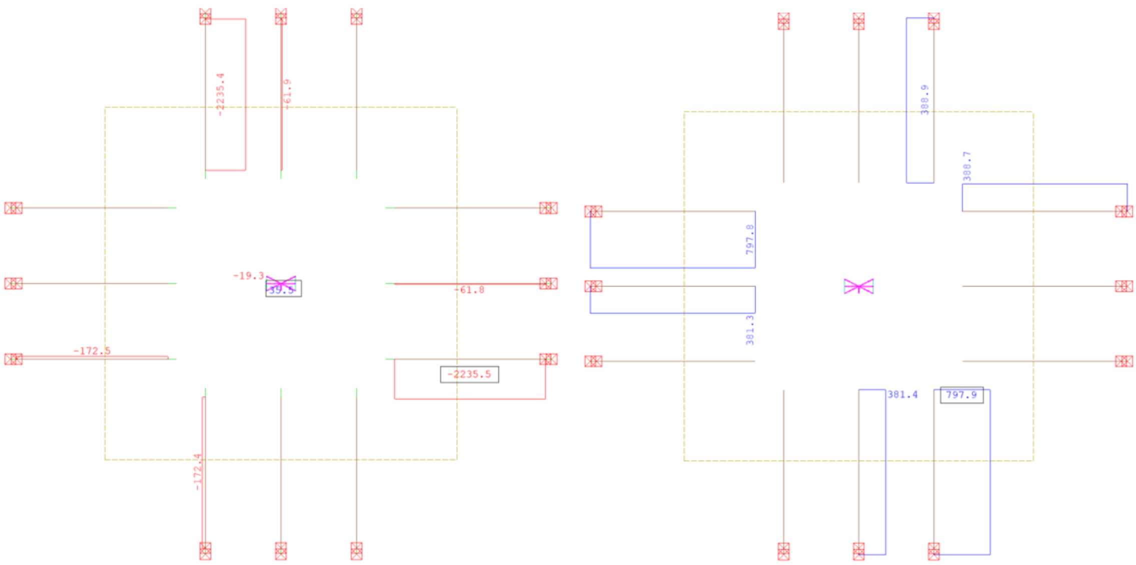

Figure A.19: Reaction force model C, load case b. Red compressive forces represents pile reactions, blue tensile forces represents anchor reactions.

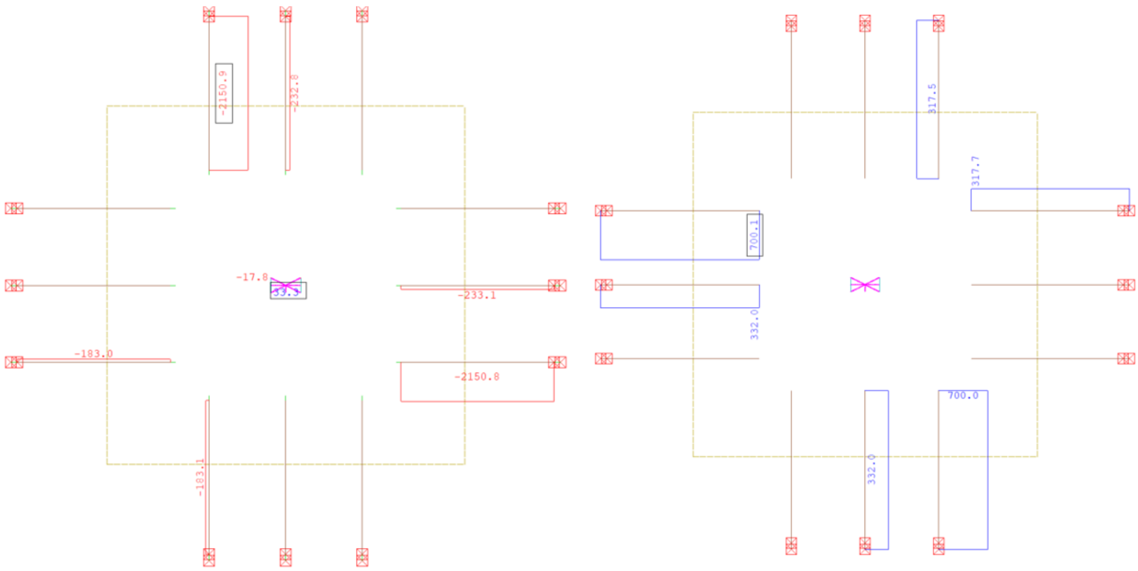

Figure A.20: Reaction force model D, load case b. Red compressive forces represents pile reactions, blue tensile forces represents anchor reactions.

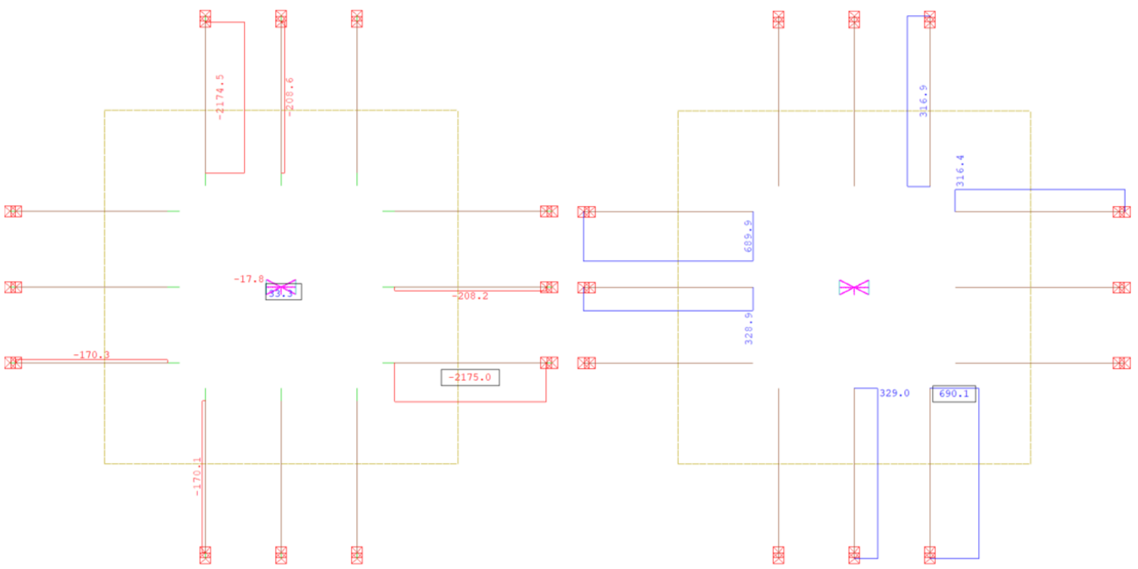

Figure A.21: Reaction force model F, load case b. Red compressive forces represents pile reactions, blue tensile forces represents anchor reactions.

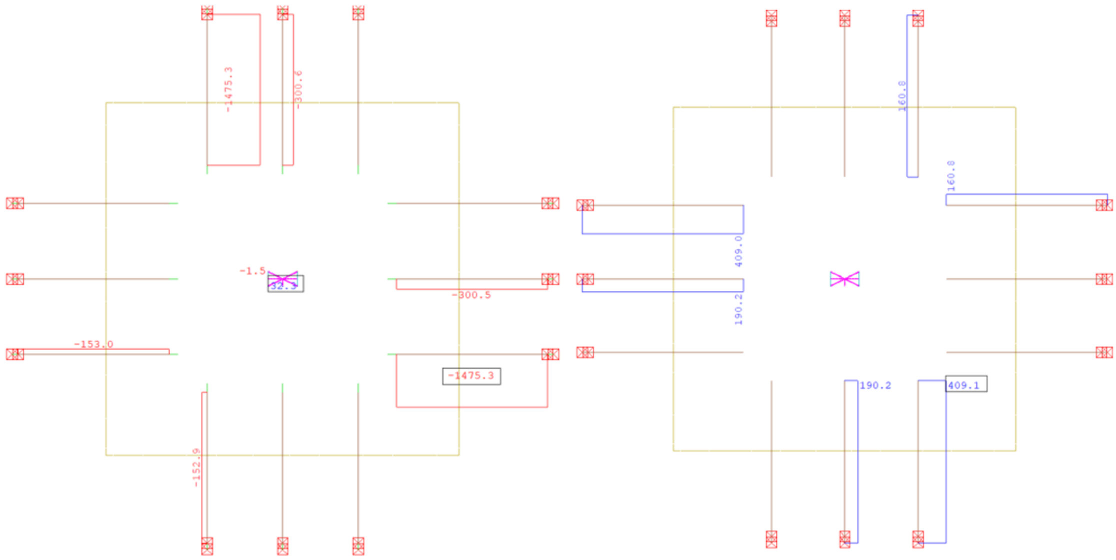

Figure A.22: Reaction force model A, load case c. Red compressive forces represents pile reactions, blue tensile forces represents anchor reactions.

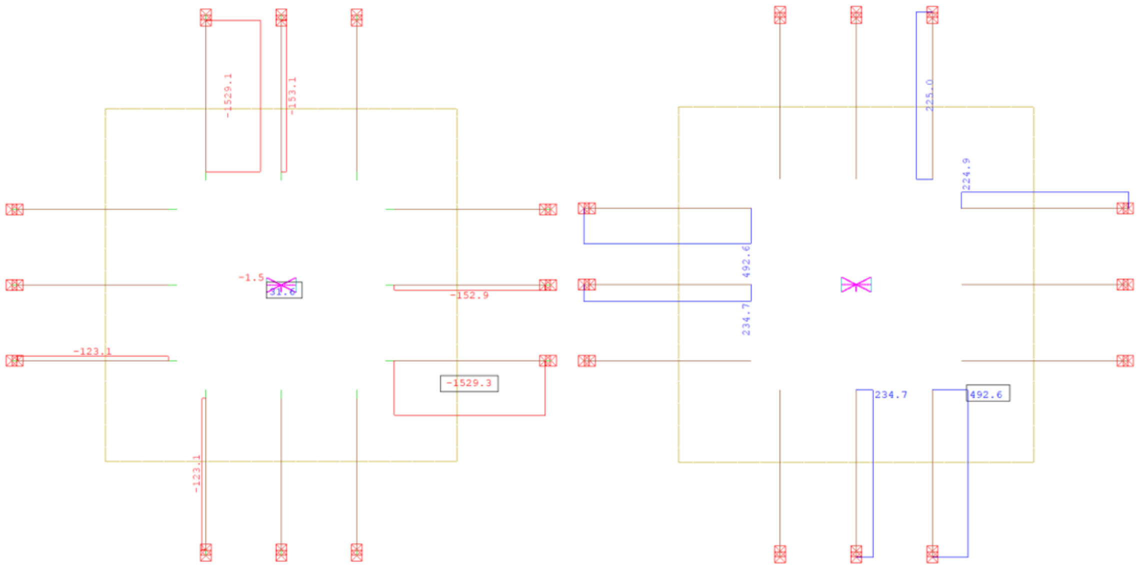

Figure A.23: Reaction force model B & E, load case c. Red compressive forces represents pile reactions, blue tensile forces represents anchor reactions.

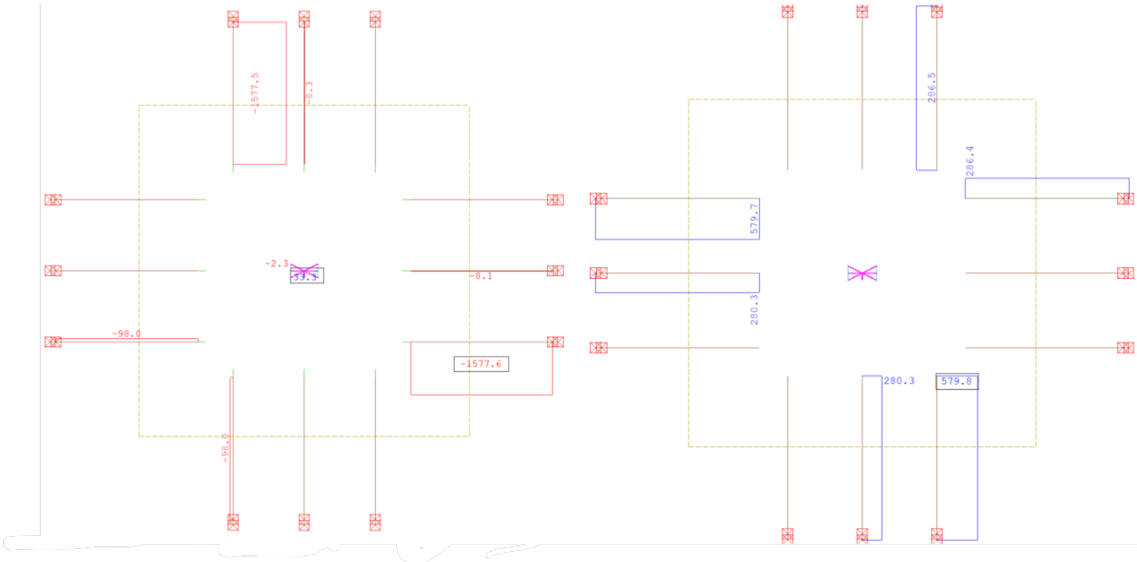

Figure A.24: Reaction force model C, load case c. Red compressive forces represents pile reactions, blue tensile forces represents anchor reactions.

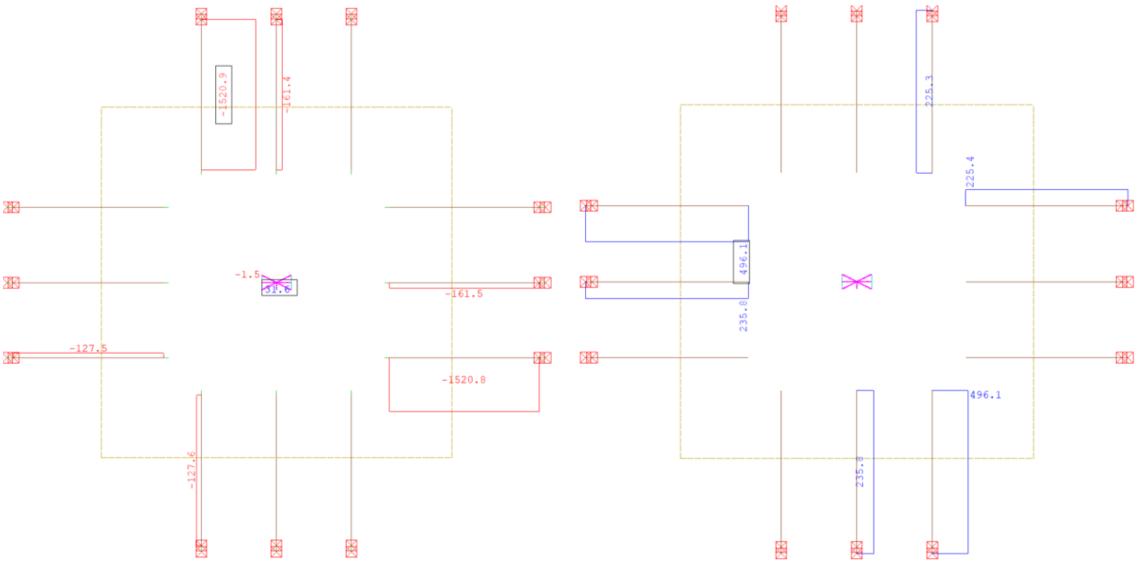

Figure A.25: Reaction force model D, load case c. Red compressive forces represents pile reactions, blue tensile forces represents anchor reactions.

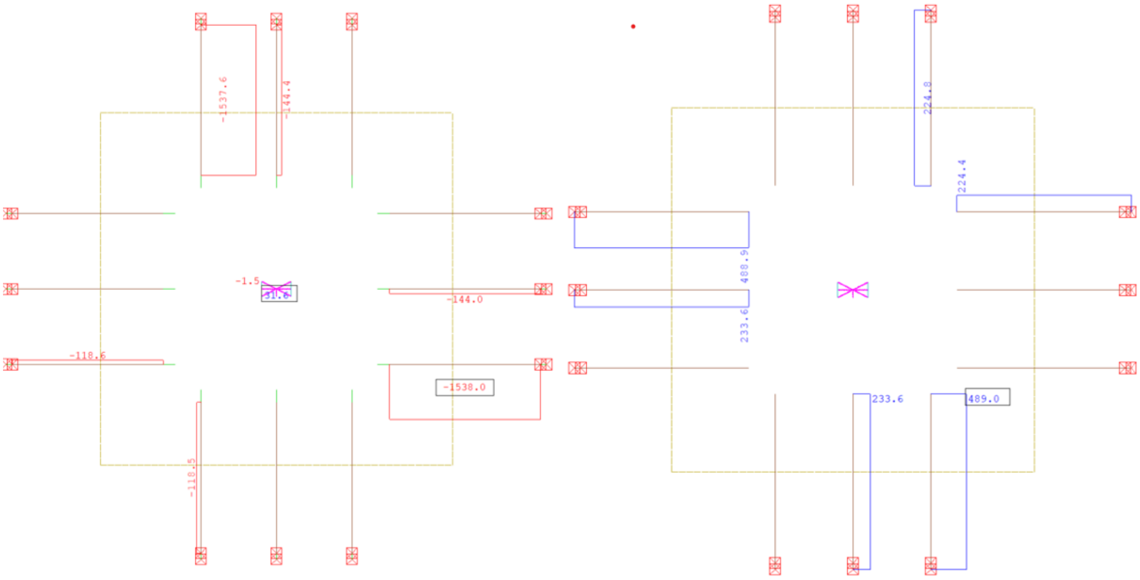

Figure A.26: Reaction force model F, load case c. Red compressive forces represents pile reactions, blue tensile forces represents anchor reactions.

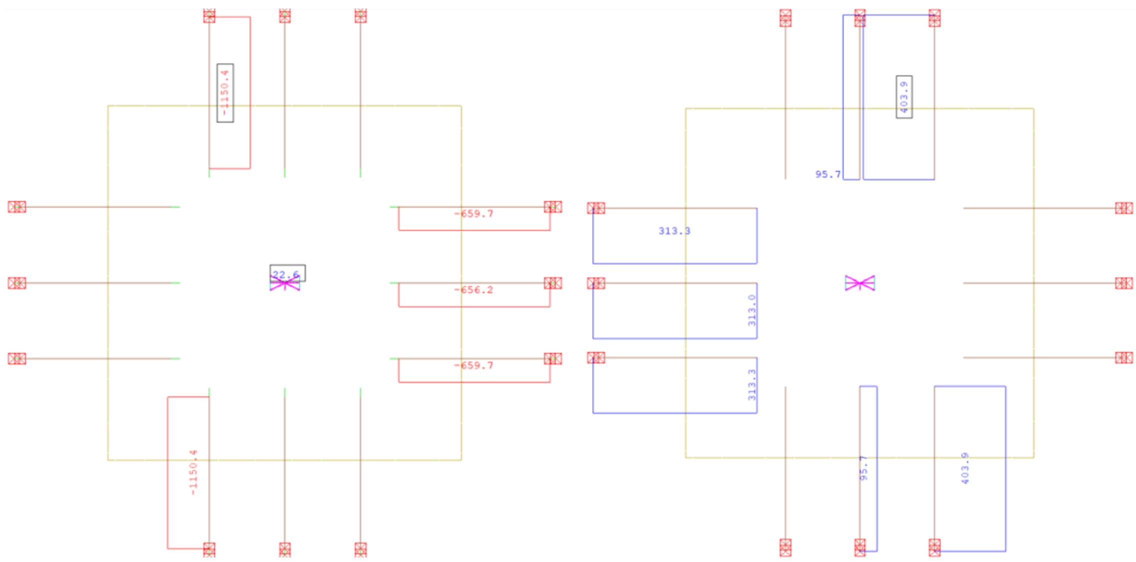

Figure A.27: Reaction force model A, load case d. Red compressive forces represents pile reactions, blue tensile forces represents anchor reactions.

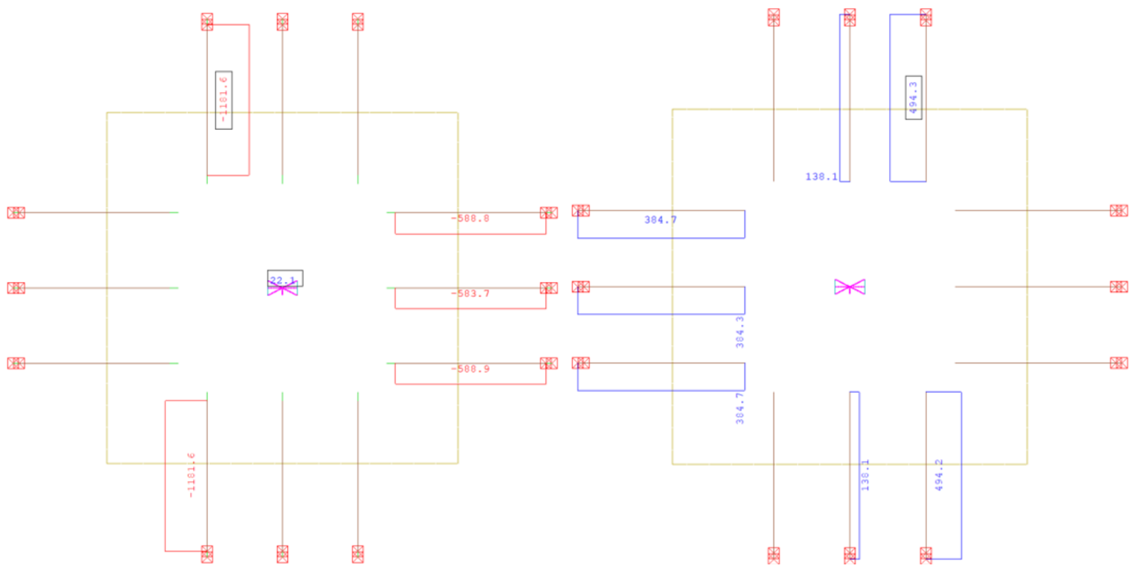

Figure A.28: Reaction force model B & E, load case d. Red compressive forces represents pile reactions, blue tensile forces represents anchor reactions.

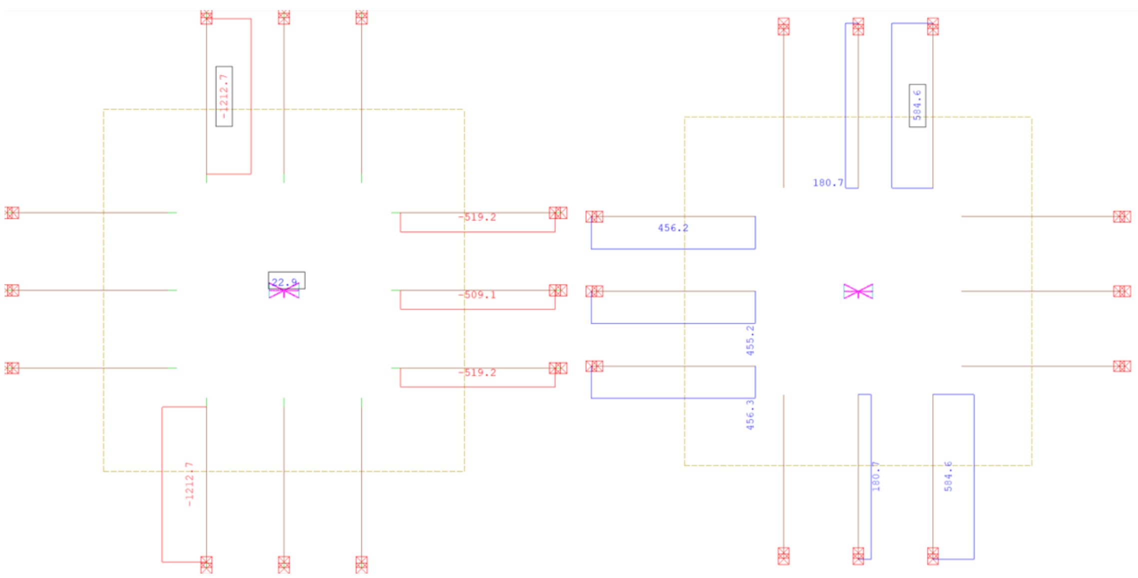

Figure A.29: Reaction force model C, load case d. Red compressive forces represents pile reactions, blue tensile forces represents anchor reactions.

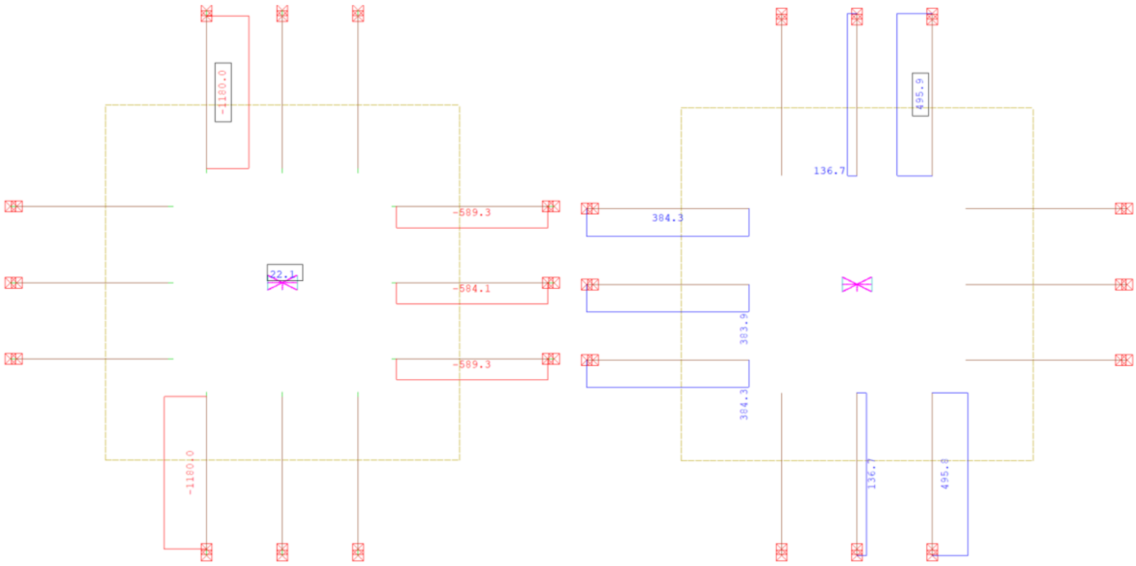

Figure A.30: Reaction force model D, load case d. Red compressive forces represents pile reactions, blue tensile forces represents anchor reactions.

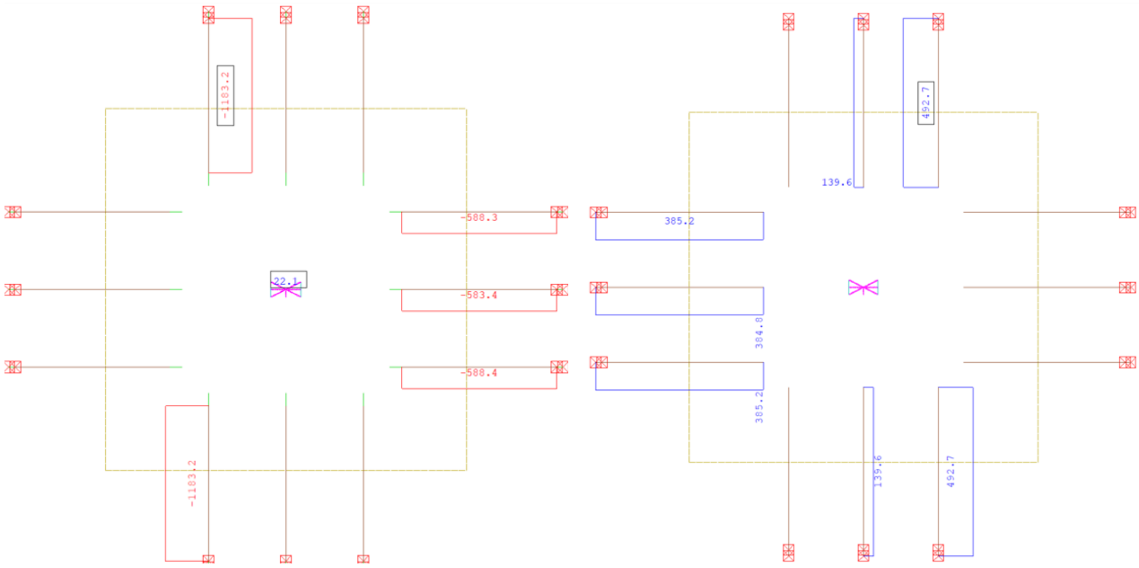

Figure A.31: Reaction force model F, load case d. Red compressive forces represents pile reactions, blue tensile forces represents anchor reactions.

A.6 Load case c

It should be noted that the plots for load case c exhibit the same strut-and-tie load transfer mechanism as load case b, despite differences in their visual representation.

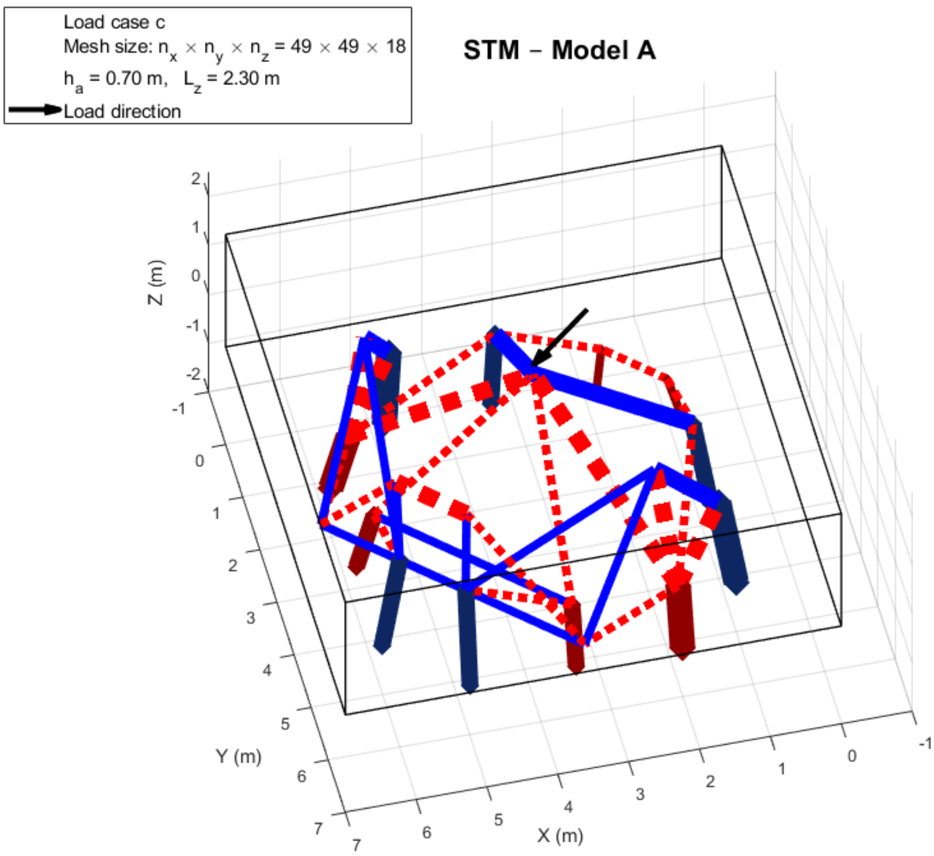

Figure A.32: STM for model A, lc c.

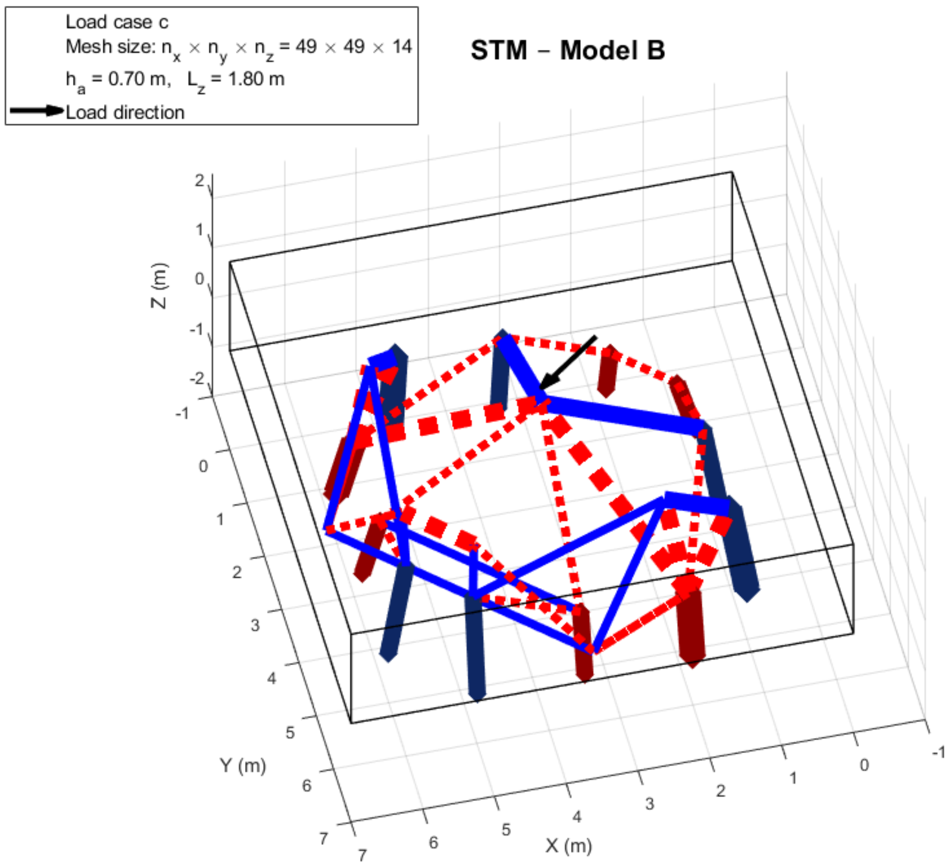

Figure A.33: STM for model B & E, lc c.

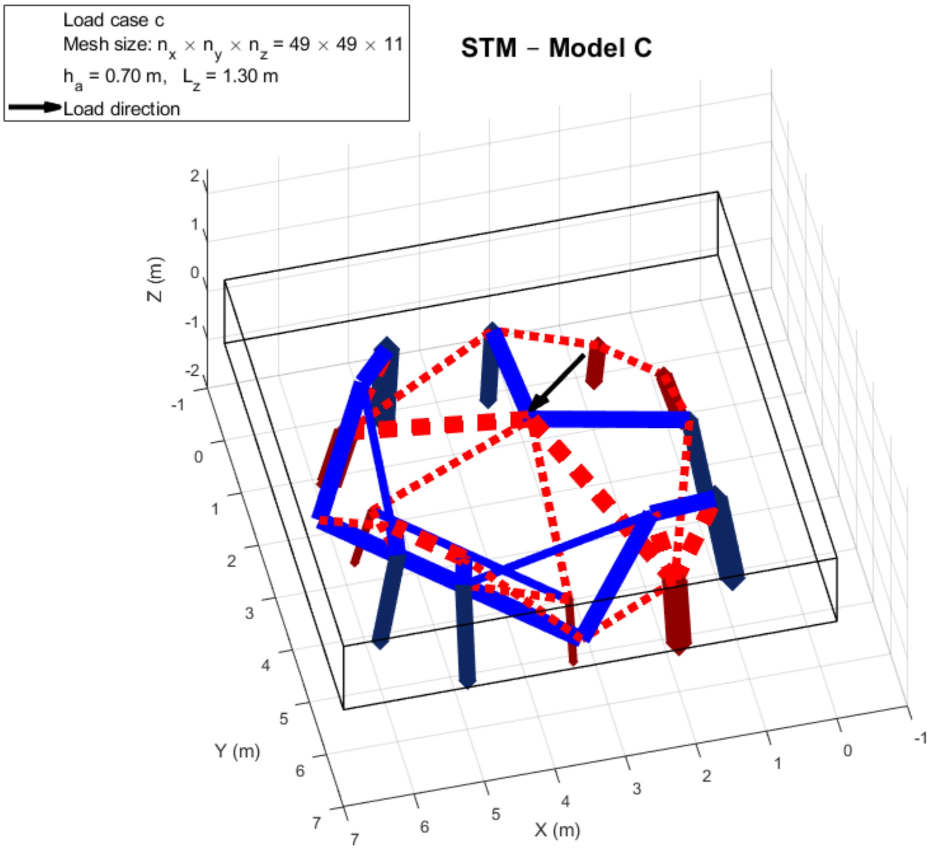

Figure A.34: STM for model C, lc c.

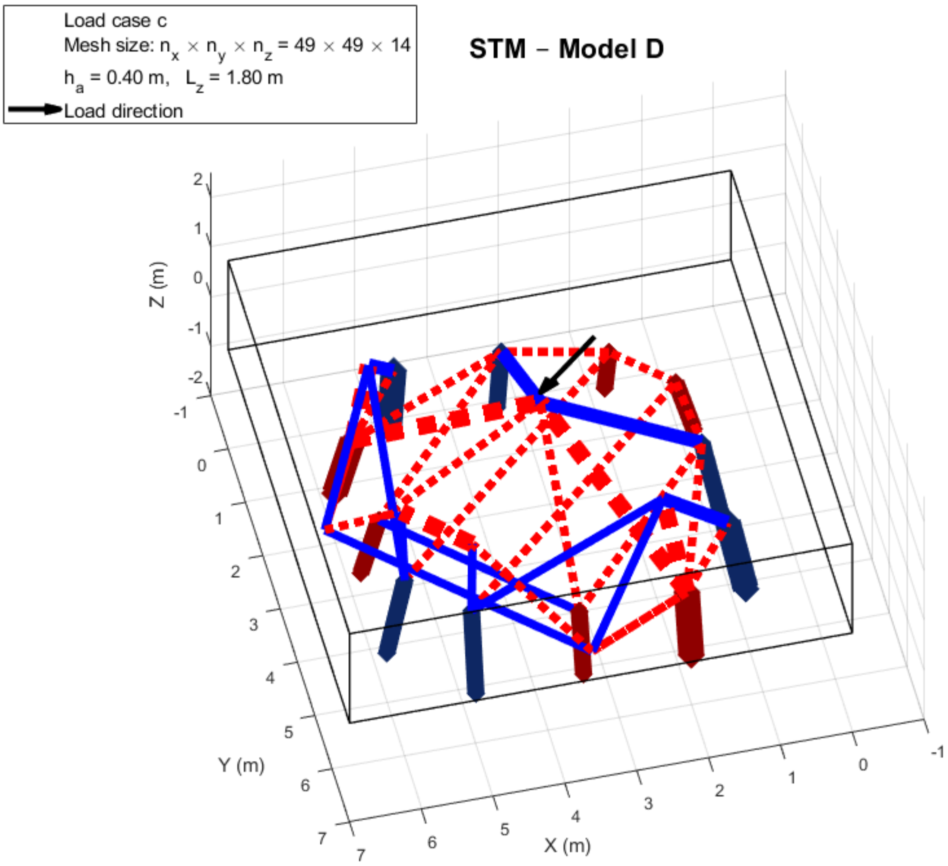

Figure A.35: STM for model D, lc c.

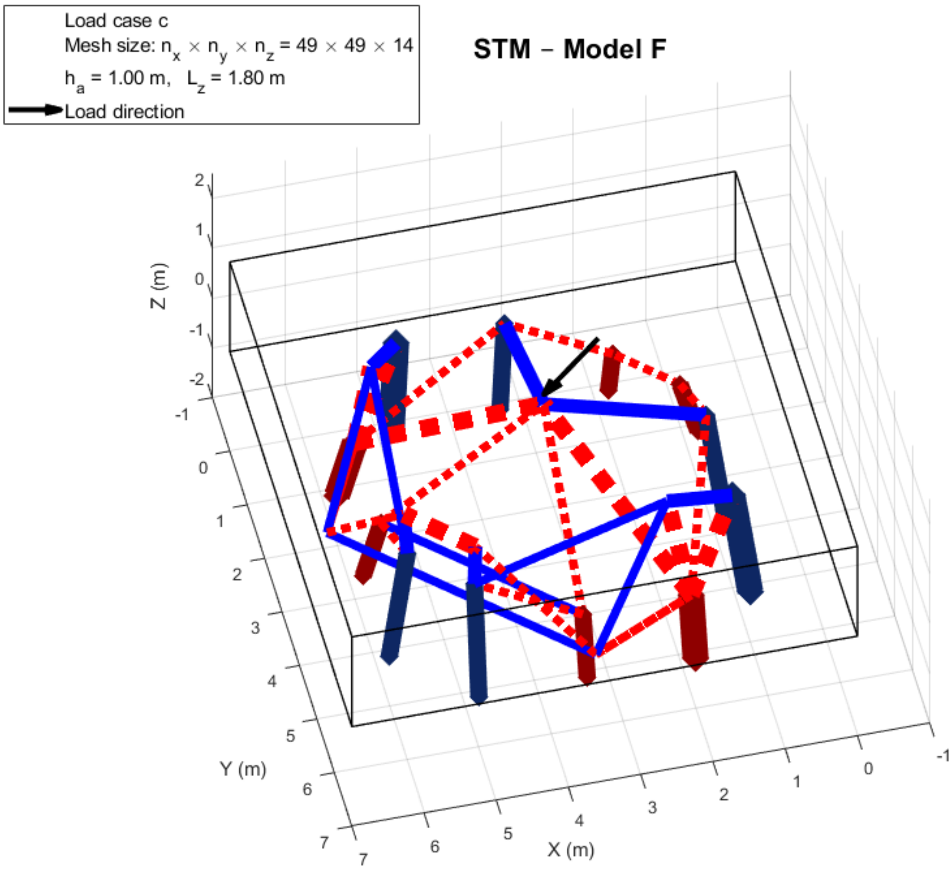

Figure A.36: STM for model F, lc c.

A.7 Load case d

It should be noted that the plots for load case d exhibit the same strut-and-tie load transfer mechanism as load case a, despite differences in their visual representation.

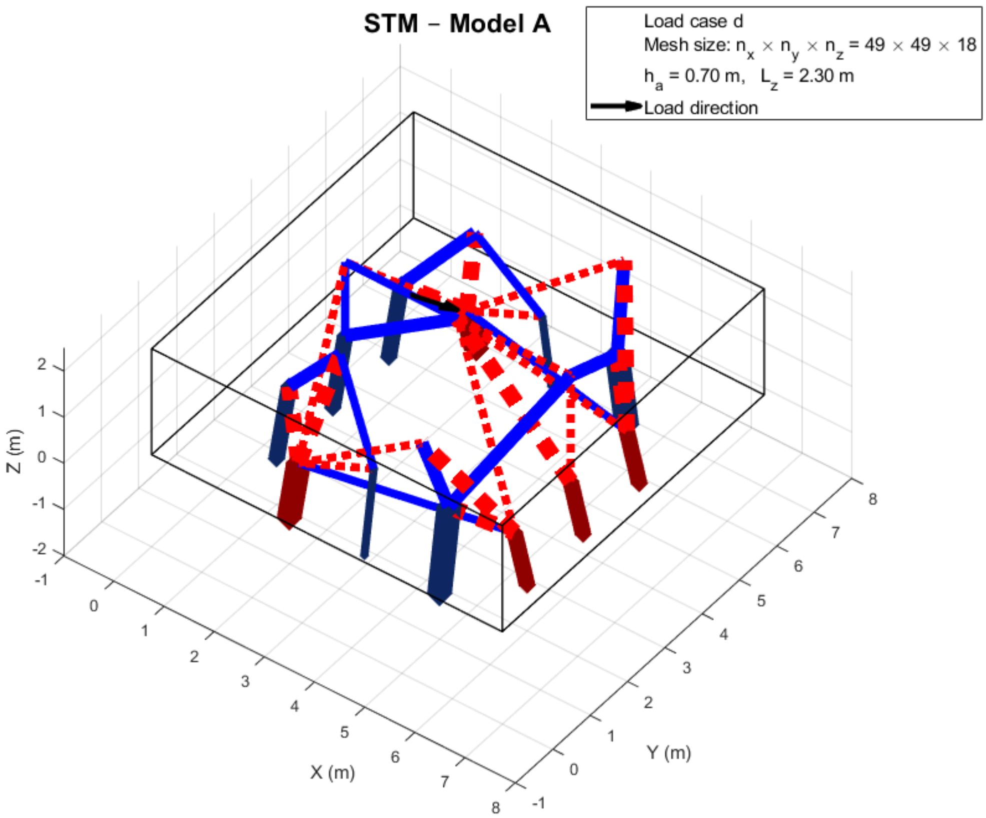

Figure A.37: STM for model A, lc d.

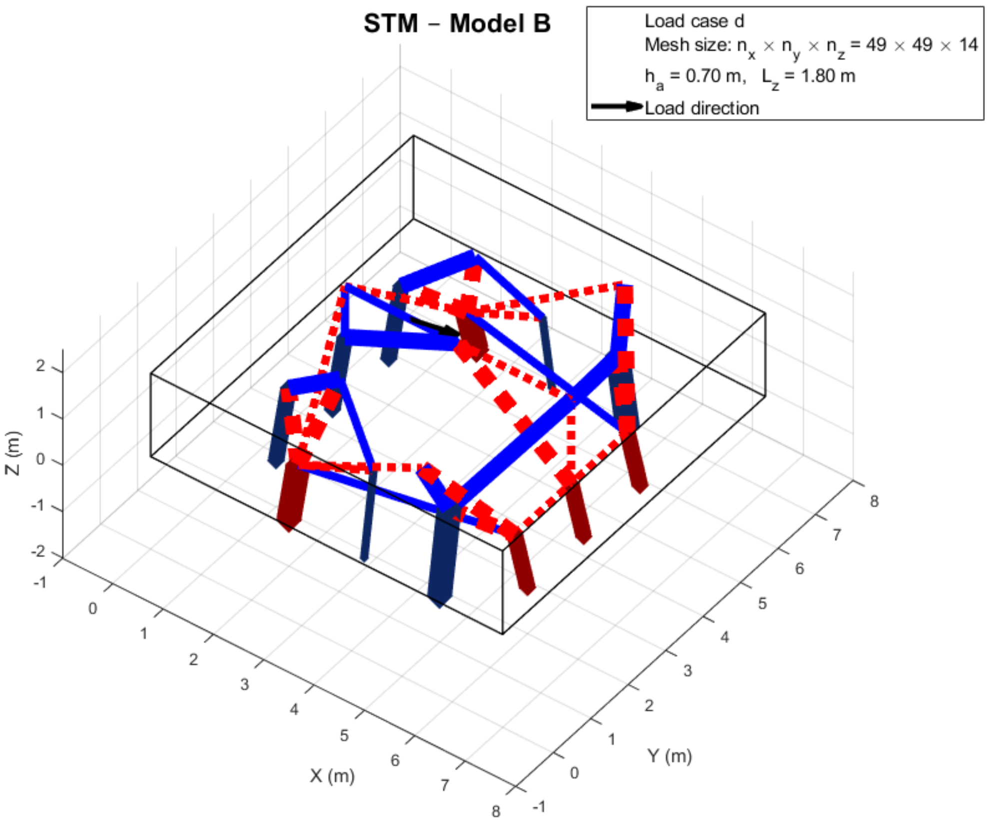

Figure A.38: STM for model B & E, lc d.

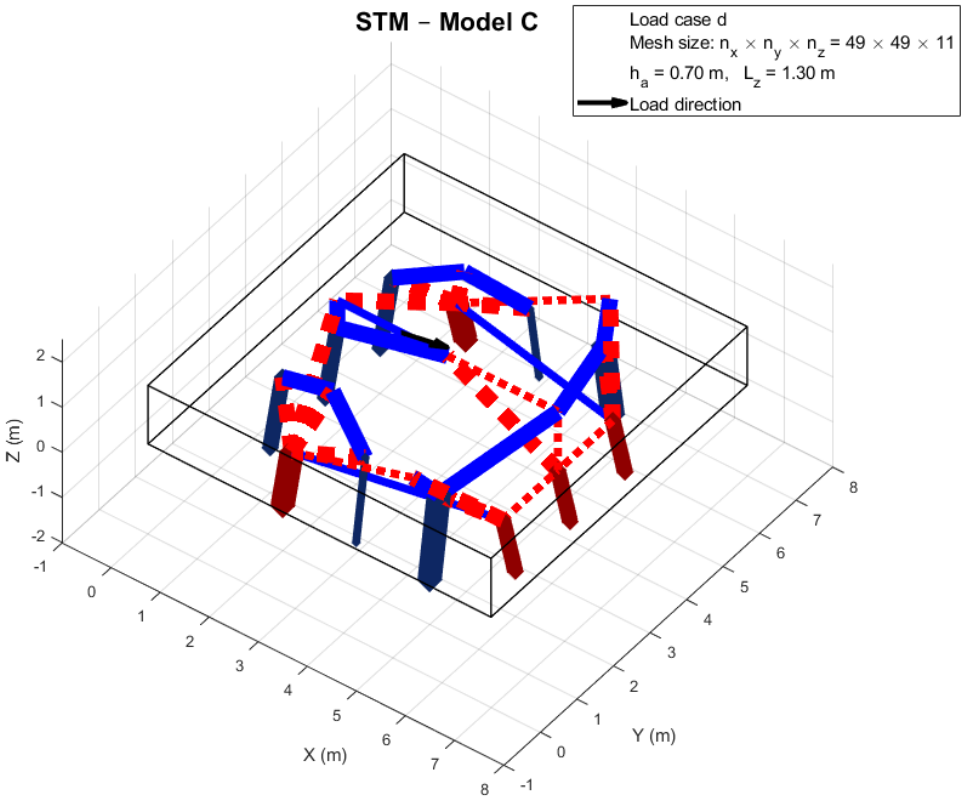

Figure A.39: STM for model C, lc d.

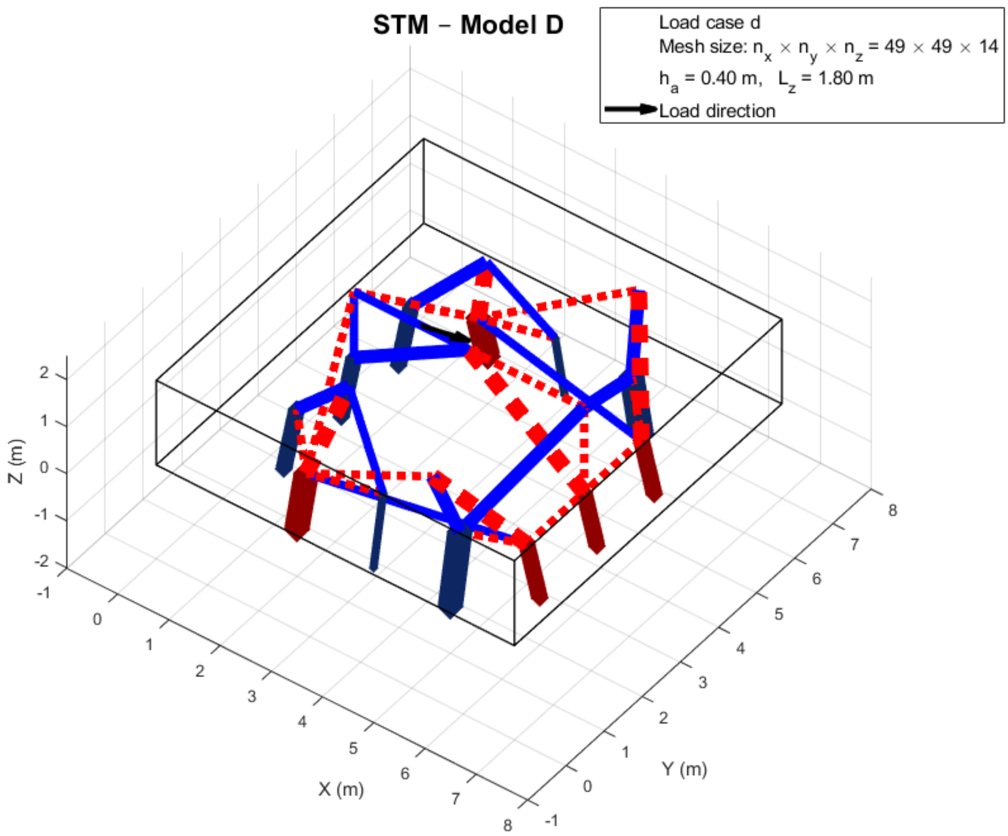

Figure A.40: STM for model D, lc d.

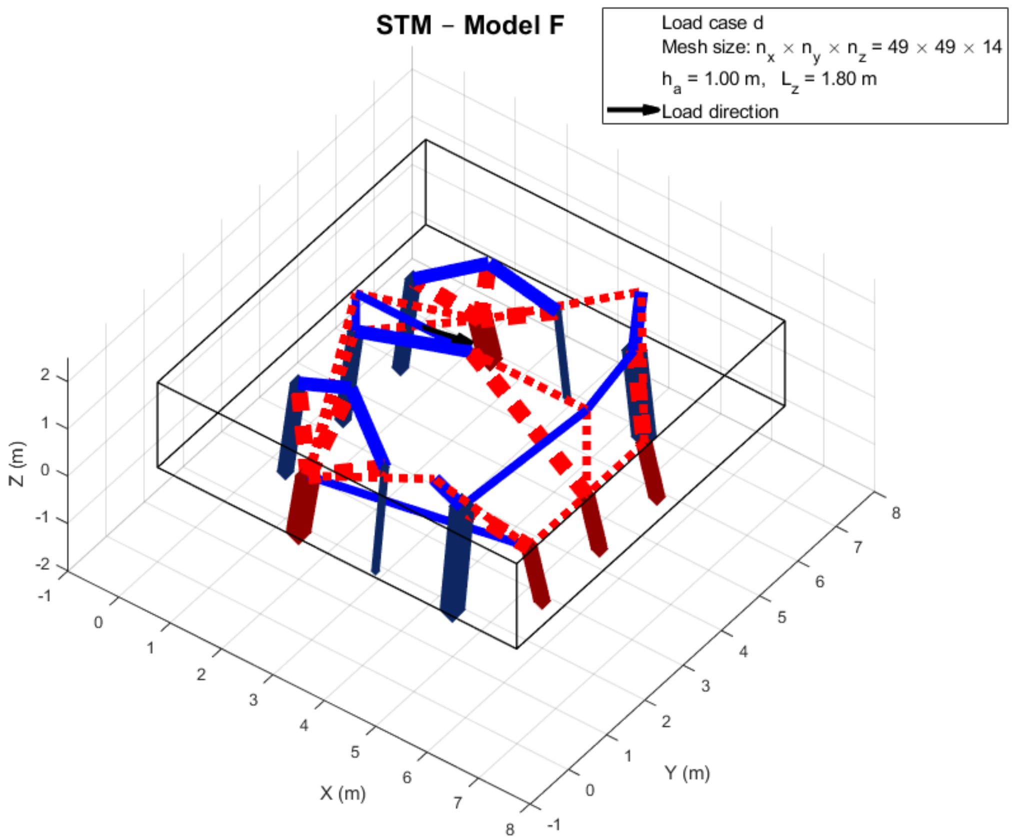

Figure A.41: STM for model F, lc d.

A.8 Verification of pile response

Control of Reaction Forces in Piles
Self weight

Material Data

Concrete C 35/45 $\rho_c := 25 \frac{kN}{m^3}$

Steel S 275 $\rho_s := 78.5 \frac{kN}{m^3}$

Pile Cap

$B := 7\ m$ $H := B$ $T := 1.8\ m$

$V_c := B \cdot H \cdot T = 88.2\ m^3$

$F_c := V_c \cdot \rho_c = \left(2.205 \cdot 10^3\right)\ kN$ Dead load pile cap

Piles

$t_p := 14.2\ mm$ Thickness

$D_{p\_o} := 508\ mm$ Outer $D_{p\_i} := D_{p\_o} - \left(2 \cdot t_p\right) = 479.6\ mm$

$A_{py} := \frac{\pi \cdot D_{p\_o}^{\ 2}}{4} = 0.203\ m^2$ $A_{pi} := \frac{\pi \cdot D_{p\_i}^{\ 2}}{4} = 0.181\ m^2$ Inner

$A_{p.tot} := 12 \cdot \left(A_{py} - A_{pi}\right) = 0.264\ m^2$

$L_p := 12.3 \frac{m}{\cos(14\ deg)} = 12.677\ m$ $V_p := L_p \cdot A_{p.tot} = 3.351\ m^3$

$F_p := V_p \cdot \rho_s = 263.052\ kN$ Dead load piles

Reaction Force / pile

$F_{tot} := F_c + F_p = \left(2.468 \cdot 10^3\right)\ kN$ $F_{pile} := \frac{F_{tot}}{12} = 205.671\ kN$

$F_{FEM} := 205\ kN$ $\Delta_F := F_{FEM} - F_{pile} = -0.671\ kN$

DEPARTMENT OF SOME SUBJECT OR TECHNOLOGY
CHALMERS UNIVERSITY OF TECHNOLOGY
Gothenburg, Sweden
www.chalmers.se